

ISSN 1881-7831 Online ISSN 1881-784X

DD & T

Drug Discoveries & Therapeutics

Volume 13, Number 5
October 2019



www.ddtjournal.com

DD & T

Drug Discoveries & Therapeutics



ISSN: 1881-7831
Online ISSN: 1881-784X
CODEN: DDTRBX
Issues/Year: 6
Language: English
Publisher: IACMHR Co., Ltd.

Drug Discoveries & Therapeutics is one of a series of peer-reviewed journals of the International Research and Cooperation Association for Bio & Socio-Sciences Advancement (IRCA-BSSA) Group and is published bimonthly by the International Advancement Center for Medicine & Health Research Co., Ltd. (IACMHR Co., Ltd.) and supported by the IRCA-BSSA and Shandong University China-Japan Cooperation Center for Drug Discovery & Screening (SDU-DDSC).

Drug Discoveries & Therapeutics publishes contributions in all fields of pharmaceutical and therapeutic research such as medicinal chemistry, pharmacology, pharmaceutical analysis, pharmaceuticals, pharmaceutical administration, and experimental and clinical studies of effects, mechanisms, or uses of various treatments. Studies in drug-related fields such as biology, biochemistry, physiology, microbiology, and immunology are also within the scope of this journal.

Drug Discoveries & Therapeutics publishes Original Articles, Brief Reports, Reviews, Policy Forum articles, Case Reports, News, and Letters on all aspects of the field of pharmaceutical research. All contributions should seek to promote international collaboration in pharmaceutical science.

Editorial Board

Editor-in-Chief:

Kazuhisa SEKIMIZU
Teikyo University, Tokyo, Japan

Co-Editors-in-Chief:

Xishan HAO
Tianjin Medical University, Tianjin, China
Munehiro NAKATA
Tokai University, Hiratsuka, Japan

Chief Director & Executive Editor:

Wei TANG
National Center for Global Health and Medicine, Tokyo, Japan

Senior Editors:

Guanhua DU
Chinese Academy of Medical Science and Peking Union Medical College, Beijing, China
Xiao-Kang LI
National Research Institute for Child Health and Development, Tokyo, Japan
Masahiro MURAKAMI
Osaka Ohtani University, Osaka, Japan
Yutaka ORIHARA
The University of Tokyo, Tokyo, Japan
Tomofumi SANTA
The University of Tokyo, Tokyo, Japan
Hongbin SUN
China Pharmaceutical University, Nanjing, China

Fengshan WANG
Shandong University, Ji'nan, China

Managing Editor:

Hiroshi HAMAMOTO
Teikyo University, Tokyo, Japan

Web Editor:

Yu CHEN
The University of Tokyo, Tokyo, Japan

Proofreaders:

Curtis BENTLEY
Roswell, GA, USA
Thomas R. LEBON
Los Angeles, CA, USA

Editorial and Head Office:

Pearl City Koishikawa 603,
2-4-5 Kasuga, Bunkyo-ku,
Tokyo 112-0003, Japan
Tel.: +81-3-5840-9697
Fax: +81-3-5840-9698
E-mail: office@ddtjournal.com

Drug Discoveries & Therapeutics

Editorial and Head Office

Pearl City Koishikawa 603, 2-4-5 Kasuga, Bunkyo-ku,
Tokyo 112-0003, Japan

Tel: +81-3-5840-9697, Fax: +81-3-5840-9698
E-mail: office@ddtjournal.com
URL: www.ddtjournal.com

Editorial Board Members

Alex ALMASAN <i>(Cleveland, OH)</i>	Rodney J. Y. HO <i>(Seattle, WA)</i>	Ken-ichi MAFUNE <i>(Tokyo)</i>	Quanxing WANG <i>(Shanghai)</i>
John K. BUOLAMWINI <i>(Memphis, TN)</i>	Hsing-Pang HSIEH <i>(Zhunan, Miaoli)</i>	Sridhar MANI <i>(Bronx, NY)</i>	Stephen G. WARD <i>(Bath)</i>
Jianping CAO <i>(Shanghai)</i>	Yongzhou HU <i>(Hangzhou, Zhejiang)</i>	Tohru MIZUSHIMA <i>(Tokyo)</i>	Yuhong XU <i>(Shanghai)</i>
Shousong CAO <i>(Buffalo, NY)</i>	Yu HUANG <i>(Hong Kong)</i>	Abdulla M. MOLOKHIA <i>(Alexandria)</i>	Bing YAN <i>(Ji'nan, Shandong)</i>
Jang-Yang CHANG <i>(Tainan)</i>	Amrit B. KARMARKAR <i>(Karad, Maharashtra)</i>	Yoshinobu NAKANISHI <i>(Kanazawa, Ishikawa)</i>	Chunyan YAN <i>(Guangzhou Guangdong)</i>
Fen-Er CHEN <i>(Shanghai)</i>	Toshiaki KATADA <i>(Tokyo)</i>	Siriporn OKONOGI <i>(Chiang Mai)</i>	Xiao-Long YANG <i>(Chongqing)</i>
Zhe-Sheng CHEN <i>(Queens, NY)</i>	Gagan KAUSHAL <i>(Philadelphia, PA)</i>	Weisan PAN <i>(Shenyang, Liaoning)</i>	Yun YEN <i>(Duarte, CA)</i>
Zilin CHEN <i>(Wuhan, Hubei)</i>	Ibrahim S. KHATTAB <i>(Kuwait)</i>	Chan Hum PARK <i>(Eumseong)</i>	Yasuko YOKOTA <i>(Tokyo)</i>
Xiaolan CUI <i>(Beijing)</i>	Shiroh KISHIOKA <i>(Wakayama, Wakayama)</i>	Rakesh P. PATEL <i>(Mehsana, Gujarat)</i>	Takako YOKOZAWA <i>(Toyama, Toyama)</i>
Shaofeng DUAN <i>(Lawrence, KS)</i>	Robert Kam-Ming KO <i>(Hong Kong)</i>	Shivanand P. PUTHLI <i>(Mumbai, Maharashtra)</i>	Rongmin YU <i>(Guangzhou, Guangdong)</i>
Mohamed F. EL-MILIGI <i>(6th of October City)</i>	Nobuyuki KOBAYASHI <i>(Nagasaki, Nagasaki)</i>	Shafiqur RAHMAN <i>(Brookings, SD)</i>	Guangxi ZHAI <i>(Ji'nan, Shandong)</i>
Hao FANG <i>(Ji'nan, Shandong)</i>	Norihiro KOKUDO <i>(Tokyo, Japan)</i>	Adel SAKR <i>(Cairo)</i>	Liangren ZHANG <i>(Beijing)</i>
Marcus L. FORREST <i>(Lawrence, KS)</i>	Toshiro KONISHI <i>(Tokyo)</i>	Gary K. SCHWARTZ <i>(New York, NY)</i>	Lining ZHANG <i>(Ji'nan, Shandong)</i>
Takeshi FUKUSHIMA <i>(Funabashi, Chiba)</i>	Chun-Guang LI <i>(Melbourne)</i>	Yuemao SHEN <i>(Ji'nan, Shandong)</i>	Na ZHANG <i>(Ji'nan, Shandong)</i>
Harald HAMACHER <i>(Tübingen, Baden-Württemberg)</i>	Minyong LI <i>(Ji'nan, Shandong)</i>	Brahma N. SINGH <i>(New York, NY)</i>	Ruiwen ZHANG <i>(Houston, TX)</i>
Kenji HAMASE <i>(Fukuoka, Fukuoka)</i>	Xun LI <i>(Ji'nan, Shandong)</i>	Tianqiang SONG <i>(Tianjin)</i>	Xiu-Mei ZHANG <i>(Ji'nan, Shandong)</i>
Junqing HAN <i>(Ji'nan, Shandong)</i>	Jikai LIU <i>(Wuhan, Hubei)</i>	Sanjay K. SRIVASTAVA <i>(Abilene, TX)</i>	Yongxiang ZHANG <i>(Beijing)</i>
Xiaojiang HAO <i>(Kunming, Yunnan)</i>	Xinyong LIU <i>(Ji'nan, Shandong)</i>	Chandan M. THOMAS <i>(Bradenton, FL)</i>	Jian-hua ZHU <i>(Guangzhou, Guangdong)</i>
Kiyoshi HASEGAWA <i>(Tokyo)</i>	Yuxiu LIU <i>(Nanjing, Jiangsu)</i>	Li TONG <i>(Xining, Qinghai)</i>	
Waseem HASSAN <i>(Rio de Janeiro)</i>	Hongxiang LOU <i>(Jinan, Shandong)</i>	Murat TURKOGLU <i>(Istanbul)</i>	
Langchong HE <i>(Xi'an, Shaanxi)</i>	Xingyuan MA <i>(Shanghai)</i>	Hui WANG <i>(Shanghai)</i>	

(As of February 2019)

Original Article

- 244 - 247 **Suppressive effects of whey protein hydrolysate on sucroseinduced hyperglycemia in silkworms.**
Yasuhiko Matsumoto, Miki Takahashi, Masahiro Umehara, Masato Asano, Hiroko Maruki-Uchida, Minoru Morita, Kazuhisa Sekimizu
- 248 - 255 **1,2,3-Triazolyl ester of ketorolac (15K), a potent PAK1 blocker, inhibits both growth and metastasis of orthotopic human pancreatic cancer xenografts in mice.**
Rene Hennig, Alia Albawardi, Saeeda Almarzooqi, Shoja Haneefa, Edward Imbaraj, Nur Elena Zaaba, Abderrahim Nemmar, Sandeep Subramanya, Hiroshi Maruta, Thomas E. Adrian
- 256 - 260 **Effects of storage temperature, storage time, and Cary-Blair transport medium on the stability of the gut microbiota.**
Naoyoshi Nagata, Mari Tohya, Fumihiko Takeuchi, Wataru Suda, Suguru Nishijima, Mitsuru Ohsugi, Kohjiro Ueki, Tetsuro Tsujimoto, Tomoka Nakamura, Takashi Kawai, Tohru Miyoshi-Akiyama, Naomi Uemura, Masahira Hattori
- 261 - 267 ***Centella asiatica* (L.) extract attenuates inflammation and improve insulin sensitivity in a coculture of lipopolysaccharide (LPS)-induced 3T3-L1 adipocytes and RAW 264.7 macrophages.**
Siska Andrina Kusumastuti, Dwi Aris Agung Nugrahaningsih, Mae Sri Hartati Wahyuningsih
- 268 - 273 **Royal jelly regulates the proliferation of human dermal microvascular endothelial cells through the down-regulation of a photoaging-related microRNA.**
Yuya Kawano, Katsunari Makino, Masatoshi Jinnin, Soichiro Sawamura, Shuichi Shimada, Satoshi Fukushima, Hironobu Ihn
- 274 - 279 **Profile and predictors of hepatitis and HIV infection in patients on hemodialysis of Quetta, Pakistan.**
Ammara Lodhi, Ashif Sajjad, Khalid Mehmood, Ayesha Lodhi, Sabeena Rizwan, Ayesha Ubaid, Kulsoom Baloch, Sheikh Ahmed, Mohkam ud din, Zahid Mehmood
- 280 - 287 **Catheter tips are a possible resource for biological study on catheter failure.**
Toshiaki Takahashi, Takeo Minematsu, Ryoko Murayama, Gojiro Nakagami, Taketoshi Mori, Hiromi Sanada

Brief Report

- 288 - 293 **Characteristics of subcutaneous tissues at the site of insertion of peripheral infusion in patients undergoing paclitaxel and carboplatin chemotherapy.**
Ryoko Murayama, Maiko Oya, Mari Abe-Doi, Makoto Oe, Chieko Komiyama, Hiromi Sanada

CONTENTS

(Continued)

Case Report

- 294 - 296 **Pediatric case of Graham Little Piccardi Lassueur syndrome – A rare entity.**
*Ayan Basu, Dyuti Basu, Arpita Chattopadhyay, Rhik Sanyal, Mehebubar Rahman,
Rama Prosad Goswami*
- 297 - 298 **A case of overlap syndrome (scleroderma and polymyositis) associated with
the development of sudden chest pain due to myocardial damage.**
Akira Kaneko, Ikko Kajihara, Azusa Miyashita, Hironobu Ihn

Guide for Authors

Copyright

Suppressive effects of whey protein hydrolysate on sucrose-induced hyperglycemia in silkworms

Yasuhiko Matsumoto^{1,2}, Miki Takahashi^{2,3}, Masahiro Umehara⁴, Masato Asano⁴, Hiroko Maruki-Uchida⁴, Minoru Morita⁴, Kazuhisa Sekimizu^{2,3,*}

¹Department of Microbiology, Meiji Pharmaceutical University, Tokyo, Japan;

²Teikyo University Institute of Medical Mycology, Tokyo, Japan;

³Genome Pharmaceuticals Institute Co., Ltd., Tokyo, Japan;

⁴Health Science Research Center, Research and Development Institute, Morinaga and Company Limited, Kanagawa, Japan.

Summary Silkworms are useful for evaluating substances that suppress postprandial hyperglycemia by oral administration. In this study, orally administered whey protein hydrolysate (WPH), obtained by enzymatic treatment of whey protein, suppressed sucrose-induced hyperglycemia in silkworms in a dose-dependent manner. WPH also inhibited glucose-induced hyperglycemia in silkworms. These findings suggest that WPH contains a bioactive peptide that inhibits glucose uptake from the intestinal tract and thereby suppresses sucrose-induced hyperglycemia.

Keywords: Hyperglycemia, silkworm, sucrose, whey protein hydrolysate

1. Introduction

Sucrose is one of the main sweeteners added to various foods (1). Increased blood glucose levels due to excessive intake of sucrose induces the development of lifestyle-related diseases (2,3). Therefore, the development of strategies to suppress postprandial hyperglycemia induced by sucrose intake will contribute to the maintenance of human health (4).

Blood glucose levels are regulated at various stages by the functions of several organs: enzymatic decomposition of sucrose in the intestine, absorption from the intestine, distribution and metabolism in various organs, and excretion outside the body (5). Therefore, experiments to accurately evaluate active substances that suppress sucrose-induced hyperglycemia must be performed using whole animals.

We previously reported diabetic silkworm models for evaluating anti-diabetic agents such as human insulin, pioglitazone, and metformin (6-9). Moreover, we established a silkworm model to search for substances

that suppress sucrose-induced hyperglycemia (10-13). *Enterococcus faecalis* YM0831, a lactic acid bacteria strain that was identified using an *in vivo* silkworm evaluation system, suppresses sucrose-induced hyperglycemia in humans (14). Therefore, the *in vivo* silkworm evaluation system is useful for identifying candidate anti-diabetic drugs and foods that control blood glucose levels in humans.

Whey protein is a fermentation liquid obtained as a byproduct of yogurt or cheese production. In young adult females, whey protein suppresses sweetened beverage-induced hyperglycemia (15). In addition, whey protein hydrolysate (WPH), obtained by enzymatic treatment of whey protein, exhibits anti-oxidative properties and inhibits angiotensin-I-converting enzyme (16,17). The mechanism of action of whey protein against postprandial hyperglycemia, however, is unclear.

In this study, we demonstrated that WPH suppressed sucrose-induced hyperglycemia in silkworms. To our knowledge, this is the first study demonstrating that WPH suppresses postprandial hyperglycemia in an animal model.

2. Materials and Methods

2.1. Reagents

Whey protein and WPH, prepared by enzymatic

Released online in J-STAGE as advance publication October 14, 2019.

*Address correspondence to:

Dr. Kazuhisa Sekimizu, Teikyo University Institute of Medical Mycology, 359 Otsuka, Hachioji, Tokyo, 192-0395, Japan.

E-mail: sekimizu@main.teikyo-u.ac.jp

hydrolysis of whey protein, were purchased from Fonterra Japan (Tokyo, Japan). The protein content of the whey protein was 80% and that of the WPH was 83%. High-performance liquid chromatography (HPLC) grade acetonitrile (> 99.8%) and special grade trifluoroacetic acid (> 98.0%) were purchased from FUJIFILM Wako Pure Chemical Corporation (Osaka, Japan).

2.2. Size exclusion chromatography

Whey protein (10.0 mg) and WPH (9.6 mg) were suspended in ultrapure water (2.0 mL). The mixture was centrifuged (20,400g, 20°C, 10 min), and the supernatant was subjected to size exclusion chromatography using a TSKgel® G2000SW_{XL} HPLC column (300 × 7.8 mm i.d., particle size: 5 µm, Tosoh Corporation, Tokyo, Japan) with a TSKgel® SW_{XL} guard column (40 × 6.0 mm i.d., particle size: 7 µm, Tosoh Corporation). The analysis was performed with an HPLC system (autosampler: AS-2057, pump: PU-2080, column oven: CO-2065, PDA detector: MD-2018, JASCO Corporation, Tokyo, Japan). The mobile phase was acetonitrile/water/trifluoroacetic acid (25/75/0.1 v/v/v). The column oven temperature was set to 30°C and the flow rate was 0.6 mL/min. Absorbance at 280 nm was monitored. The data was analyzed using ChromNAV (version 1.18.04, JASCO Corporation).

2.3. Silkworm rearing conditions and sucrose tolerance test

Silkworms were reared as reported previously (6,18). Sucrose or glucose tolerance tests using the silkworms were performed according to a previous report (10). Briefly, test samples were mixed with artificial diet containing 10% glucose or 10% sucrose. The diet was fed to the silkworms for 1 h and the glucose level in the silkworm hemolymph was measured using a glucometer (Accu-Chek, Roche, Basel, Switzerland).

2.4. Statistical analysis

All experiments were performed at least twice. The significance of differences was calculated using a two-tailed Student's t-test. A p value of less than 0.05 was considered significant.

3. Results

3.1. Characterization of whey protein and WPH by size exclusion chromatography

We compared the size exclusion chromatography patterns between whey protein and WPH. Each sample was subjected to size exclusion chromatography. The

whey protein produced major peaks at elution times ranging from 11.5 to 13.5 min (Figure 1). The WPH, in contrast, did not have these two major peaks, and instead multiple peaks were observed at elution times ranging from 14 to 20 min (Figure 1). This finding suggests that the WPH comprised whey proteins digested into low molecular mass peptides.

3.2. Suppressive effect of WPH on sucrose-induced hyperglycemia in silkworms

When an artificial diet containing 10% sucrose is fed to silkworms for 1 h, the glucose level in the silkworm hemolymph increases to 300-400 mg/dL (10). In the present study, we investigated the effects of whey protein and WPH on the sucrose-induced hyperglycemia in silkworms. The blood glucose level was lower in silkworms fed the 10% sucrose diet supplemented with 10% WPH than in control silkworms (Figure 2). Supplementation with acarbose, an α -glycosidase inhibitor used as a positive control, also exhibited a suppressive effect (Figure 2). In contrast, when whey protein was added to the 10% sucrose diet, the blood glucose level of the silkworms did not decrease (Figure 2). We next examined the dose dependence of the inhibitory effect of WPH on sucrose-induced hyperglycemia in silkworms in a sucrose tolerance test. WPH in the range of 0-10% of the diet suppressed the sucrose-induced hyperglycemia in silkworms in a dose-dependent manner (Figure 3).

3.3. Suppressive effect of WPH on glucose-induced hyperglycemia in silkworms

To clarify the mechanism of the suppression of the

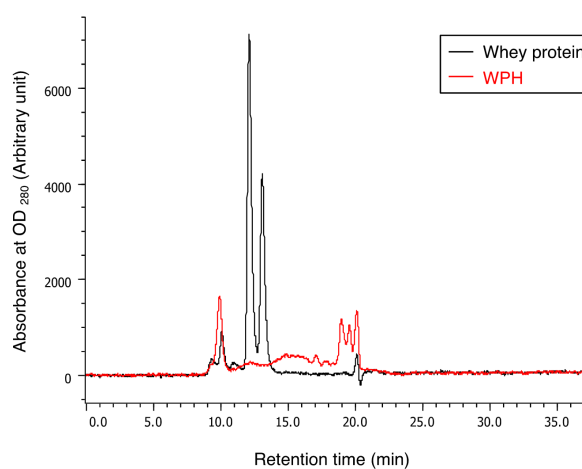


Figure 1. Molecular weight distribution by size exclusion chromatography of whey protein and whey protein hydrolysate. Whey protein (10.0 mg) and whey protein hydrolysate (WPH, 9.6 mg) were suspended in 2 mL ultrapure water. The suspensions were centrifuged, and the supernatant was subjected to size exclusion chromatography. Absorbance at 280 nm was monitored.

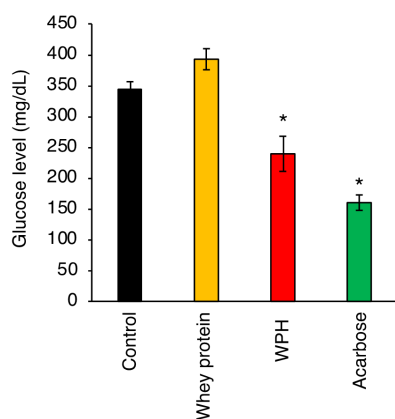


Figure 2. Effects of whey protein and whey protein hydrolysate on sucrose-induced hyperglycemia in silkworms. A 10% sucrose diet without sample (Control) or with 10% whey protein (Whey protein), whey protein hydrolysate (WPH), or 4% acarbose (Acarbose) was fed to silkworms for 1 h. After feeding, the blood sugar level of the silkworms was measured. Data represent mean \pm SEM. Statistically significant differences between control and other groups were evaluated using Student's *t*-test. * $p < 0.05$. $n = 7$ /group.

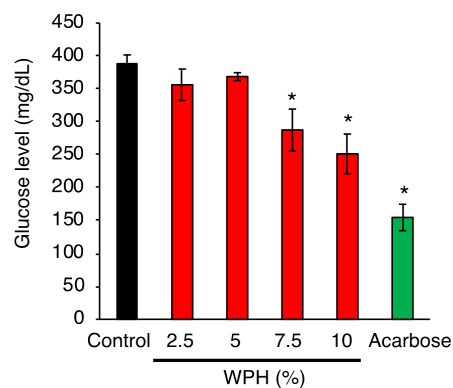


Figure 3. Dose dependence of the suppressive effect of whey protein hydrolysate on sucrose-induced hyperglycemia in silkworms. A 10% sucrose diet without sample (Control) and with 2.5, 5, 7.5, 10% whey protein hydrolysate (WPH) or 4% acarbose (Acarbose) was fed to silkworms for 1 h. After feeding, the blood sugar level of the silkworms was measured. Data represent mean \pm SEM. Statistically significant differences between control and other groups were evaluated using the Student's *t*-test. * $p < 0.05$. $n = 4-10$ /group.

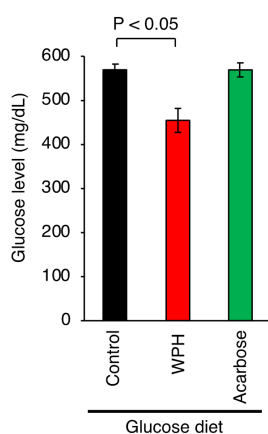


Figure 4. Suppressive effects of whey protein hydrolysate on glucose-induced hyperglycemia in silkworms. A 10% glucose diet without sample (Control) and with 7.5% whey protein hydrolysate (WPH) or 4% acarbose (Acarbose) was fed to silkworms for 1 h. After feeding, the blood sugar level of the silkworms was measured. Data represent mean \pm SEM. Statistically significant differences between the control and other groups were evaluated using the Student's *t*-test. $n = 7$ /group.

sucrose-induced hyperglycemia by WPH, we tested whether WPH also suppresses glucose-induced hyperglycemia. When artificial diet containing 10% glucose is fed to silkworms for 1 h, the glucose level in the silkworm hemolymph increases to 500 mg/dL or more (10). The increase in the blood glucose level of the silkworms is not suppressed by acarbose, an α -glycosidase inhibitor (10). The blood sugar level was lower in silkworms fed a 10% glucose diet containing 7.5% WPH than in the control silkworms (Figure 4). These findings indicate that WPH suppresses glucose-induced hyperglycemia.

4. Discussion

The findings of the present study demonstrated that WPH inhibited sucrose-induced hyperglycemia in an *in vivo* evaluation system using silkworms, whereas whey protein did not have the same effect. Further, WPH suppressed glucose-induced hyperglycemia. This finding indicates that the anti-hyperglycemic effect of WPH cannot be explained by the inhibition of α -glycosidase. Sucrose in the intestine is degraded to glucose and fructose by α -glycosidase, and these monosaccharides are transferred into the blood via sugar transporters on the intestinal cells. WPH may inhibit the activity of sugar transporters responsible for the uptake of monosaccharides from the intestine into the blood. Another possibility is that WPH promotes the uptake of monosaccharides into the organs from the bloodstream.

Whey protein has an inhibitory effect on sweetened beverage-induced hyperglycemia in young adult females (15). We demonstrated that whey protein did not suppress sucrose-induced hyperglycemia in silkworms. In humans, whey protein may be degraded to WPH by proteases in the stomach and small intestine. In silkworms, whey protein may not be fully degraded to active WPH. Otherwise WPH may have a different hypoglycemic effect compared to whey protein, because it is hydrolyzed by enzyme and may have special peptides.

In conclusion, WPH has the potential to suppress postprandial hyperglycemia, but inhibition of α -glycosidase does not explain the suppressive activity of WPH. We suggest that the use of WPH in combination with α -glycosidase inhibitors might prevent the onset of life-related diseases such as diabetes and obesity.

Acknowledgements

We thank Kana Hashimoto and Mari Maeda (Genome Pharmaceuticals Institute Co., Ltd, Tokyo, Japan) for technical assistance in rearing the silkworms. The project was supported by JSPS KAKENHI grant number JP15H05783 (Scientific Research (S) to KS), JSPS KAKENHI grant number JP17K08288 (Scientific Research (C) to YM), and the Supporting Industry Program by Ministry of Economy, Trade and Industry. The project was also supported by Genome Pharmaceuticals Institute Co., Ltd. (Tokyo, Japan).

References

1. Newens KJ, Walton J. A review of sugar consumption from nationally representative dietary surveys across the world. *J Hum Nutr Diet.* 2016; 29:225-240.
2. Johnson RJ, Nakagawa T, Sanchez-Lozada LG, Shafiu M, Sundaram S, Le M, Ishimoto T, Sautin YY, Lanasa MA. Sugar, uric acid, and the etiology of diabetes and obesity. *Diabetes.* 2013; 62:3307-3315.
3. Pereira MA. Sugar-sweetened and artificially-sweetened beverages in relation to obesity risk. *Adv Nutr.* 2014; 5:797-808.
4. Ochoa M, Lallès JP, Malbert CH, Val-Laillet D. Dietary sugars: their detection by the gut-brain axis and their peripheral and central effects in health and diseases. *Eur J Nutr.* 2015; 54:1-24.
5. Lewis AS, McCourt HJ, Ennis CN, Bell PM, Courtney CH, McKinley MC, Young IS, Hunter SJ. Comparison of 5% versus 15% sucrose intakes as part of a eucaloric diet in overweight and obese subjects: effects on insulin sensitivity, glucose metabolism, vascular compliance, body composition and lipid profile. A randomised controlled trial. *Metab Clin Exp.* 2013; 62:694-702.
6. Matsumoto Y, Sumiya E, Sugita T, Sekimizu K. An invertebrate hyperglycemic model for the identification of anti-diabetic drugs. *PLoS ONE.* 2011; 6:e18292.
7. Matsumoto Y, Ishii M, Ishii K, Miyaguchi W, Horie R, Inagaki Y, Hamamoto H, Tatematsu KI, Uchino K, Tamura T, Sezutsu H, Sekimizu K. Transgenic silkworms expressing human insulin receptors for evaluation of therapeutically active insulin receptor agonists. *Biochem Biophys Res Commun.* 2014; 455:159-164.
8. Matsumoto Y, Ishii M, Hayashi Y, Miyazaki S, Sugita T, Sumiya E, Sekimizu K. Diabetic silkworms for evaluation of therapeutically effective drugs against type II diabetes. *Sci Rep.* 2015; 5:10722.
9. Matsumoto Y, Sekimizu K. Evaluation of anti-diabetic drugs by using silkworm, *Bombyx mori*. *Drug Discov Ther.* 2016; 10:19-23.
10. Matsumoto Y, Ishii M, Sekimizu K. An *in vivo* invertebrate evaluation system for identifying substances that suppress sucrose-induced postprandial hyperglycemia. *Sci Rep.* 2016; 6:26354.
11. Ishii M, Matsumoto Y, Sekimizu K. Inhibitory effects of alpha-cyclodextrin and its derivative against sucrose-induced hyperglycemia in an *in vivo* evaluation system. *Drug Discov Ther.* 2018; 12:122-125.
12. Ishii M, Matsumoto Y, Sekimizu K. Bacterial polysaccharides inhibit sucrose-induced hyperglycemia in silkworms. *Drug Discov Ther.* 2018; 12:185-188.
13. Ishii M, Matsumoto Y, Katada T, Sekimizu K. Additive effects of Kothala himbutu (*Salacia reticulata*) extract and a lactic acid bacterium (*Enterococcus faecalis* YM0831) for suppression of sucrose-induced hyperglycemia in an *in vivo* silkworm evaluation system. *Drug Discov Ther.* 2019; 13:133-136.
14. Matsumoto Y, Ishii M, Hasegawa S, Sekimizu K. *Enterococcus faecalis* YM0831 suppresses sucrose-induced hyperglycemia in a silkworm model and in humans. *Commun Biol.* 2019; 2:157.
15. Zafar TA, Waslien C, AlRaefaei A, Alrashidi N, Al Mahmoud E. Whey protein sweetened beverages reduce glycemic and appetite responses and food intake in young females. *Nutr Res.* 2013; 33:303-310.
16. Jiang B, Na J, Wang L, Li D, Liu C, Feng Z. Separation and enrichment of antioxidant peptides from whey protein isolate hydrolysate by aqueous two-phase extraction and aqueous two-phase flotation. *Foods.* 2019; 8:34.
17. Guo Y, Jiang X, Xiong B, Zhang T, Zeng X, Wu Z, Sun Y, Pan D. Production and transepithelial transportation of angiotensin-I-converting enzyme (ACE)-inhibitory peptides from whey protein hydrolyzed by immobilized *Lactobacillus helveticus* proteinase. *J Dairy Sci.* 2019; 102:961-975.
18. Matsumoto Y, Sekimizu K. Silkworm as an experimental animal to research for fungal infections. *Microbiol Immunol.* 2019; 63:41-50.

(Received September 21, 2019; Accepted September 29, 2019)

1,2,3-Triazolyl ester of ketorolac (15K), a potent PAK1 blocker, inhibits both growth and metastasis of orthotopic human pancreatic cancer xenografts in mice

Rene Hennig¹, Alia Albawardi², Saeeda Almarzooqi², Shoja Haneefa³, Edward Imbaraj³, Nur Elena Zaaba³, Abderrahim Nemmar³, Sandeep Subramanya³, Hiroshi Maruta^{4,*}, Thomas E. Adrian^{3,5,*}

¹Department of General and Visceral Surgery, Freudenstadt University Hospital, Freudenstadt, Germany;

²Department of Pathology, United Arab Emirates University, Al Ain, UAE;

³Department of Physiology, United Arab Emirates University, Al Ain, UAE;

⁴PAK Research Center, Melbourne, Australia;

⁵Mohammed Bin Rashid University of Medicine and Health Sciences, Dubai, UAE.

Summary

More than 90% of human pancreatic cancers carry the oncogenic mutant of Ki-RAS and their growth depends on its downstream kinase PAK1, mainly because PAK1 blocks the apoptosis of cancer cells selectively. We developed a highly cell-permeable PAK1-blocker called 15K from an old pain-killer (ketorolac), that is shown here to inhibit the growth of three pancreatic cancer cell lines with IC₅₀ values ranging 41-88 nM *in vitro*. The anti-cancer effect of 15K was further investigated in an orthotopic xenograft model with gemcitabine (GEM)-resistant human pancreatic cancer cell lines (AsPC-1 and BxPC-3) expressing luciferase in athymic mice. During 4 weeks, 15K blocks total burden (growth) of both AsPC-1 and BxPC-3 tumors (measured as radiance/sec) with the IC₅₀ below daily dose of 0.1 mg/kg, *i.p.* In a similar manner 15K reduced both their invasion and metastases as well, while it had no effect on either body weight or hematological parameters even at 5 mg/kg/day. To the best of our knowledge, 15K is so far the most potent among synthetic PAK1-blockers *in vivo*, and could be potentially useful for therapy of GEM-resistant cancers.

Keywords: 1,2,3-Triazolyl ester of ketorolac (15K), PAK1, pancreatic cancer, gemcitabine-resistance, xenografts

1. Introduction

The oncogenic/ageing kinase PAK1 (RAC/CDC42-activated kinase 1) is abnormally activated by the oncogenic RAS mutants, and essential for both growth and metastasis of RAS-transformed malignant cells

(RAS cancers) such as those seen in more than 90% of pancreatic cancers, 50% of colon cancers and 30% of lung cancers in humans (1). Moreover, only 10% of human pancreatic cancers are sensitive to gemcitabine (GEM), and the rest is highly resistant to GEM treatment. Interestingly, a major reason for GEM-resistance is GEM-induced abnormal activation of PAK1 (2). Thus, potent PAK1-blockers could effectively overcome their GEM-resistance. Indeed, the combination of AG879 (inhibitor of a Tyr-kinase ETK, 20 mg/kg) and PP1 (inhibitor of another Tyr-kinase Src, 20 mg/kg) that block the activation of PAK1 strongly suppresses almost completely the growth of human pancreatic cancer xenografts in mice (3). However, both AG879 and PP1 are water-insoluble, and their low-bioavailability renders them clinically unfeasible. Thus, we have been developing a series of water-soluble

Released online in J-STAGE as advance publication October 27, 2019.

§These authors contributed equally to this work.

*Address correspondence to:

Dr. Hiroshi Maruta, PAK Research Center, Melbourne, Australia.

E-mail: maruta20420@yahoo.co.jp

Dr. Thomas E. Adrian, Mohammed Bin Rashid University of Medicine and Health Sciences, Dubai, UAE.

E-mail: thomas.adrian@mbru.ac.ae

and highly cell permeable PAK1 blockers which are potentially useful for clinical use.

Recently, we synthesized 1,2,3-triazolyl ester of an old pain-killer (ketorolac) *via* Click Chemistry which is both highly cell-permeable and water-soluble (4). Ketorolac is a synthetic COOH-bearing "racemic" pain-killer that inhibits directly COX-2 in S-form (5). However, recently R-form of ketorolac was found to inhibit RAC/CDC42 directly, therefore blocking the down-stream kinase PAK1 (6). Unfortunately, due to its COOH moiety that hampers the free penetration through the negatively charged phospholipid-bilayers of target cell membranes, its cell-permeability *per se* is very poor (anti-cancer IC₅₀ around 13 μM). Thus, *via* Click Chemistry, we have esterized ketorolac with the water-soluble 1,2,3-triazolyl alcohol, making 15K which is over 500 times more cell-permeable than ketorolac, and inhibits the growth of RAS-transformed lung cancer cell line (A549) with IC₅₀ around 24 nM. Furthermore, 15K was found to extend the healthy lifespan of *C. elegans* 15-30% at 50 nM (depending on the temperature) and boost its heat-resistance over 9 times (7). Thus, it is strongly suggested that 15K, a potent anti-cancer (anti-PAK1/anti-COX-2) and anti-aging drug, could overcome the GEM-resistance of human pancreatic cancers without any serious side-effects.

In the present study we examined the effect of 15K *in vitro* and on both growth and metastasis of GEM-resistant human pancreatic cancers orthotopically grafted in athymic mice.

2. Materials and Methods

2.1. Chemicals

1,2,3-Triazolyl ester of ketorolac (15K) was chemically synthesized from the racemic mixture of ketorolac *via* Click Chemistry as previously described in detail (4). A stock solution of 15K of 10 mg/mL in DMSO was made. Fresh daily dilutions were made at concentrations of 10, 100 and 500 μg/mL for the low, medium and high doses of drug for daily injection, respectively.

2.2. Cell lines and culture

Firefly luciferase stably expressing human pancreatic adenocarcinoma cell lines, including AsPC-1 (pLL3.7-luc transfected; AsPC-1/CMV-Luc) and BxPC-3 (pMSCV-luc transfected; BxPC-3-Luc#2) cells, were obtained from Takashi Murakami, Faculty of Medicine, Saitama Medical University 38 Moro-Hongo, Moroyama, Saitama 350-0495, Japan. AsPC-1 cells are poorly differentiated and carry a homozygous KRAS mutation in codon12: GGT(Gly)>GAT(Asp) (8). BxPC-3 cells have a moderate degree of differentiation (9), have no KRAS mutation (8), but have high expression

of cancer stem cell markers (10). Both of these cell lines are relatively resistant to gemcitabine and become more resistant following treatment with the drug (11-13). In previous studies IC₅₀ of GEM against BxPC-3 have been reported as ~100 nM and against AsPC-1 cells ~200-500 nM (13,14). Parent AsPC-1 and BxPC-3 cells were purchased from the American Type Culture Collection (Manassas VA), while S2013 cells were a generous gift from Dr. Takeshi Iwamura (Miyazaki Medical College, Japan). All Human pancreatic cancer cell lines were cultured in RPMI 1640 medium (Gibco) supplemented with L-glutamine and 10% fetal bovine serum (Sigma) as described previously (14).

2.3. Monitoring the cell viability of pancreatic cancer cell lines *in vitro* under 15K treatment

The cells were regularly seeded into 75-cm² flasks with media changes every second or third day. For experiments, cells were grown to 70% confluence, digested with trypsin-EDTA, and plated in 24-well plates and incubated at 37°C for 24 h with 10% fetal calf serum, allowing cells to adhere to the substratum. After cultured in a serum-free medium for another 24 h, they were treated with 15K at different concentrations for 72 h. RAS-transformed cells such as the majority of pancreatic cancer cells need no serum growth factor for their growth *per se*, as they produce/secrete the essential autocrine growth factors that activate PAK1. At the end of each time period, the cells were trypsinized to produce a single cell suspension, and the viable cell number, determined by trypan blue exclusion, in each well was counted using an improved Neubauer chamber.

2.4. Orthotropic xenografts of human pancreatic cancers in mice

For cancer xenografts, 12-16 week-old athymic NMRI nude mice (nu/nu, Charles River, Suizfeld, Germany) were bred in the UAEU animal facility. Forty 40 female mice were used for the experiment with AsPC-1 cell transplants and 40 male animals for the BxPC-3 transplants.

The mice were housed in micro-isolator cages in a filtered-air laminar flow cabinet (EuroBioConcept, Paris, France), handled under aseptic conditions and fed with autoclaved laboratory rodent food pellets. The animal protocol was approved by the Institutional Animal Care and Use Committee and all procedures were conducted to conform with Institutional Guidelines that are in compliance with College of Medicine & Health Sciences, National and International Laws and Policies (EEC Council Directive 86/609, OJ L 358, 1, 12th December 1987; and NIH Guide for Care and Use of Laboratory Animals, NIH Publication No. 85-23, 1985). Animal weight was recorded weekly.

Transplants were performed as previously described in detail (15). For surgery, mice were anesthetized intraperitoneally with 0.05 mL of a mixture of 0.4 mL of ketamine (Fort Dodge Animal Health, Fort Dodge, IO), 0.1 mL of xylazine (Phoenix Scientific, Inc., St. Joseph, MO), and 0.5 mL of NaCl. The abdomen was sterilized with alcohol pads and a 0.5-cm midline incision was performed. The abdominal wall was wrapped with wet gauze. After pulling the stomach on the surface, the pancreas was then carefully exposed and tumor cells (5×10^5 in 10 μ L of DMEM) were injected into the duodenal lobe using a Monoject 200 27-gauge x 1/2 in. polypropylene hub hypodermic needle (Kendall, Mansfield, MA) and a 50- μ L sterile glass syringe (Hamilton Company, Reno, NV). Female mice received transplants of AsPC-1 cells and male mice received BxPC-3 transplants. The needle was kept in place for 30 seconds and then carefully withdrawn and the injection sealed with a dry cotton tip to prevent leakage from the injection site. After the stomach and pancreas were returned to the peritoneal cavity, the incision was closed in two layers with vicryl-coated Rapide sutures 4-0 (Ethicon, Inc., Somerville, NJ). The animals were kept under a heating lamp and once they were ambulatory, they were returned to the laminar flow cabinet. The mice were kept in a sterile environment throughout the procedure.

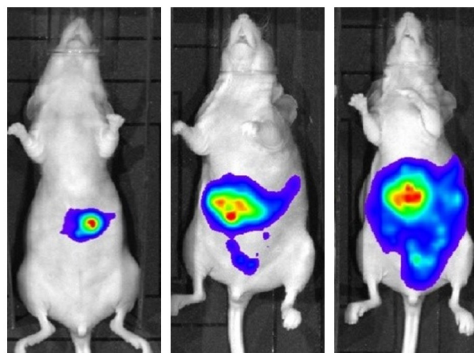
2.5. 15K therapy *in vivo*

One day after surgery, the male and female mice were each randomized into four groups of ten mice: Four days after transplant treatment began. Group I (Control) received daily *i.p.* injection of 0.9% NaCl solution at 10 μ L/gram body weight. Groups 2, 3 and 4 received 15K at doses of 100 μ g, 1 mg, and 5 mg/kg/day, respectively (10 μ L/gram of each of the fresh dilutions mentioned above).

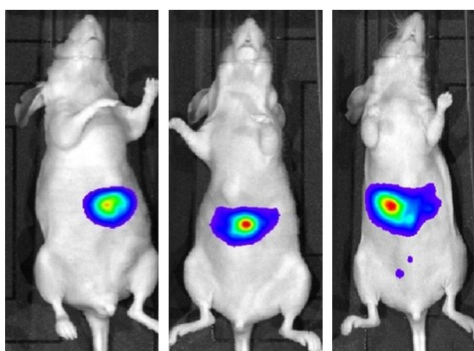
2.6. Measurement of tumor burden (growth) in mice using the IVIS Spectrum animal imaging system

Mice were anesthetized using inhaled isoflurane, then injected intraperitoneally with 3 mg of luciferin in 100 μ L PBS. After 10 minutes, to reach a pre-established luciferase signal plateau, three mice were placed on their backs on the stage of the Lumina II imaging system (Perkin-Elmer), where anesthesia was maintained by the onboard isoflurane system. Radiance of the image is expressed as photons/second. White light and bioluminescence images were captured using the Living Image software with auto exposure, binning factor 8, field of view 12.5 cm, subject height 1.5 cm, F-stop 1 (16). After imaging the mice were removed from the inhaled anesthetic and allowed to recover. Animals were imaged once per week for four weeks prior to euthanasia. For detail of imaging the

Control mouse



15K-treated mouse



2 W

3 W

4 W

Figure 1. Imaging the luciferase-labeled cancer xenografts in mice (control vs 15K-treated). Top: an AsPC-1-bearing mouse (control); at 2, 3 and 4 weeks, from left to right. Bottom: an AsPC-1-bearing mouse treated with 15K (5 mg/kg); at 2, 3, and 4 weeks, from left to right. 15K clearly suppresses both growth and metastasis of the GEM-resistant pancreatic cancer during 3-4 weeks after the graft.

luciferase-labeled cancer xenografts in mice (control vs 15K-treated), see Figure 1.

2.7. Autopsy and histological analysis

Animals were anesthetized with ketamine/xylazine as described above for surgery. Blood was taken from the vena cava for hematological analysis and peritoneal organs and heart and lungs removed for histological analysis.

Tissues from autopsy were fixed in 10% formalin, dehydrated in increasing concentrations of ethanol, cleared with xylene and embedded in paraffin (Thermo Shandon Ltd, Cheshire, UK). 3-5 μ m sections were prepared from the paraffin blocks using Shandon Finesse 325 microtome (Thermo Scientific Ltd., Cheshire, UK) and stained with hematoxylin and eosin (Thermo Shandon Ltd., Cheshire, UK), dehydrated in ascending concentrations of ethanol, cleared in xylene and mounted in DPX (Sigma Aldrich Steinheim, Germany). Histologic evaluation was performed under light microscopy.

2.8. Statistical analysis

The effects of 15K on growth of AsPC-1 and BxPC-3 tumors in athymic mice, measured as total flux (photons/sec) was analysed by two-way analysis of variance with drug dose and time as the variables and with Bonferroni post-hoc tests for the different time points. Statistical analysis of the occurrence of metastases was carried out using Fisher's exact test. Data analysis was performed using SPSS software (IBM).

3. Results

3.1. Effects of 15K on the growth of cultured human pancreatic cancer cells

Addition of 15K to the culture media caused a concentration-dependent decrease in viable cell number in all three GEM-resistant cancer cell lines (see Figure

2). The potency of 15K was greater in AsPC-1 and S2013 cells compared with that in BxPC-3 cells as judged by the IC_{50} for 15K in these cell lines (AsPC-1: 41 nM; BxPC-3: 88 nM; and S2013: 52 nM).

3.2. Anti-pancreatic cancer activity of 15K in orthotopically transplanted pancreatic cancers in athymic mice

Administration of 15K caused statistically significant, dose-responsive inhibition of total tumor burden (growth) in animals with either AsPC-1 (ANOVA: $p < 0.0001$, Dose $F = 8.78$, Df = 3; Time $F = 28.4$, Df = 3; Interaction $F = 4.28$, Df = 9) or BxPC-3 (ANOVA: $p < 0.0001$, Dose $F = 11.73$, Df = 3; Time $F = 19.30$, Df = 3; Interaction $F = 6.35$, Df = 9) orthotopic transplants (see Figure 3).

During 4 weeks, 15K had reduced total burden of AsPC-1 tumors by 53%, 69% and 85% with daily doses

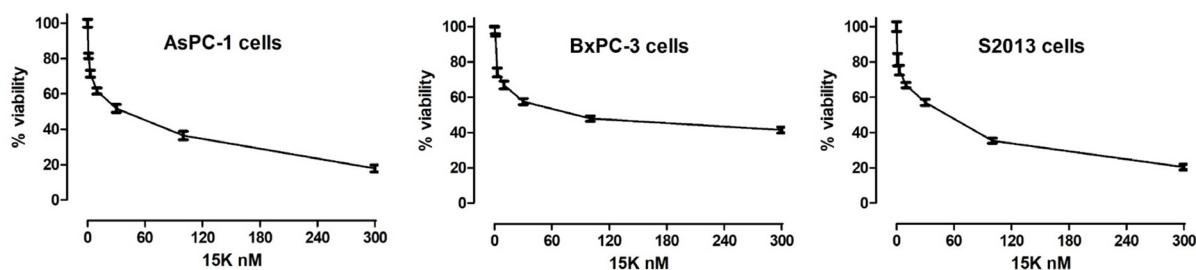


Figure 2. Effect of 15K on the growth/viability of human pancreatic cancer cell lines. **Left:** AsPC-1; **Middle:** BxPC-3; and **Right:** S2013. Each cell line was treated with 15K in serum free conditions at given concentrations for 72 h, and its viability was monitored by counting viable cell number. Results are expressed as percentage of control untreated cells.

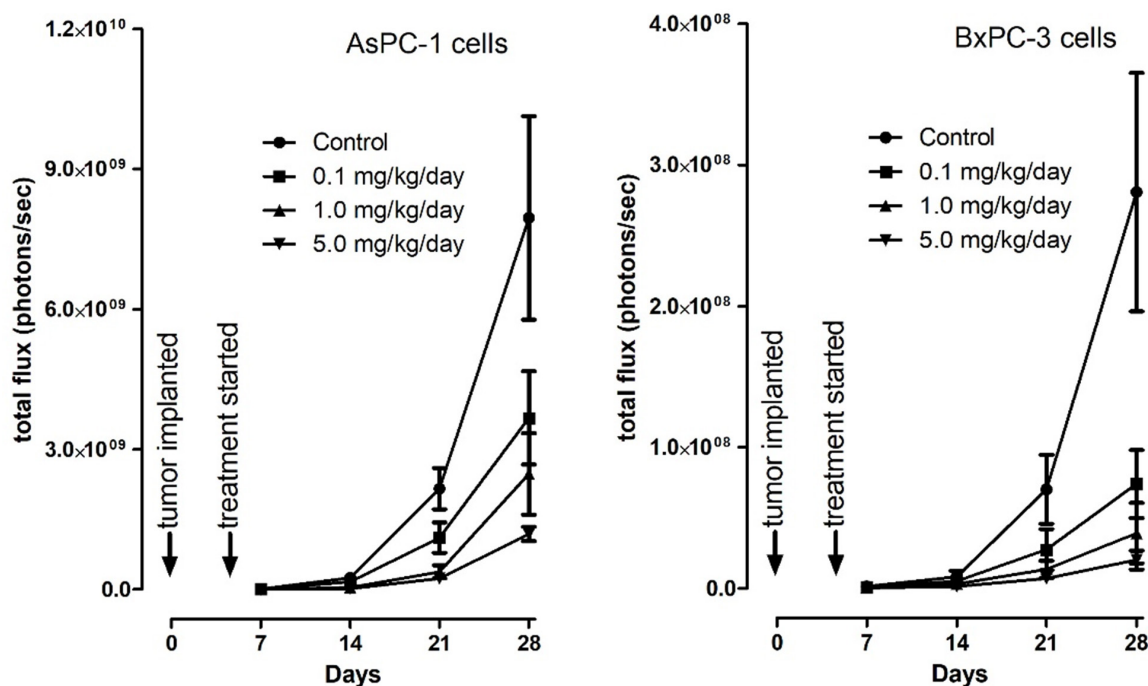


Figure 3. Effect of 15K on total tumor burden of GEM-resistant human pancreatic cancer xenograft in mice. **Left:** Female mice with AsPC-1 xenografts; **Right:** male mice with BxPC-3 xenografts. Total tumor burden was measured by bioluminescence (photons/sec) at weekly intervals after transplant.

Table 1. Number of female mice with AsPC-1 cancer xenografts showing tissue tumor invasion or metastases. Table shows numbers of animals and % in parentheses

Groups	Control, 0 mg/kg/day	15K, 0.1 mg/kg/day	15K, 1 mg/kg/day	15K, 5 mg/kg/day	Significance
Number of Mice	10	10	8	10	
Pancreas	10 (100%)	10 (100%)	6 (75%)	5 (50%)	NS
Abdominal Wall	8 (80%)	8 (80%)	4 (50%)	4 (40%)	NS
Esophagus	6 (60%)	3 (30%)	1 (12.5%)	0 (0%)	$P < 0.05$
Stomach	9 (90%)	3 (30%)	4 (50%)	3 (30%)	NS
Small Intestine	8 (80%)	8 (80%)	5 (62.5%)	4 (40%)	NS
Colon	0 (0%)	1 (10%)	1 (12.5%)	0 (0%)	NS
Liver	9 (90%)	6 (60%)	0 (0%)	1 (10%)	$P < 0.01$
Spleen	3 (30%)	2 (20%)	1 (12.5%)	0 (0%)	NS
Kidney	7 (70%)	1 (10%)	1 (12.5%)	1 (10%)	NS
Lung	2 (20%)	4 (40%)	1 (12.5%)	0 (0%)	NS
Lymph Nodes or LVI	9 (90%)	7 (70%)	7 (87.5%)	3 (30%)	NS
Peritoneum	10 (100%)	8 (80%)	6 (75%)	4 (40%)	NS

Table 2. Number of male mice with BxPC-3 cancer xenografts showing tissue tumor invasion or metastases. Table shows numbers of animals and % in parentheses

Groups	Control, 0 mg/kg/day	15K, 0.1 mg/kg/day	15K, 1 mg/kg/day	15K, 5 mg/kg/day	Significance
Number of Mice	8	10	9	8	
Pancreas	8 (100%)	9 (90%)	4 (44.4%)	2 (25%)	NS
Abdominal Wall	8 (100%)	4 (40%)	4 (44.4%)	2 (25%)	NS
Esophagus	4 (50%)	2 (20%)	2 (22.2%)	0 (0%)	NS
Stomach	8 (100%)	6 (60%)	4 (44.4%)	2 (25%)	NS
Small Intestine	3 (37.5%)	3 (30%)	1 (11.1%)	2 (25%)	NS
Liver	5 (62.5%)	1 (10%)	1 (11.1%)	0 (0%)	$P < 0.05$
Spleen	2 (25%)	0 (0%)	0 (0%)	0 (0%)	NS
Kidney	2 (25%)	3 (30%)	2 (22.2%)	0 (0%)	NS
Heart	0 (0%)	1 (10%)	0 (0%)	0 (0%)	NS
Lymph Nodes or LVI	5 (62.5%)	4 (40%)	1 (11.1%)	1 (12.5%)	NS
Peritoneal Invasion	4 (50%)	2 (20%)	3 (33.3%)	0 (0%)	NS

of 0.1, 1 and 5 mg/kg, *i.p.*, respectively (see Figure 1 and Figure 3, left, all $p < 0.001$). Similarly, with the same corresponding doses, 15K had reduced total burden of BxPC-3 tumors by 74%, 86% and 93%, respectively (see Figure 3, right, all $p < 0.001$). Thus, in both cases, the *in vivo* IC₅₀ of 15K against the growth of these human pancreatic cancers was below 0.1 mg/kg/day.

3.3. Effect of 15K on both tumor invasion and metastasis

The results of histological analysis showing the presence of tumor cells in the pancreas and other tissues of AspC-1 and BxPC-3 transplanted animals are shown in Tables 1 and 2, respectively. Tumor burden observed grossly and microscopic was larger in the AsPC-1 cancer xenografts mice in comparison to those seen in the BxPC-3 cancer xenografts mice. In the majority of the control animals, with both cell lines, the pancreatic tumor had invaded into the serosal surface of the stomach and/or the small intestine, as well as the abdominal wall adjacent to the laparotomy scar. The latter invasion was presumably triggered by the growth factor responses from the healing tissue. There is a possibility that seeding occurred during the surgical

procedure in some animals, but no leakage was apparent from the injection site. Indeed, a macroscopically well-defined bubble was evident in the duodenal lobe of the pancreas of all transplanted animals. Imaging immediately after transplantation would have revealed any leakage, this was intended by unfortunately could not be carried out because the IVIS imaging system was not working at that time.

AsPC-1 Cancer Xenografts: All female mice with AsPC-1 cancer xenografts in the control group had tumor in the pancreas and peritoneum. The majority had tumor present in organs adjacent to the pancreas. The serosal surface +/- variable thickness of wall was involved in stomach (9/10), duodenum/small intestine (8/10) and esophagus (6/10). Tumor was present in 7/10 control mice in the peri-renal adipose tissue in the form of tumor nodules without invasion of the renal or adrenal parenchyma except for one case that had parenchymal invasion. Metastasis was present in the liver (9/10), pelvic lymph nodes (5/10), peri-tumoral lymph nodes (4/10), spleen (3/10), and lung (2/10) as well, but no tumor was detected in the uterus or ovaries in the control or treated mice. Lymph-vascular invasion and/or lymph node metastasis was present in 9/10 (90%) of AsPC-1 control cases. The frequency decreased from

70% to 30% with increasing dose of 15K. The tumor was detected in the pancreas, peritoneum, stomach and adjacent small intestine and esophagus with a decreased frequency as the dose of 15K increased in both the AsPC-1 (Table 1), however this reduction only reached statistical significance in the liver and esophagus. Two animals with AsPC-1 tumors had lung micro-metastases. In two animals of the AsPC-1, 5 mg/kg group, no tumor was detected in any organ including the pancreas and the adjacent peritoneal/adipose tissue or stomach/duodenum or the surgical scar. However, in one case, tumor mass was detected around the sternum. In the other mouse, no tumor was detected in any organ. The histological observations were confirmed by the imaging which showed lack of tumor burden in these cases. This could reflect the effect of high dose 15K in these animals. In three cases from this 15K-treated group where tumor was no longer seen in the pancreas, it was detected in adjacent tissue including stomach, duodenum or peritoneum.

BxPC-3 Cancer Xenografts: All male mice with BxPC-3 cancer xenografts in the control group had tumor in the pancreas stomach and abdominal wall. Tumor was present in small intestine (37.5%), esophagus (50%), liver (62.5%), spleen (25%), and surface of kidney (25%). Peritoneal tumor nodules were present in 50% of the control group. Tumor detected in the pancreas decreased in frequency from 90% in the 0.1 mg/kg to 44% and 25% in the 1 and 5 mg/kg groups, respectively. Similarly, there was a reduction in tumors detected in the abdominal wall and stomach from 40% and 60% in the 0.1 mg group to 25% and 25% in the 5 mg/kg group, respectively.

Tumor was detected in the spleen of 20% of untreated animals but was not detected in the spleen in any of the treated animals. Tumor was present in the liver in 50% of untreated animals and this decreased frequency of 10%, 10% and 0% as the dose of 15K increased.

Lymph-vascular invasion and/or lymph node metastasis was detected in 5/8 (62.5%) of BxPC-3 control cases. The frequency decreased from 40% to 12.5% with increasing dose of 15K. No tumor metastasis was found in either testis, colon or heart of the control group. Tumor detected in the pancreas, peritoneum, liver, stomach and adjacent small intestine, esophagus, kidney with a decreased frequency as the dose of 15K increased in both the BxPC-3 mice (Table 2), however this reduction only reached statistical significance in the liver.

Tumor presence in liver and kidney with both cell lines was mostly found on the surface of these tissues, suggestive of peritoneal seeding rather than vascular invasion. Indeed, nine of the AsPC-1 group and four of the BxPC-3 group had peritoneal metastases, supporting tumor seeding through this route. Numbers of animals with local invasion and metastatic spread were lower

in the treated groups in a dose-dependent pattern and generally tumor volumes were clearly lower in treated animals as reflected in the total tumor burden. One animal in the high dose AsPC-1 group and four animals in the high dose BxPC-3 group were tumor-free at autopsy.

3.4. No effect of 15K on body weight, and hematological parameters

The tested doses of 15K on mice, up to 5 mg/kg/day, were well-tolerated as evidenced by the lack of any side effect on either body weight throughout the experiment or hematological parameters measured at the time of euthanasia. Body weights measured at weekly intervals (see Figure S1, <http://www.ddtjournal.com/action/getSupplementalData.php?ID=47>). There were no significant changes in haemoglobin, red cell counts, white cell counts or platelet counts between the two groups (see Figure S2, <http://www.ddtjournal.com/action/getSupplementalData.php?ID=47>). Hematocrit, mean corpuscular volume, mean corpuscular hemoglobin, and mean corpuscular haemoglobin concentration were also no different between the groups (data not shown).

4. Discussion

First of all, orthotopic graft of luciferase-expressing cancer cell lines on pancreas was quite helpful for non-invasive (luminescence-based) weekly quantification of the cancer mass growth or burden. The main reason why we have chosen the orthotopic graft (instead of technically far easier subcutaneous graft) of these cancers is that the latter approach prevents pancreatic cancers from significant metastases. Injection of cancer cells into tail vein was not our choice for metastasis model, simply because it is very far from human conditions. Nevertheless, we managed to confirm the extremely potent anti-mitotic and anti-metastatic property of 15K *in vivo* (against xenograft of human GEM-resistant pancreatic cancers in mice).

In the past, several distinct anti-cancer drugs including a few PAK1 inhibitors have been shown to overcome the GEM-resistance of human pancreatic cancers *in vivo*. For example, frondoside A (FRA) from a sea cucumber, that directly inhibits PAK1 with IC₅₀ around 1 μM (17), inhibits the growth of GEM-resistant human pancreatic cancer cells (AsPC-1, S2013, MiaPaCa2) in culture with the same IC₅₀. Furthermore, frondoside A inhibits the growth of pancreatic cancer xenografts of AsPC-1 and S2013 cells in mice with an IC₅₀ below 100 μg/kg/day (18). Another natural PAK1-blocker called triptolide or its prodrug (phosphorylated derivative) called minnelide inhibited the growth of GEM-resistant human pancreatic cancer xenografts in mice with the IC₅₀ around 0.3 mg/kg/day (19).

Among the synthetic PAK1-blockers, YM155 has been the most potent, suppressing survivin expression by blocking PAK1 signalling, but inhibits the growth of GEM-resistant human pancreatic cancer *in vivo* with IC₅₀ around 10 mg/kg/day (20). Thus, to the best of our knowledge, so far 15K appears to be among the most potent PAK1-blockers that suppress both growth and metastasis of GEM-resistant human pancreatic cancers *in vivo* without apparent side effects. Interestingly, among these potent PAK1-blockers, 15K is able to extend the healthy lifespan of *C. elegans* at 50 nM (7), while triptolide needs over 1000 times higher concentrations (around 140 μM) to show a similar lifespan extending effect (21). Moreover, 15K has a great advantage in the mass production for clinical use over natural PAK1-blockers, because its starting material (ketorolac) is a generic synthetic pain-killer developed and sold more than three decades ago (4,5). Thus, we look forward to commencing its clinical trials for GEM-resistant pancreatic cancers shortly.

Finally, it is worth noting that the "brand-new" role of BETs (bromodomain and external domain proteins) was recently identified. BETs are responsible for expression of both the receptor PD-1 in T-cells and its ligand PD-L1 in cancer cells *via* β-catenin-MYC pathway (22), which eventually destroys our "immune-surveillance" of cancers. Furthermore, a few years ago, a series of 1,2,3-triazol compounds have been found to inhibit BETs (23). Since 15K is also among 1,2,3-triazol compounds, it is most likely that 15K suppresses both PD-1 and PD-L1 by blocking not only PAK1 but also BETs, both of which are essential for the activation of the oncogenic β-catenin-MYC pathway. Thus, 15K could be a more effective (safer and less expensive as well) therapeutic than the current monoclonal-based immune (check-point) therapeutics which have never worked for the treatment of brain tumors and pancreatic cancers (24).

Acknowledgements

We are very grateful to Dr. Yoshihiro Uto at Tokushima University for his kindly mass production of 15K. This study was supported in part by a research grants from the Al Jalila Foundation (AJF2018006) and Mohammed Bin Rashid University (CM-RG2019-01).

References

- Maruta H, Ahn MR. From bench (laboratory) to bed (hospital/home): How to explore natural and synthetic PAK1-blockers/Longevity-promoters for cancer therapy, *Eur J Med Chem.* 2017; 142:229-243.
- Jagadeeshan S, Venkatraman G, Rayala SK. Targeting p21 activated kinase 1 (Pak1) to PAKup pancreatic cancer. *Expert Opin Ther Targets.* 2016; 20:1283-1285.
- Hirokawa Y, Levitzki A, Lessene G, Baell J, Xiao Y, Zhu H, Maruta H. Signal therapy of human pancreatic cancer and NF1-deficient breast cancer xenograft in mice by a combination of PP1 and GL-2003, anti-PAK1 drugs (Tyrosine kinase inhibitors). *Cancer Lett.* 2007; 245:242-251.
- Nguyen BCQ, Takahashi H, Uto Y, Shahinozzaman MD, Tawata S, Maruta H. 1,2,3-Triazolyl ester of Ketorolac: A "click chemistry"-based highly potent PAK1-blocking cancer-killer. *Eur J Med Chem.* 2017; 126:270-276.
- Vit JP, Ohara PT, Tien DA, Fike JR, Eikmeier L, Beitz A, Wilcox GL, Jasmin L. The analgesic effect of low dose focal irradiation in a mouse model of bone cancer is associated with spinal changes in neuro-mediators of nociception. *Pain.* 2006; 120:188-201.
- Guo Y, Kenney Jr SR, Muller CY, Adams S, Rutledge T, Romero E, Murray-Krezan C, Prekeris R, Sklar LA, Hudson LG, Wandinger-Ness A. R-ketorolac targets Cdc42 and Rac1 and alters ovarian cancer cell behaviors critical for invasion and metastasis. *Mol Cancer Ther.* 2015; 14:2215-2227.
- Nguyen BC, Kim SA, Won SM, Park SK, Uto Y, Maruta H. 1,2,3-Triazolyl ester of ketorolac (15K): Boosting both heat-endurance and lifespan of *C. elegans* by down-regulating PAK1 at nM levels. *Drug Discov Ther.* 2018; 12:92-96.
- Deer EL, Gonzalez-Hernandez J, Coursen JD, Shea JE, Ngatia J, Scaife CL, Firpo MA, Mulvihill SJ. Phenotype and genotype of pancreatic cancer cell lines. *Pancreas.* 2010; 39:425-435.
- Tan MH, Nowak NJ, Loor R, Ochi H, Sandberg AA, Lopez C, Pickren JW, Berjian R, Douglass HO Jr, Chu TM. Characterization of a new primary human pancreatic tumor line. *Cancer Invest.* 1986; 4:15-23.
- Fredebohm J, Boettcher M, Eisen C, Gaida MM, Heller A, Keleg S, Tost J, Greulich-Bode KM, Hotz-Wagenblatt A, Lathrop M, Giese NA, Hoheisel JD. Establishment and characterization of a highly tumorigenic and cancer stem cell enriched pancreatic cancer cell line as a well-defined model system. *PLOS One.* 2012; 7:e48503.
- Amrutkar M, Gladhaug IP. Pancreatic cancer chemoresistance to gemcitabine. *Cancers.* 2017; 9:E57.
- Arlt A, Gehrz A, Muerkoster S, Vorndamm J, Kruse ML, Folsch UR, Schafer H. Role of NF-kappaB and Akt/PI3K in the resistance of pancreatic carcinoma cell lines against gemcitabine-induced cell death. *Oncogene.* 2003; 22:3243-3251.
- Rathos MJ, Joshi K, Khanwalkar H, Manohar SM, Joshi KS. Molecular evidence for increased antitumor activity of gemcitabine in combination with a cyclin-dependent kinase inhibitor, P276-00 in pancreatic cancers. *J Transl Med.* 2012; 10:161.
- Al Shemali J, Mensah-Brown E, Parekh K, Thomas SA, Attoub S, Hellman B, Nyberg F, Adem A, Collin P, Adrian TE. Frondoside A enhances the antiproliferative effects of gemcitabine in pancreatic cancer. *Eur J Cancer.* 2014; 50:1391-1398.
- Hennig R, Ventura J, Segersvard R, Ward E, Ding XZ, Rao SM, Jovanovic BD, Iwamura T, Talamonti MS, Bell RH Jr, Adrian TE. LY293111 improves efficacy of gemcitabine therapy on pancreatic cancer in a fluorescent orthotopic model in athymic mice. *Neoplasia.* 2005; 7:417-425.
- Lim E, Modi KD, Kim J. *In vivo* bioluminescent imaging of mammary tumors using IVIS Spectrum. *J Vis Exp.* 2009; 26:e1210.
- Nguyen BCQ, Yoshimura K, Kumazawa S, Tawata S, Maruta H. Frondoside A from sea cucumber and nymphaeols from Okinawa propolis: Natural anti-cancer agents that selectively inhibit PAK1 *in vitro*. *Drug Discov*

- Ther. 2017; 11:110-114.
18. Adrian TE, Collin P. The anti-cancer effects of frondoside A. *Mar Drugs*. 2018; 16:E64.
 19. Chugh R, Sangwan V, Patil SP, Dudeja V, Dawra RK, Banerjee S, Schumacher RJ, Blazar BR, Georg GI, Vickers SM, Saluja AK. A preclinical evaluation of minnelide as a therapeutic agent against pancreatic cancer. *Sci Transl Med*. 2012; 4:156ra139.
 20. Zhao X, Puszyk WM, Lu Z, Ostrov DA, George TJ, Robertson KD, Liu C. Small molecule inhibitor YM155-mediated activation of death receptor 5 is crucial for chemotherapy-induced apoptosis in pancreatic carcinoma. *Mol Cancer Ther*. 2015; 14:80-89.
 21. Kim SJ, Beak SM, Park SK. Supplementation with triptolide increases resistance to environmental stressors and lifespan in *C. elegans*. *J Food Sci*. 2017; 82:1484-1490.
 22. Andrieu GP, Shafran JS, Smith CL, Belkina AC, Casey AN, Jafari N, Denis GV. BET protein targeting suppresses the PD-1/PD-L1 pathway in triple-negative breast cancer and elicits anti-tumor immune response. *Cancer Lett*. 2019. pii: S0304-3835(19)30450-1.
 23. Sharp PP, Garnier JM, Hatfaludi T, *et al*. Design, synthesis, and biological activity of 1,2,3-triazolobenzodiazepine BET bromodomain inhibitors. *ACS Med Chem Lett*. 2017; 8:1298-1303.
 24. Maruta H. Breakthrough: PAK1-dependent expression of PD-L1 (programmed death ligand). *Integr Mol Med*. 2019; 6:1-2.

(Received September 5, 2019; Revised September 24, 2019; Accepted October 13, 2019)

Effects of storage temperature, storage time, and Cary-Blair transport medium on the stability of the gut microbiota

Naoyoshi Nagata^{1,2,*}, Mari Tohya^{3,4}, Fumihiko Takeuchi⁵, Wataru Suda⁶, Suguru Nishijima^{7,8}, Mitsuru Ohsugi⁹, Kohjiro Ueki⁹, Tetsuro Tsujimoto⁹, Tomoka Nakamura⁹, Takashi Kawai², Tohru Miyoshi-Akiyama³, Naomi Uemura^{2,10}, Masahira Hattori^{6,8}

¹ Department of Gastroenterology and Hepatology, National Center for Global Health and Medicine, Tokyo, Japan;

² Gastroenterological Endoscopy, Tokyo Medical University, Tokyo, Japan;

³ Pathogenic Microbe Laboratory, Research Institute, National Center for Global Health and Medicine, Tokyo, Japan;

⁴ Department of Microbiology, Juntendo University School of Medicine, Tokyo, Japan;

⁵ Department of Gene Diagnostics and Therapeutics, National Center for Global Health and Medicine, Tokyo, Japan;

⁶ RIKEN Center for Integrative Medical Sciences, Tokyo, Japan;

⁷ Computational Bio-Big Data Open Innovation Lab., National Institute of Advanced Science and Technology, Tokyo, Japan;

⁸ Graduate School of Advanced Science and Engineering, Waseda University, Tokyo, Japan;

⁹ Department of Diabetes, Endocrinology, and Metabolism, Center Hospital, National Center for Global Health and Medicine, Tokyo, Japan;

¹⁰ Department of Gastroenterology and Hepatology, National Center for Global Health and Medicine, Kohnodai Hospital, Tokyo, Japan.

Summary

How long fecal samples can withstand a period of refrigeration or room temperature, and the appropriate preservative, are largely unknown. Cary-Blair transport medium has been used for many years because it is inexpensive and prevents bacterial overgrowth. However, its effectiveness for metagenomic analyses has never been tested. We found that the microbial compositions using a 16S rRNA sequence of samples left at 4°C for 3 or 7 days or at 25°C for 1, 3, or 7 days differed significantly from samples stored at -80°C in no-preservative method. Whereas samples stored in Cary-Blair medium remained unchanged for longer periods. The relative abundances of phylum Bacteroidetes and Actinobacteria, changed significantly at 25°C, whereas Cary-Blair medium inhibited the reduction in Bacteroidetes and the increase in Actinobacteria. The bacterial survival counts were significantly lower in the RNAlater samples than in the Cary-Blair samples under aerobic and anaerobic culture conditions. In conclusion, storage time and storage temperature significantly affect the gut microbial composition in fecal samples. Given the low cost, inhibitory effect on bacterial changes, and potential utility in bacterial isolation, Cary-Blair medium containers are suitable for large-scale or hospital-based microbiome studies, especially if direct freezing at -80°C is unavailable.

Keywords: Gut microbiome, Cary-Blair transport medium, RNAlater, fecal sampling, bacterial survival rate

1. Introduction

Immediate DNA extraction from fresh feces or

Released online in J-STAGE as advance publication October 11, 2019.

*Address correspondence to:

Dr. Naoyoshi Nagata, Department of Gastroenterology and Hepatology, National Center for Global Health and Medicine, 1-21-1 Toyama, Shinjuku-ku, Tokyo 162-8655, Japan.

E-mail: nnagata_ncgm@yahoo.co.jp

immediate freezing at -80°C is the gold standard procedure in microbiome studies, but this can be challenging (1-4). To date, several preservatives have been reported (5-8), but most preservatives do not distinguish between DNA obtained from live or dead cells, and the bacteria are unculturable. Cary-Blair medium consisting predominantly of buffered salts with no nutrients (9), which suppresses bacterial overgrowth, potentially allows for long-term survival of enteric pathogens (9) and can be used for the isolation of

organisms. However, the effectiveness of this medium for 16S rRNA sequencing analyses of human fecal samples has never been tested. Therefore, we examined the stability of the gut microbiota in Cary-Blair medium.

2. Materials and Methods

2.1. Human fecal sample collection and storage methods

Various storage methods were tested using 231 fecal samples from 11 healthy adults: (i) immediate DNA extraction from fresh samples (fresh); (ii) immediate freezing at -80°C ; and (iii) preservation under different conditions: 4°C or 25°C for 1, 3, or 7 days (Figure 1). Microbial composition was compared between the no preservative method and Cary-Blair medium-containing method (Toyobo Co., Ltd., Tokyo, Japan) (9). Written consent was obtained from all the participants. The study was approved by the Ethics Committee of the National Center for Global Health and Medicine (No. 2014).

2.2. Bacterial DNA extraction and sequencing 16S ribosomal RNA gene amplicons

To extract the fecal bacterial DNA, we used an enzymatic lysis method with lysozyme (Sigma-Aldrich Co., St. Louis, MO, USA) and achromopeptidase (Wako Pure Chemical Industries, Ltd., Osaka, Japan) (10). The 16S amplicon PCR forward primer (5'-TCGTCGGCAGCGTCAGATGTGTATAAGAGACAGCCTACGG GNGGCWGCAG-3') and 16S amplicon PCR reverse primer (5'-GTCTCGTGGGCTCGGAGATGTGTATA AGAGACAGGACTACHVGGGTATCTAATCC-3'), with adaptor sequences for Illumina indexing, were used to amplify the bacterial 16S rRNA gene V3-V4 regions. PCRs were run for 25 cycles, using the KAPA HiFi HotStart ReadyMix PCR Kit (Nippon Genetics Co., Ltd., Tokyo, Japan). The PCR amplicons were purified with AMPure[®] XP magnetic purification beads (Beckman Coulter, Inc., Brea, CA, USA) and quantified with 4200 TapeStation (Agilent Technologies Japan, Ltd). Equal amounts of amplicons from all the samples were sequenced with the MiSeq System (Illumina, Inc., Tokyo Japan), according to the manufacturer's instructions (10).

2.3. Bioinformatic and statistical analyses

After the quality of the filter-passed reads with average quality values of > 25 was checked for chimeras, the taxonomy of the high-quality reads was assigned with three publically databases: the Ribosomal Database Project (RDP) v. 10.27, CORE (<http://microbiome.osu.edu/>), and a reference genome sequence database obtained from the National Center for Biotechnology Information FTP site (<ftp://ftp.ncbi.nih.gov/genbank/>, December 2011). We then selected those reads with BLAST matches of $> 90\%$ with a representative

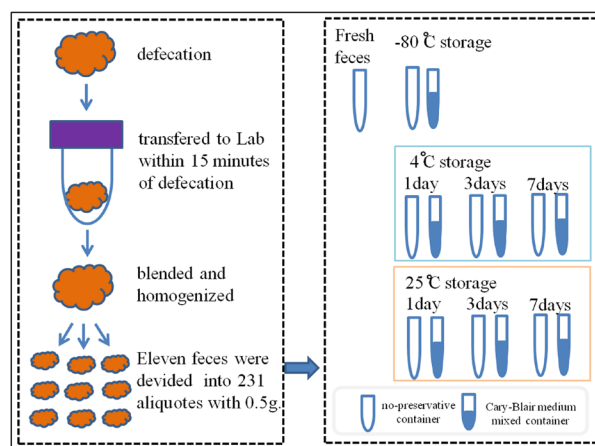


Figure 1. Sample collection and storage method.

sequence in one of the three databases. A total of 1,992,156 high-quality reads were obtained after quality filtering. We randomly selected 3,000 reads per sample and analyzed them to minimize the overestimation of the species richness in the clustering due to intrinsic sequencing error (4,10). Good's coverage index (11) of the 3,000 reads per sample in this study was 0.96, indicating high coverage, and the number of reads is sufficient for microbiome analysis. After both primer sequences were removed, the reads were sorted and grouped into operational taxonomic units (OTUs) with a sequence identity threshold of 97%. The taxonomic assignment of each OTU was made with the GLSEARCH program. Taxonomic groups with relative abundances of $\geq 0.1\%$ in any subject were included in the subsequent analyses. All reads were deposited in the DDBJ/GenBank/EMBL database under accession number DRA 006625. Pairwise Pearson's correlation coefficients were used to analyze the microbial compositions under different storage conditions. For the UniFrac distance analyses, phylogenetic-tree-based metrics were used to measure the differences in the overall bacterial compositions under different storage conditions (12). We defined the "reference" as the distance or coefficient between the fresh sample and those stored at -80°C . Values of $p < 0.05$ were considered statistically significant. All statistical analyses were performed with the R software package (v3.2.2).

3. Results

At 4°C , weighted UniFrac distance of samples stored without preservative at 3 and 7 days was significantly larger than the reference (Figure 2A); at 25°C , the distance was significantly greater for samples at 1, 3, and 7 days (Figure 2B). In contrast, the distance for samples stored in Cary-Blair medium remained unchanged for up to 7 days at 4°C (Figure 2A) and for 24 h at 25°C (Figure 2B). Similar results were obtained at the genus level

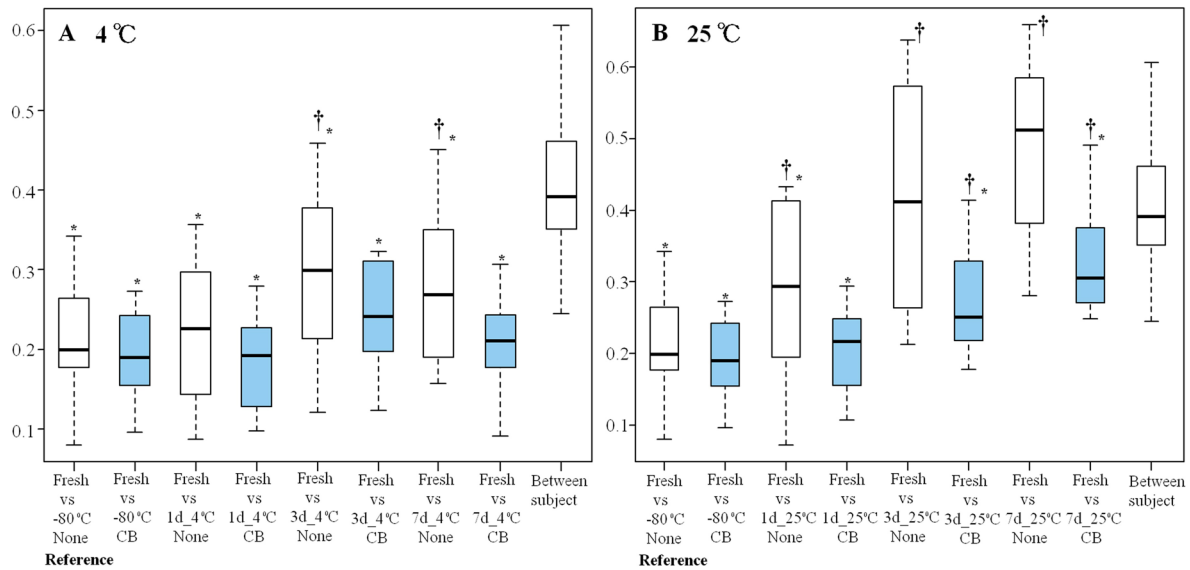


Figure 2. Box-and-whisker plot of UniFrac distances at 4°C (A) and 25°C (B) stored without preservative (white box) or in Cary-Blair (CB) medium (blue box). † $p < 0.05$ for differences between fresh samples and stored samples relative to the reference distance. * $p < 0.05$ for differences between (i) between-subject distances and (ii) within-subject distances between fresh samples and stored samples. Boxes represent the interquartile range (IQR) and lines inside show the median. Whiskers indicate the lowest and highest values within 1.5 times the IQR.

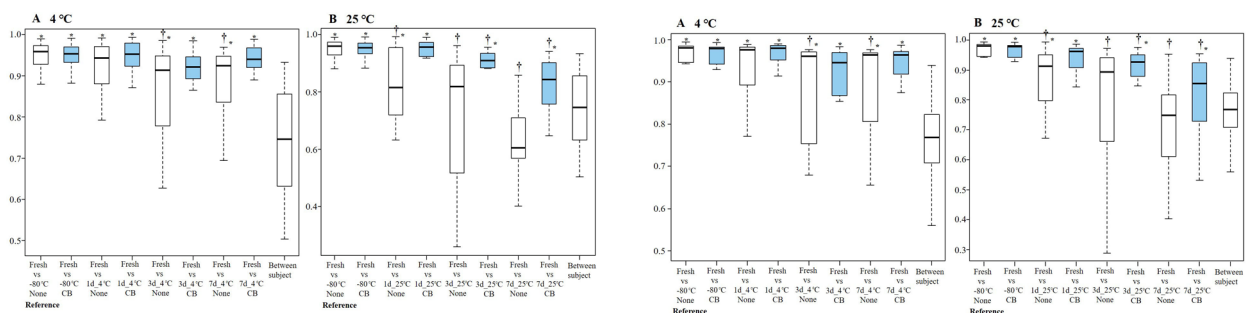


Figure 3. Box-and-whisker plot of the coefficient value at the genus level for samples stored at 4°C (A) and 25°C (B) without preservative (white box) or in Cary-Blair (CB) medium (blue box). † $p < 0.05$ for differences between fresh samples and stored samples relative to the reference distance. * $p < 0.05$ for differences between (i) between-subject distances and (ii) within-subject distances between fresh samples and stored samples. Boxes represent the interquartile range (IQR) and the lines inside show the median. Whiskers indicate the lowest and highest values within 1.5 times the IQR.

Figure 4. Box-and-whisker plot of the coefficient value at the species level for samples stored at 4°C (A) and 25°C (B) without preservative (white box) or in Cary-Blair (CB) medium (blue box). † $p < 0.05$ for differences between fresh samples and stored samples relative to the reference distance. * $p < 0.05$ for differences between (i) between-subject distances and (ii) within-subject distances between fresh samples and stored samples.

(Figure 3) and species level (Figure 4).

Relative abundance at the phylum level was significantly reduced for Firmicutes but significantly increased for Actinobacteria without preservative at 4°C at 3 and 7 days compared with the reference (Figure 5A); at 25°C, relative abundance continued to decrease for Firmicutes and Bacteroidetes from 1 day and was significantly increased for Actinobacteria at 3 and 7 days and for Proteobacteria at 1, 3, and 7 days (Figure 5B). In contrast, Cary-Blair medium inhibited the reduction in Bacteroidetes at 25°C and the increase in Actinobacteria at 3 days at 4°C and 25°C (Figure 5).

Lastly, we analyzed 9 fecal samples from 3 healthy subjects to investigate bacterial survival. We found

that survival counts were significantly higher in Cary-Blair samples than in the RNAlater samples, and were not significantly different from the samples without preservative under aerobic and anaerobic culture conditions (Figure 6).

4. Discussion

This is the first study to show that the effect of Cary-Blair medium on the stability of the gut microbiomes to be used for 16S rRNA analyses. Cary-Blair medium is a nonnutritive transport medium for Gram-negative and anaerobic organisms in stool samples (9), and importantly, prevents the overgrowth of

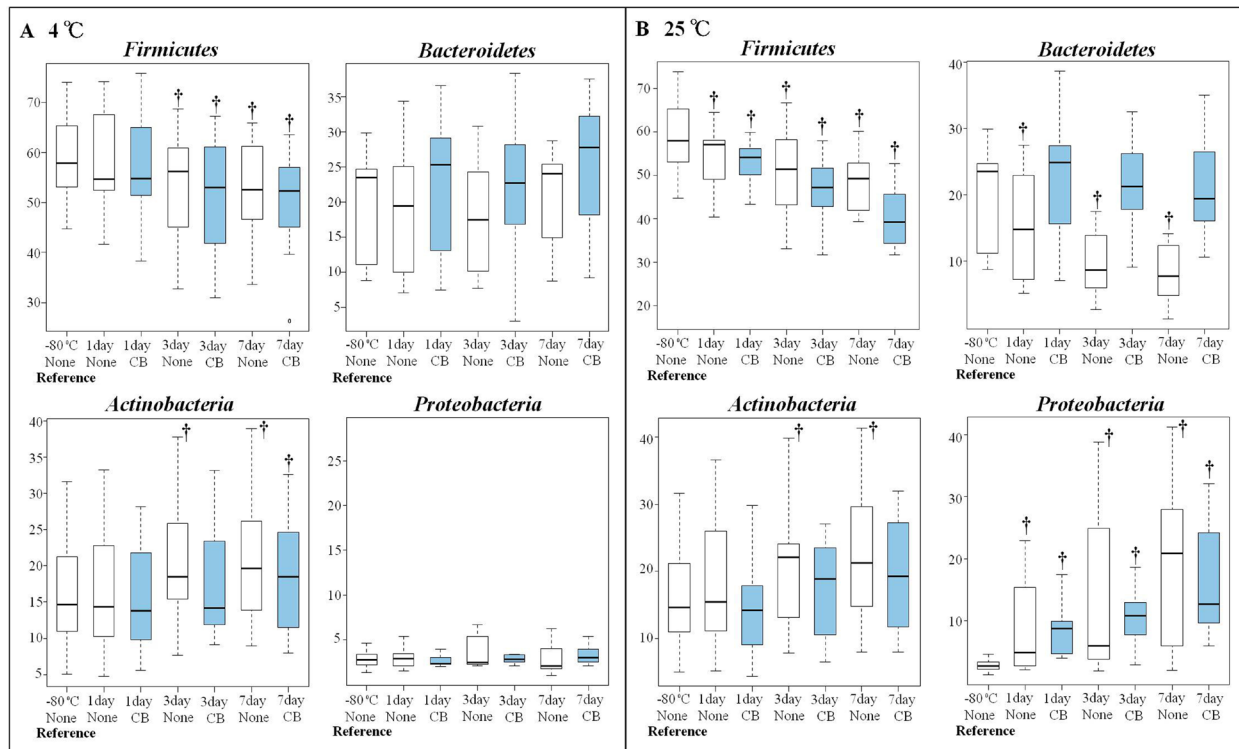


Figure 5. Time courses of relative abundance of four phyla at 4°C (A) or 25°C (B) stored without preservative (white box) or in Cary-Blair (CB) medium (blue box). * $p < 0.05$ for differences between the -80°C sample (reference) and samples stored by other methods. Boxes represent the interquartile range (IQR) and lines inside show the median. Whiskers indicate the lowest and highest values within 1.5 times the IQR.

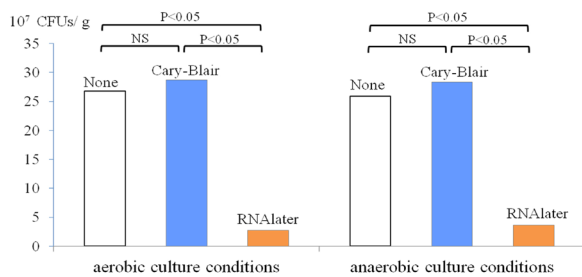


Figure 6. Bacterial survival count of fecal samples stored in Cary-Blair medium, without preservative, and in RNAlater solution under aerobic (A) and anaerobic (B) culture conditions. Survival counts were calculated as the number of colony-forming units (CFUs) and compared between fresh samples and samples stored at -80°C for 7 days. Bar chart illustrating the mean numbers of CFUs.

Enterobacteriaceae and allows the long-term survival of enteric pathogens (13,14). In this study, Cary-Blair medium inhibited the reduction of Bacteroidetes in samples left for up to 7 days at 25°C, and the increase in Actinobacteria in samples left for 3 or 7 days at 25°C, whereas the no-medium method did not. Consistent with these findings, Gorzelak *et al.* have shown that the detection of Bacteroidetes in no-medium fecal samples decreased after 30 min at room temperature. Therefore, one explanation of the stability of the gut microbiome in Cary-Blair medium is that it allows some bacteria to withstand longer periods at room temperature.

Another advantage of Cary-Blair medium use is that it can potentially be used for the isolation of organisms associated with specific diseases (15), whereas most preservatives do not distinguish between the DNA obtained from live or dead cells (5-8). To confirm this hypothesis, we examined the bacterial survival counts in no preservative, Cary-Blair medium, or RNAlater in the fresh and -80°C samples. We found that the survival counts were significantly lower in the RNAlater samples than in the Cary-Blair samples. In addition to this advantage, Cary-Blair medium is the least expensive of the preservatives used in microbiome studies, at less than US\$0.50 dollar per container.

Our results are consistent with those of previous studies, which showed no significant change in the microbial composition of frozen fecal samples and samples stored at 4°C for up to 24 h (3,16-18). Few data are available regarding the effects on the gut microbiota when samples are stored at 4°C for more than 3 days. As in the present study, Choo *et al.* reported that stool storage at 4°C for 3 days significantly affected the composition of the gut microbiome compared with storage at -80°C (5). These results suggest that the composition of the microbiome is associated with the length of storage, even when refrigerated, and that samples should be stored at 4°C for only 3 days after defecation.

In contrast, the microbial compositions of samples left for 1, 3, or 7 days at 25°C changed substantially

compared with the reference. Consistent with this, Shaw *et al.* showed that storage for 12 h at room temperature significantly increased the weighted UniFrac distances relative to -80°C storage (19). Two other studies have also demonstrated a significant change in microbial composition within 3 h at room temperature (20,21). These findings imply that fecal samples should not be left at room temperature after defecation.

In conclusion, fecal samples without preservative should be transferred to the laboratory within 24 h of defecation when stored at room temperature or within 3 days when stored refrigerated. Given the inhibitory effect on bacterial changes, potential utility in bacterial isolation, and low cost, Cary-Blair medium containers are useful for microbiome studies, especially when direct freezing at -80°C is unavailable.

Acknowledgements

This work was partially supported by Grants-in-Aid for Research from the National Center for Global Health and Medicine (28-2401, 29-2001, 29-2004, 19A1011, 19A1022, and 29-1025), JSPS KAKENHI Grant (JP17K09365), Smoking Research Foundation, Pancreas Research Foundation of Japan, DANONE RESEARCH GRANT, Research funding of Japan Dairy Association (J-Milk), and Takeda Science Foundation. The funding body had no role in the study design, data collection or analysis, decision to publish, or preparation of the manuscript. The authors thank Kuniko Miki, Kenko Yoshida, Eiko Izawa, Chiharu Matsuoka, Chikako Toyoda, and Hisae Kawashiro, for their help with the data collection.

References

- Fouhy F, Deane J, Rea MC, O'Sullivan O, Ross RP, O'Callaghan G, Plant BJ, Stanton C. The effects of freezing on faecal microbiota as determined using MiSeq sequencing and culture-based investigations. *PLoS One*. 2015; 10:e0119355.
- Bahl MI, Bergstrom A, Licht TR. Freezing fecal samples prior to DNA extraction affects the firmicutes to bacteroidetes ratio determined by downstream quantitative PCR analysis. *FEMS Microbiol Lett*. 2012; 329:193-197.
- Wu GD, Lewis JD, Hoffmann C, Chen YY, Knight R, Bittinger K, Hwang J, Chen J, Berkowsky R, Nessel L, Li H, Bushman FD. Sampling and pyrosequencing methods for characterizing bacterial communities in the human gut using 16S sequence tags. *BMC Microbiol*. 2010; 10:206.
- Nagata N, Tohya M, Fukuda S, *et al.* Effects of bowel preparation on the human gut microbiome and metabolome. *Sci Rep*. 2019; 9:4042.
- Choo JM, Leong LE, Rogers GB. Sample storage conditions significantly influence faecal microbiome profiles. *Sci Rep*. 2015; 5:16350.
- Chomezynski P, Sacchi N. The single-step method of RNA isolation by acid guanidinium thiocyanate-phenol-chloroform extraction: Twenty-something years on. *Nat Protoc*. 2006; 1:581-585.
- Song SJ, Amir A, Metcalf JL, Amato KR, Xu ZZ, Humphrey G, Knight R. Preservation methods differ in fecal microbiome stability, affecting suitability for field studies. *mSystems*. 2016; 1:e00021-16.
- Roesch LF, Casella G, Simell O, Krischer J, Wasserfall CH, Schatz D, Atkinson MA, Neu J, Triplett EW. Influence of fecal sample storage on bacterial community diversity. *Open Microbiol J*. 2009; 3:40-46.
- CARY SG, BLAIR EB. New transport medium for shipment of clinical specimens. I. fecal specimens. *J Bacteriol*. 1964; 88:96-98.
- Kim SW, Suda W, Kim S, Oshima K, Fukuda S, Ohno H, Morita H, Hattori M. Robustness of gut microbiota of healthy adults in response to probiotic intervention revealed by high-throughput pyrosequencing. *DNA Res*. 2013; 20:241-253.
- Singleton DR, Furlong MA, Rathbun SL, Whitman WB. Quantitative comparisons of 16S rRNA gene sequence libraries from environmental samples. *Appl Environ Microbiol*. 2001; 67:4374-4376.
- Lozupone C, Ladser ME, Knights D, Stombaugh J, Knight R. UniFrac: An effective distance metric for microbial community comparison. *ISME J*. 2011; 5:169-172.
- STUART RD. Transport medium for specimens in public health bacteriology. *Public Health Rep*. 1959; 74:431-438.
- Neumann DA, Benenson MW, Hubster E, Thi-nhu-Tuan N, Le-tien-Van. *Vibrio parahemolyticus* in the republic of vietnam. *Am J Trop Med Hyg*. 1972; 21:464-466.
- Lagier JC, Armougom F, Million M, Hugon P, Pagnier I, Robert C, Bittar F, Fournous G, Gimenez G, Maraninchi M, Trape JF, Koonin EV, La Scola B, Raoult D. Microbial culturomics: Paradigm shift in the human gut microbiome study. *Clin Microbiol Infect*. 2012; 18:1185-1193.
- Bassis CM, Moore NM, Lolans K, Seekatz AM, Weinstein RA, Young VB, Hayden MK; CDC Prevention Epicenters Program. Comparison of stool versus rectal swab samples and storage conditions on bacterial community profiles. *BMC Microbiol*. 2017; 17:78.
- Tedjo DI, Jonkers DM, Savelkoul PH, Masclee AA, van Best N, Pierik MJ, Penders J. The effect of sampling and storage on the fecal microbiota composition in healthy and diseased subjects. *PLoS One*. 2015; 10:e0126685.
- Carroll IM, Ringel-Kulka T, Siddle JP, Klaenhammer TR, Ringel Y. Characterization of the fecal microbiota using high-throughput sequencing reveals a stable microbial community during storage. *PLoS One*. 2012; 7:e46953.
- Shaw AG, Sim K, Powell E, Cornwell E, Cramer T, McClure ZE, Li MS, Kroll JS. Latitude in sample handling and storage for infant faecal microbiota studies: The elephant in the room? *Microbiome*. 2016; 4:40.
- Cardona S, Eck A, Cassellas M, Gallart M, Alastrue C, Dore J, Azpiroz F, Roca J, Guarner F, Manichanh C. Storage conditions of intestinal microbiota matter in metagenomic analysis. *BMC Microbiol*. 2012; 12:158.
- Gorzalak MA, Gill SK, Tasnim N, Ahmadi-Vand Z, Jay M, Gibson DL. Methods for improving human gut microbiome data by reducing variability through sample processing and storage of stool. *PLoS One*. 2015; 10:e0134802.

(Received September 17, 2019; Revised September 29, 2019; Accepted October 2, 2019)

***Centella asiatica* (L.) extract attenuates inflammation and improve insulin sensitivity in a coculture of lipopolysaccharide (LPS)-induced 3T3-L1 adipocytes and RAW 264.7 macrophages**

Siska Andrina Kusumastuti¹, Dwi Aris Agung Nugrahaningsih^{2,*},
Mae Sri Hartati Wahyuningsih²

¹ Center of Pharmaceutical and Medicine Technology, Agency for the Assessment and Application of Technology (BPPT), Jakarta, Indonesia;

² Department of Pharmacology and Therapy, Medical Faculty, Universitas Gadjah Mada, Yogyakarta, Indonesia.

Summary

Insulin resistance in obese condition is related to chronic low-grade inflammation which leads to insulin signaling impairment. *Centella asiatica* (L.) is an herb that exhibits anti-inflammatory and blood sugar-lowering activity (hypoglycemia). The study aims to investigate the molecular mechanism of *C. asiatica* extract in insulin sensitivity improvement in a coculture of lipopolysaccharide (LPS)-induced 3T3-L1 adipocytes and RAW 264.7 macrophages. A coculture of 3T3-L1 adipocytes and RAW 264.7 macrophages were incubated with LPS to induce insulin resistance in the adipocytes. An extract of *C. asiatica* was added to coculture cells and after 24 hours, insulin sensitivity and inflammatory response were determined, including glucose consumption, glucose transporter-4 (GLUT-4), insulin receptor substrate-1 (IRS-1), and interleukin-6 (IL-6) mRNA expression. *C. asiatica* extract at a concentration of 500 µg/mL increased glucose consumption and induced GLUT-4 and IRS-1 mRNA expression significantly in a coculture of LPS-induced 3T3-L1 adipocytes and RAW 264.7 macrophages. The pro-inflammatory cytokines IL-6 mRNA expression was decreased in the coculture cells after treatment with *C. asiatica* extract at a concentration of 500 µg/mL. This result indicates that *C. asiatica* has an effect to stimulate glucose consumption in the coculture cells that might be mediated via GLUT-4/IRS-1 pathway as a result of IL-6 inhibition. These findings suggest that the *C. asiatica* extract inhibits inflammation and improves insulin sensitivity in a coculture of LPS-induced 3T3-L1 adipocytes and RAW 264.7 macrophages.

Keywords: *Centella asiatica* L., insulin sensitivity, coculture, 3T3-L1 adipocytes, RAW 264.7 macrophages

1. Introduction

Type 2 diabetes mellitus (T2DM) is a metabolic disorder caused by a defect in insulin action called insulin resistance (1). Insulin resistance in obesity is associated with chronic low-grade inflammation resulting from an increase of macrophages infiltration into adipose tissues (2). An interaction between excessive adipocytes and the higher amount of

macrophages promotes the macrophage activation into inflammatory macrophages (M2) followed by the secretion of pro-inflammatory cytokines such as interleukin-6 (IL-6), tumor necrosis factor- α (TNF- α), and monocyte chemoattractant protein-1 (MCP-1) (3). Pro-inflammatory cytokines secreted from both adipocytes and activated macrophages may alter insulin sensitivity in adipocytes through the degradation and deactivation of insulin receptor substrate-1 (*IRS-1*), one of essential protein in the insulin receptor substrate-1/phosphoinositide 3-kinases/Akt (*IRS-1/PI3K/Akt*) insulin signaling pathway (3,4). The degradation of *IRS-1* may trigger the downregulation of proteins downstream in the *IRS-1/PI3K/Akt* pathway, including glucose transporter-4 (*GLUT-4*) expression leading to

*Address correspondence to:

Dr. Dwi Aris Agung Nugrahaningsih, Department of Pharmacology and Therapy, Medical Faculty, Universitas Gadjah Mada, Yogyakarta, Indonesia.
E-mail: dwi.aris.a@ugm.ac.id

the disruption of glucose uptake in adipocytes (5).

Anti-diabetic drugs efficacy in controlling blood glucose in diabetic patients has been established. However, they also have undesirable side effects such as weight gain, bone loss and increased cardiovascular risk (6). Therefore, safer and more effective alternative agents are needed and developing new drugs from herbal is a promising method.

Centella asiatica (L.) or Pegagan in Bahasa Indonesia is one of the most important herbal medicine used empirically in Indonesia. The herb has been proven to possess hypoglycemic activity in in-vivo models. Recent studies reported that *C. asiatica* extract decreased glucose plasma levels in high fat diet (HFD)-induced and streptozotocin-induced diabetic mice in dose- dependent manner (7,8). One of the active compounds in *C. asiatica*, asiatic acid has also been shown as an anti-inflammatory and a hypoglycemic agent (10,11). Recent studies reported that asiatic acid decrease secretion of pro-inflammatory cytokines in the liver tissues of diabetic mice and inhibit LPS-induced inflammatory response in endometrial epithelial cells (12,13). However, there is minimal information about molecular mechanism of *C. asiatica* extract in improving insulin sensitivity related to insulin resistance caused by inflammation. In the present study, we investigated the effect of *C. asiatica* extract on the insulin sensitivity of adipocytes using a coculture of LPS-induced RAW 264.7 macrophages and 3T3-L1 adipocytes. This study also evaluated involvement of the IRS-1/GLUT-4 pathway in relation to insulin sensitivity effect. The expression of the pro-inflammatory cytokine IL-6 was also investigated to determine *C. asiatica* effect on the inflammatory changes related to insulin sensitivity impairment.

2. Materials and Methods

2.1. *C. asiatica* extract preparation

A standardized *C. asiatica* extracts was produced by Javaplant PT, Tri Rahardja Tawangmangu Surakarta Indonesia, in September of 2016. Extraction was performed using water as a solvent and following good manufacturing practices. *C. asiatica* herbs were soaked in water at boiling point followed by stirring with a magnetic stirrer for 5 h. Herbs were removed from the heat sources then filtered to obtain the concentrated extract. The freeze-drying method was used to obtain dried powder and then extract powder was dissolved in a Dimethyl Sulfoxide (DMSO) to prepare samples for testing.

2.2. Cell lines and culture

3T3-L1 preadipocyte cells and RAW 264.7 murine macrophage cells were obtained from the Food and

Science Technology Department of National Pingtung Science Technology (NPUST, Pingtung, Taiwan). Both cell lines were maintained in Dulbecco's modified Eagle's medium (DMEM, Gibco, New York, USA) containing 1% penicillin/streptomycin (PS, 100 units of penicillin/mL and 100 pg streptomycin/mL, Gibco, New York, USA) and supplemented with 10% New-born Calf Serum (NBCS, Gibco, New York, USA) to culture the 3T3-L1 cells and 10% Fetal Bovine Serum (FBS, Gibco, New York, USA) to culture RAW 264.7 cells. The cells were incubated at 37°C in a humidified 5% CO₂ atmosphere and the medium was replaced every 2 days.

2.3. Viability assay

RAW 264.7 macrophages were seeded at 2.4×10^4 cells/well and 3T3-L1 pre-adipocytes were seeded at 1.5×10^4 cells/well. Cells were cultured in a various concentrations (62.5-1,000 µg/mL) of the *C. asiatica* extract and then, the cells were incubated at 37°C in a humidified 5% CO₂ atmosphere for 24 h. Viability assay of the 3T3-L1 pre-adipocyte cells and RAW 264.7 macrophage cells were performed using a previously described 3-[4,5- dimethylthiazol-2-yl]-2,5 diphenyl tetrazolium bromide (MTT) assay protocol (14). Safe concentrations of the extract were determined and used in further experiment.

2.4. Coating the plates

Gelatin 1.3% (Sigma Aldrich, Saint Louis, USA) was dissolved in phosphate buffered saline (PBS). Transferred 2 mL of gelatin working solution into each well and then, plates were incubated at 37°C for 1 h. The plates were dried for 30 min and sterilized by an Ultraviolet (UV) lamp for 15 min.

2.5. Differentiation and coculture of 3T3-L1 adipocyte cells and RAW 264.7 macrophage cells

3T3-L1 pre-adipocytes were differentiated into mature adipocytes in gelatin-coated 6 well plate using a previously described protocol (15). RAW 264.7 macrophages were plated onto differentiated 3T3-L1 in serum-starved DMEM and incubated at 37°C in a humidified 5% CO₂ atmosphere for 3 h. Lipopolysaccharide (Sigma Aldrich, Saint Louis, USA) at a concentration of 0.125 µg/mL was added to the cells in the FBS-supplemented DMEM medium and the cells were incubated at 37°C in a humidified 5% CO₂ atmosphere for 48 h. As a control, equal numbers of RAW 264.7 macrophages and differentiated 3T3-L1 cells were cultured separately in the same medium with a coculture. After 48 h, *C. asiatica* extract dissolved in DMEM containing FBS 2% was added to a coculture cells at three different concentration (125, 250 and 500

µg/mL) followed by incubation at 37°C in a humidified 5% CO₂ atmosphere for an additional 24 h. Cells were incubated in serum-starved DMEM containing 1 µg/mL insulin (Sigma Aldrich, Saint Louis, USA) for 30 min. The medium and cells were collected and stored at -20°C until use.

2.6. Determination of glucose consumption

Glucose concentration contained in the cell medium was measured using Glucose GOD FS glucose kit assay (Diasys Diagnostics, Holzheim, Germany) and was performed following the manufacturer's protocol with slight modifications. Reagents were added after 20 µL of cells media was plated onto 96 well-plate. The plates were then incubated at 25°C for 20 min. Absorbance at 540 nm was recorded using a microplate reader (Thermo Fisher Scientific Multiskan, Ratastie, Finland). All the samples were measured in triplicate.

2.7. Quantitative of polymerase chain reaction

A coculture of adipocytes and macrophages treated with the extract was harvested after 24 h of incubation. Control of RAW 264.7 macrophages and differentiated 3T3-L1 were harvested separately and then mixed in a single tube as a control without a coculture. Total RNA was isolated in each group according to manufacturer protocol (Geneaid biotech Ltd, New Taipei, Taiwan). Expression of GLUT-1, IRS-1 and IL-6 mRNA were measured by quantitative polymerase chain reaction (qPCR) using a Sensifast SYBR No-ROX One-Step Kit Master Mix Kit (Bioline, London, United Kingdom) and analyzed on an Eco™ Real-Time PCR instrument (Illumina Inc, San Diego, USA). The following primers were used for the qPCR: GLUT-4, 5'-TTGCACACGGCTTCCGAACG-3' (forward) and 5'-GATCTGCTGGAAACCCGACGG-3'; IRS-1 5'-CCATGAGCGATGAGTTTCGC-3' (reverse) and 5'-GCAGTGATGCTCTCAGTTTCG; IL-6 5'-GAGTCACAGAAGGAGTGGCTAAG-3' (forward) and 5'-ACCACAGTGAGGAATGTCCAC-3' (reverse); and β-actin 5'-CTCTGGCTCCTAGCACCATGAAGA-3' (forward) and 5'-GTAAAACGCAGCTCAGTAACAGTCCG-3' (reverse). The qPCR reaction cycling parameters for all genes were performed at 45°C for 10 min for reverse transcriptase activation, followed by a pre-incubation condition step at 95°C for 2 min and amplification for 40 cycles at 95°C for 5 sec, 62°C for 15 sec and 72°C for 5 sec. Gene expression was calculated using the relative expression $2^{-\Delta\Delta Cq}$ method and β-actin was used as a normalizer. All samples were amplified in duplicate.

2.8. Statistical analysis

Data were expressed as the mean ± SD. Statistical analysis were performed using the unpaired Student t-test

and analysis of variance (ANOVA) followed by post-hoc tests. A value of $p < 0.05$ was considered significant.

3. Results

3.1. Viability assay of the *C. asiatica* extract on 3T3-L1 preadipocytes and RAW 264.7 macrophages

To investigate *C. asiatica* extract effect on insulin sensitivity related to inflammatory changes in a coculture of differentiated 3T3-L1 and RAW 264.7 macrophages, we first evaluated its cytotoxicity at various concentration. Cells were treated with *C. asiatica* extract at concentrations up to 500 µg/mL showed viability more than 90% (Figure 1), suggesting that *C. asiatica* extract is safe and non-toxic up to a concentration of 500 µg/mL in both of 3T3-L1 preadipocytes and RAW 264.7 macrophages.

3.2 Coculture of RAW 264.7 macrophages in contact with 3T3-L1 adipocytes induced insulin resistance in adipocytes and altered macrophages morphology

Before we examine insulin sensitivity effect of *C. asiatica* extract on coculture cells, we evaluated adipocytes insulin responsiveness in a direct coculture of LPS-induced 3T3-L1 adipocytes and RAW 264.7 macrophages. Cellular contact in direct coculture under LPS treatment triggered morphological changes in the macrophages. RAW 264.7 macrophages appeared rounded without the LPS treatment and the macrophages became elongated with short extension appearance after LPS treatment. With 48 hours of the direct coculture, macrophages showed an elongated appearance with a long cellular extension between and

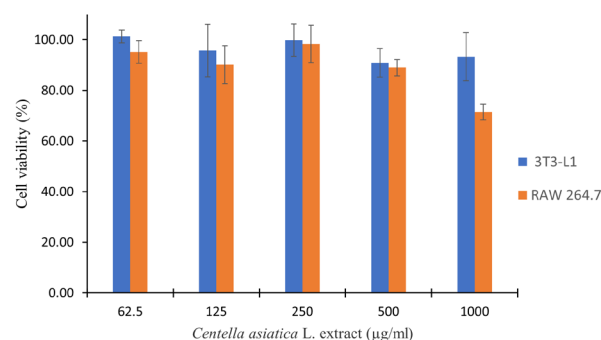


Figure 1. Effects of *Centella asiatica* (L.) extract on RAW 264.7 macrophages and 3T3-L1 pre-adipocytes viability. RAW 264.7 macrophages and 3T3-L1 preadipocytes were culturing in DMEM high glucose supplemented by New Calf Bovine Serum (NCBS) 10% for culturing 3T3-L1 preadipocytes and Fetal Bovine Serum (FBS) 10% for culturing RAW 264.7 macrophages in 96 well plate for 24 h. The cells then were incubated at 37°C in a humidified 5% CO₂ with various concentration of *Centella asiatica* (L.) extract for 24 h and cell viability was determined using the MTT assay. Extract at a concentration up to 500 µg/mL showed cell viability more than 90% in both of the cells. Values are expressed as means ± SD.

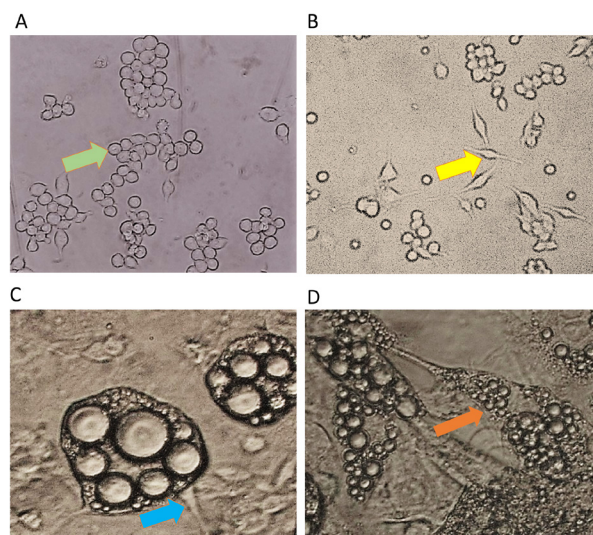


Figure 2. Morphological changes of RAW 264.7 macrophages without coculture and a direct coculture with adipocytes. Both of cells were culturing in DMEM high glucose supplemented by fetal bovine serum (FBS) 10% in 6 well plate and incubated at 37°C in a humidified 5% CO₂ for 48 h. Morphology of the cells were observed under microscope: (A) RAW 264.7 macrophages without LPS appeared small rounded (green arrow); (B) RAW 264.7 macrophages under LPS treatment showed elongated appearance with a short extension (yellow arrow); (C) Culture RAW 264.7 macrophages in contact with adipocytes under LPS treatment showed elongated appearance with a long cellular extension of RAW 264.7 macrophages between and along the surrounding adipocytes (blue arrow) and (D) Direct coculture between RAW 264.7 macrophages and differentiated 3T3-L1 adipocytes under LPS treatment developed lipid vacuoles accumulated in the macrophages cytoplasm (orange arrow).

along the surrounding adipocytes (Figure 2) resembling the morphology of adipose tissue macrophages (ATM) isolated from obese mice (16). However, direct contact between 3T3-L1 adipocytes and RAW 264.7 macrophages developed an accumulation of lipid vacuoles in the macrophages cytoplasm referred to as lipid-laden giant multinucleated. The results showed that a direct coculture of 3T3-L1 adipocytes and RAW 264.7 macrophages under LPS induction for 48 h stimulates changes in the macrophages behavior.

Insulin sensitivity was assessed by evaluating insulin-stimulated glucose consumption in a coculture of 3T3-L1 adipocytes and RAW 264.7 macrophages. Glucose concentration contained in a coculture medium indicates how much glucose was taken up by the coculture cells. Our study showed there were higher glucose concentration contained in the coculture of adipocytes and macrophages medium compared to the adipocytes medium only ($p = 0.046$, Figure 3A) indicating that an interaction between the adipocytes and macrophages under LPS treatment stimulated glucose uptake impairment in the adipocytes.

In this study, we determined insulin-stimulated GLUT-4 mRNA expression as a glucose transporter in adipocytes cells in contact with RAW 264.7 macrophages. We observed significantly lower GLUT-

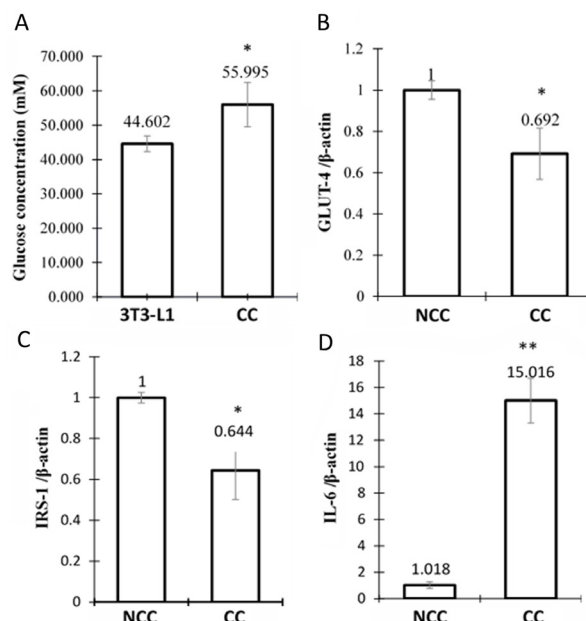


Figure 3. Insulin sensitivity and inflammatory response in control of coculture of LPS-induced adipocytes and macrophages (CC) and control of adipocytes and macrophages without co-culture (NCC). Parameters were measured after cells were incubated at 37°C in a humidified 5% CO₂ for 48 h and insulin induction for 30 minutes. (A) Glucose concentration; (B) GLUT-4 mRNA; (C) IRS-1 mRNA; (D) IL-6 mRNA. Glucose concentration were measured using glucose assay kit and expression of target genes were quantified using qPCR. Values are mean \pm Standard Deviation. * $p < 0.05$, vs. NCC; ** $p < 0.01$, vs. NCC.

4 mRNA expression in a coculture of LPS-induced 3T3-L1 adipocytes and RAW 264.7 macrophages compared to the sum of the GLUT-4 mRNA expression by adipocytes and macrophages without a co-culture ($p = 0.016$, Figure 3A). This result is consistent with the glucose consumption data previously.

Glucose transport involves insulin signaling pathways after insulin stimulation. The IRS1/PI3K/Akt pathway is essential for insulin-regulated glucose transport by activating and translocating GLUT-4 from intracellular vesicles to the plasma membrane. This study determined the mRNA expression of IRS-1. The result showed that IRS-1 mRNA expression in coculture of LPS-induced adipocytes and macrophages was significantly lower ($p = 0.045$) compared to the sum of the IRS-1 mRNA expression by adipocytes and macrophages without a co-culture (Figure 3C).

To evaluate inflammatory changes caused by the interaction between adipocytes and macrophages under LPS treatment, we assessed pro-inflammatory cytokine IL-6 mRNA expression in a coculture of 3T3-L1 adipocytes and RAW 264.7 macrophages. The coculture cells showed significantly higher of IL-6 mRNA expression compared to the sum of the IL-6 mRNA expression by adipocytes and macrophages without a co-culture ($p < 0.01$, Figure 3D). This result suggested that direct contact between adipocytes and macrophages under LPS treatment induced an

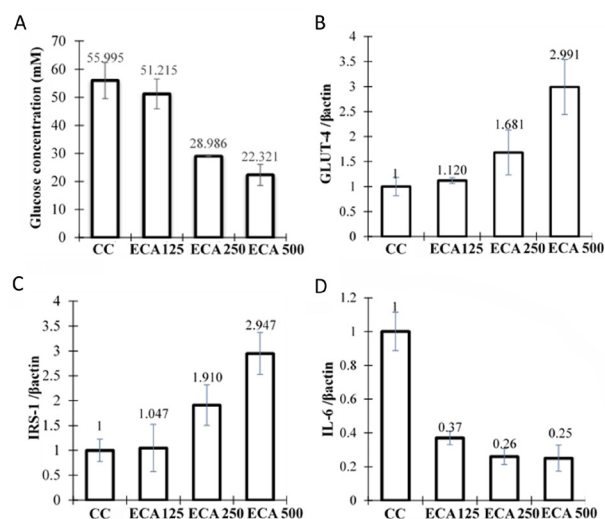


Figure 4. Insulin sensitivity and inflammatory response in control of coculture (CC) and coculture after treatment with *Centella asiatica* (L.) extract (ECA). Parameters were measured after both of cells incubated with a various concentration of *Centella asiatica* L. extract (125, 250, and 500 $\mu\text{g/mL}$) at 37°C in a humidified 5% CO_2 for 24 h, followed by insulin induction for 30 min. (A) glucose concentration; (B) GLUT-4 mRNA; (C) IRS-1 mRNA; (D) IL-6 mRNA. Glucose concentration were measured using glucose assay kit and expression of target genes were quantified using qPCR. Values are mean \pm Standard Deviation. * $p < 0.05$, vs. CC; *** $p < 0.001$, vs. CC.

inflammatory response, which in turn, influence the adipocytes insulin sensitivity that might have mediated via the IRS-1/GLUT-4 pathway.

3.3. Glucose consumption in a coculture of LPS-induced 3T3-L1 adipocytes and RAW 264.7 macrophages after 24 h treatment of *C. asiatica* extract

To evaluate *C. asiatica* extract effect to improve insulin sensitivity, we determined glucose concentration contained in a coculture of LPS-induced adipocytes and macrophages medium after treated by *C. asiatica* extract at a various concentration (125, 250, and 500 $\mu\text{g/mL}$) for 24 h. Glucose concentration contained in a coculture LPS-induced of adipocytes and macrophages medium after treated with *C. asiatica* extract at concentration 250 and 500 $\mu\text{g/mL}$ showed significantly lower concentrations compared to a differentiated adipocytes in a dose-dependent manner ($p < 0.01$ and $p < 0.01$, respectively, Figure 4A). This result indicated that *C. asiatica* extract improved glucose consumption in a coculture cells.

3.4. GLUT-4 and IRS-1 mRNA expression in a coculture of LPS-induced 3T3-L1 adipocytes and RAW 264.7 macrophages after a 24 h treatment with *C. asiatica* extract

A co-culture of adipocytes and macrophages treated with *C. asiatica* extract at a concentration of 500 $\mu\text{g/}$

mL showed significantly higher GLUT-4 and IRS-1 mRNA expression compared to a control of coculture of adipocytes and macrophages ($p < 0.01$ and $p < 0.01$, respectively) as shown in Figures 4B and 4C. This result suggested that improvement of glucose consumption in a coculture cells after treated with *C. asiatica* extract at a concentration of 500 $\mu\text{g/mL}$ might be related to the upregulation of GLUT-4 and IRS-1 mRNA expression in the adipocytes.

3.5. Pro-inflammatory cytokine IL-6 mRNA expression in a coculture of LPS-induced 3T3-L1 adipocytes and RAW 264.7 macrophages after 24 h treatment with *C. asiatica* extract

A direct interaction between adipocytes and macrophages aggravates inflammatory changes in adipose tissue marked by the increased production of pro-inflammatory cytokines such as IL-6, TNF- α and IL-1 β . This study determined pro-inflammatory cytokine IL-6 mRNA expression in a coculture of LPS-induced adipocytes and macrophages after treatment with *C. asiatica* extract. We observed that extract at a concentration of 500 $\mu\text{g/mL}$ attenuates inflammatory response in cells marked by significantly lower IL-6 mRNA expression in a coculture of adipocytes and macrophages compared to control of coculture of adipocytes and macrophages as shown in Figure 4D ($p = 0.026$).

4. Discussion

C. asiatica is a promising herb with anti-inflammatory and hypoglycemic activity. This study aimed to investigate the effect of *C. asiatica* extract on insulin sensitivity improvement related to the inflammatory response and its insulin signaling mechanism in a coculture of LPS-induced 3T3-L1 adipocytes and RAW 264.7 macrophages.

Direct contact between adipocytes and macrophages stimulates cytokines pro-inflammatory production such as IL-6, TNF- α , MCP-1, and IL-1 β which may, in turn alter insulin sensitivity in adipocytes (16,17). In this study, a direct coculture of 3T3-L1 adipocytes and RAW 264.7 macrophages treated with TLR-4 lipopolysaccharide (LPS) showed that direct contact between adipocytes and macrophages under LPS induction stimulated insulin resistance in the adipocytes. A coculture of adipocytes and macrophages showed glucose consumption impairment followed by degradation of GLUT-4 and IRS-1 mRNA. The coculture of adipocytes and macrophages under LPS induction also elevated IL-6 mRNA expression compared to the sum of IL-6 expression in adipocytes and macrophages without a co-culture. This result suggested that upregulated of *IL-6* gene expression caused by direct contact and LPS induction in a

coculture cells might lead to IRS-1 degradation resulting in GLUT-4 downregulation. GLUT-4 as a glucose transport is a key protein in the regulation of glucose in adipose tissue thus decreasing GLUT-4 mRNA expression should affect insulin sensitivity in adipocytes. It means that higher expression of pro-inflammatory cytokines in adipocyte tissue plays a pivotal role in the disruption of insulin sensitivity.

Insulin signaling impairment caused by pro-inflammatory cytokines might be influenced by upregulation of suppressor of cytokine signaling (SOCS)1/3 protein. A study conducted by Rui found that the activation and upregulation of the SOCS1/3 protein caused by pro-inflammatory cytokines altered insulin sensitivity in inflammation-induced adipocytes that have been shown to reduce IRS1/2 proteins by targeting them through ubiquitin-mediated proteasomal degradation (18).

C. asiatica extract at a concentration of 500 µg/mL was shown to improve insulin sensitivity in a coculture of LPS-induced 3T3-L1 adipocytes and RAW 264.7 macrophages. Increasing glucose consumption in a coculture of LPS-induced adipocytes and macrophages after treatment with the extract at a concentration of 500 µg/mL was followed by upregulation of *GLUT-4* and *IRS-1* gene expression in adipocytes. This result indicates that upregulation of *GLUT-4* and *IRS-1* gene expression in a coculture cells after treated with extract at a concentration of 500 µg/mL might be contributed to insulin sensitivity improvement in adipocytes.

C. asiatica extract at a concentration of 500 µg/mL attenuated inflammatory response in a coculture of LPS-induced 3T3-L1 adipocytes and RAW 264.7 macrophages by inhibiting the pro-inflammatory cytokine IL-6. This finding is consistent with the gene expression of *GLUT-4/IRS-1* and the glucose consumption results, indicating that the effect of *C. asiatica* extract to improve insulin sensitivity might be mediated through the IRS-1/GLUT-4 pathway as a result of inhibiting the pro-inflammatory cytokine IL-6.

Recent studies reported that leaf aqueous extract of *C. asiatica* at a concentration of 50 mg/kg of body weight has a glucose-lowering effect in alloxan-induced diabetic rats compared to diabetic and anti-diabetic drug groups (19). Other studies have also shown that an ethanol extract of *C. asiatica* has an anti-diabetic effect at a concentration of 200 mg/kg of body weight based on blood-glucose serum level compared to the control group (20). However, asiatic acid, as an active compound in *C. asiatica*, has anti-inflammatory activity by downregulating the pro-inflammatory cytokines IL-6, IL-1 β , and TNF- α in human corneal epithelial cells and the liver tissue of diabetic-induced mice (12,13). In addition, asiatic acid exerts anti-hyperglycemia effect in high fat diet (HFD)-induced diabetes mice through the PI3K/Akt/GSK β signaling pathway (21). Another previous study showed that asiatic acid at a dose of 20

mg/kg body decreased blood-glucose level in diabetic-induced rat using streptozotocin (STZ) followed by improved glucose uptake into skeletal muscle tissues via the IRS-1/PI3K-Akt signaling pathway (22).

IRS-1 is a key intracellular molecule that mediates insulin signaling through the IRS-1/PI3K/Akt pathway. Defects in or degradation of IRS-1 in adipocytes may be causes of insulin resistance (23). *IRS-1* gene disruption in obese mice impaired glucose transports, suggesting that insulin sensitivity in adipocytes is dependent on the expression of the IRS-1 protein (24-26). Upregulated *IRS-1* gene expression after treatment with *C. asiatica* at a concentration of 500 µg/mL might be related to its inflammation inhibition effect inducing macrophages to polarize into "macrophage alternatively activated" M2. A study conducted by Hawas found that treatment with *C. asiatica* at doses of 500 and 100 mg/kg of body weight prevented M1/M2 ratio from increasing in diabetic rats (27). This effect might trigger the deactivation of c-Jun-NH terminal kinase (JNK) and decrease SOCS1/3 expression which in turn affects IRS-1 upregulation. Increasing *GLUT-4* and *IRS-1* gene expression in adipocytes after treatment with *C. asiatica* might contribute to the adipocytes ability to take up glucose upon insulin stimulation.

In conclusion, *C. asiatica* extract alleviated the inflammatory response by inhibiting the pro-inflammatory cytokine IL-6 and improved insulin sensitivity in adipocytes marked by stimulated glucose consumption in a coculture cells that might be mediated via IRS-1/GLUT-4 insulin signaling pathway. However, further studies are required to evaluate more fully understanding about molecular actions of *C. asiatica* extract in insulin sensitivity improvement in adipocytes related to inflammatory changes.

Acknowledgments

We thank Professor Huang from the Department of Biological Science at NPUST Taiwan for providing us with the 3T3-L1 cells and RAW 264.7 cells as well as the Molecular Biology and Cell Culture Laboratory at LAPTIAB BPPT for supporting this experiment by providing access to its facilities and reagents.

References

1. Scheen A. Pathophysiology of type 2 diabetes. *Acta Clin Belg.* 2014; 110:335-341.
2. Sun K, Kusminski C, Scherer P. Adipose tissue remodeling and obesity. *J Clin Invest.* 2011; 121:2094-2101.
3. Pahlavani M, Ramalho T, Koboziev I, Lemieux M, Jayarathne S, Ramalingam L, Filgueiras L, Moustaid-Moussa N. Adipose tissue inflammation in insulin resistance: Review of mechanisms mediating anti-inflammatory effects of omega-3 polyunsaturated fatty acids. *J Investig Med.* 2017; 65:1021-1027.

4. Rotter V, Nagaev I, Smith U. Interleukin-6 (IL-6) induces insulin resistance in 3T3-L1 adipocytes and is, like IL-8 and tumor necrosis factor- α , overexpressed in human fat cells from insulin-resistant subjects. *J Biol Chem.* 2003; 278:45777-45784.
5. Pederson T, Kramer D, Rondinone C. Serine/threonine phosphorylation of IRS-1 triggers its degradation. *Diabetes.* 2001; 50:24-31.
6. Piera-Mardemootoo C, Lambert P, Faillie JL. Efficacy of metformin on glycemic control and weight in drug-naive type 2 diabetes mellitus patients: A systematic review and meta-analysis of placebo-controlled randomized trials. *Therapie.* 2018. pii: S0040-5957(18)30019-2.
7. Mutayabarwa C, Sayi J, Jande M. Hypoglycaemic Activity of *Centella Asiatica* (L) Urb. East Cent. Afr J Pharm Sci. 2003; 6:30-35.
8. Gayathri V, Lekshmi P, Padmanabhan R. Anti-diabetes activity of ethanol extract of *Centella asiatica* (L.) Urban (whole plant) in streptozotocin-induced diabetic rats, isolation of an active fraction and toxicity evaluation of the extract. *Int J Med Arom Plants.* 2011; 1:278-286.
9. Sasikala S, Lakshminarasiah S, Naidu M. Antidiabetic activity of *Centella asiatica* on streptozotocin induced diabetic male albino rats. *World J Pharm Sci.* 2015; 3:1701-1705.
10. Hashim P, Sidek H, Helan M, Sabery A, Palanisamy U, Ilham M. Triterpene composition and bioactivities of *Centella asiatica*. *Molecules.* 2011; 16:1310-1322.
11. Chen H, Hua X, Ze B, Wang B, Wei L. The anti-inflammatory effects of asiatic acid in lipopolysaccharide-stimulated human corneal epithelial cells. *Int J Ophthalmol.* 2017; 10:179-185.
12. Oyenih A, Chegou N, Oguntibeju O. *Centella asiatica* enhances hepatic antioxidant status and regulates hepatic inflammatory cytokines in type 2 diabetic rats. *Pharm Biol.* 2017; 55:1671-1678.
13. Cao SY, Wang W, Nan FF, Liu YN, Wei SY, Li FF, Chen L. Asiatic acid inhibits LPS-induced inflammatory response in endometrial epithelial cells. *Microb Pathog.* 2018; 116:195-199.
14. Twentyman P, Luscombe M. A study of some variables in a tetrazolium dye (MTT) based assay for cell growth and chemosensitivity. *Br J Cancer.* 1987; 56:279-285.
15. Zebisch K, Voigt V, Wabitsch M, Brandsch M. Protocol for effective differentiation of 3T3-L1 cells to adipocytes. *Anal Biochem.* 2012; 425:88-90.
16. Lumeng C, Deyoung S, Saltiel A. Macrophages block insulin action in adipocytes by altering expression of signaling and glucose transport protein. *Am J Physiol Endocrinol Metab.* 2007; 292:1-23.
17. Nakarai H, Yamashita A, Nagayasu S, Iwashita M, Kumamoto S, Ohyama H, Hata M, Soga Y, Kushiyama A, Asano T, Abiko Y, Nishimura F. Adipocyte-macrophage interaction may mediate LPS-induced low-grade inflammation: Potential link with metabolic complications. *Innate Immun.* 2012; 18:164-170.
18. Rui L, Yuan M, Frantz D, Shoelson S, White MF. SOCS-1 and SOCS-3 block insulin signaling by ubiquitin-mediated degradation of IRS1 and IRS2. *J Biol Chem.* 2002; 277:42394-42398.
19. Emran T, Dutta M, Uddin M, Nath, A, Uddin, Md. Antidiabetic potential of the leaf extract of *Centella asiatica* in alloxan-induced diabetic rats. *Jahangirnagar Univ J Biol Sci.* 2015; 4:51-59.
20. Gayathri V, Lekshmi P, Padmanabhan R. Anti-diabetes activity of ethanol extract of *Centella asiatica* (L.) Urban (whole plant) in streptozotocin-induced diabetic rats, isolation of an active fraction and toxicity evaluation of the extract. *Int J Med Arom Plants.* 2011; 1:278-286.
21. Sun W, Xu G, Guo X, Luo G, Wu L, Hou Y, Guo X, Zhou J, Xu T, Qin L, Fan Y, Han L, Matsabisa M, Ma X, Liu T. Protective effects of asiatic acid in a spontaneous type 2 diabetic mouse model. *Mol Med Rep.* 2017; 16:1333-1339.
22. Ramachandran V, Saravanan R. Glucose uptake through translocation and activation of GLUT4 in PI3K/Akt signaling pathway by asiatic acid in diabetic rats. *Hum Exp Toxicol.* 2015; 34:884-893.
23. Hoehn K, Hohnen-behrens C, Cederberg A, Wu L, Turner N, Yuasa T, Ebina Y, James D. IRS1-independent defects define major nodes of insulin resistance. *Cell Metab.* 2010; 7:421-433.
24. Araki E, Lipes M, Patti M, Bruning J, Haag BL III, Johnson RS, Kahn C. Alternative pathway of insulin signaling in mice with targeted disruption of the *IRS-1* gene. *Nature.* 1994; 372:186-190.
25. Tamemoto H, Kadowaki T, Tobe K, *et al.* Insulin resistance and growth retardation in mice lacking insulin receptor substrate-1. *Nature.* 1994; 372:182-186.
26. Patti M, Sun X, Bruning J, Araki E, Lipes M, White M, Kahn C. 4PS/IRS-2 is the alternative substrate of the insulin receptor in IRS-1 deficient mice. *J Biol Chem.* 1995; 270:24670-24673.
27. Hawas A., Nugrahaningsih A, Solikhah E, Syarifuddin A, Wijayaningsih R, Ngatidjan, Anti-inflammatory effect of *Centella asiatica* L. extract on prevented aortic intima-media thickening in diabetic rats. *J Pharm Sci.* 2017; 41:1-7.

(Received July 8, 2019; Revised August 24, 2019; Accepted October 22, 2019)

Royal jelly regulates the proliferation of human dermal microvascular endothelial cells through the down-regulation of a photoaging-related microRNA

Yuya Kawano¹, Katsunari Makino^{1,*}, Masatoshi Jinnin^{1,2,*}, Soichiro Sawamura¹, Shuichi Shimada¹, Satoshi Fukushima¹, Hironobu Ihn¹

¹Department of Dermatology and Plastic Surgery, Faculty of Life Sciences, Kumamoto University, Kumamoto, Japan;

²Department of Dermatology, Wakayama Medical University Graduate School of Medicine, Kimiidera, Wakayama, Japan.

Summary

Although royal jelly is believed to prevent skin aging, the underlying mechanism is not known in detail. In the present study, we investigated the plausibility of the involvement of microRNAs in the manifestation of this effect of royal jelly. The expression of microRNAs was determined by PCR array analysis and real-time PCR and the number of cells was counted with a cell counter. Using PCR array, we identified four microRNAs that were downregulated by royal jelly in cultured human dermal microvascular endothelial cells (HDMEC). Upon comparison of the expression of the four microRNAs between young and senescent facial skin, miR-129-5p was found to be significantly upregulated in senescent skin. Consistently, the expression of miR-129-5p in HDMEC was significantly increased by UVB radiation, suggesting that this microRNA is related to photoaging. The royal jelly treatment increased the number of HDMEC. Furthermore, forced overexpression of miR-129-5p resulted in significant decrease in the number of HDMEC, and its forced downregulation increased the number of cells. The number and density of vessels is reported to be decreased in aged skin. Our results indicate that miR-129-5p is induced in damaged endothelial cells upon exposure to UV radiation, which decreases the cell number. Furthermore, administration of royal jelly downregulated the expression of miR-129-5p in endothelial cells, and might prevent skin aging by maintaining the number of cells. The present study elucidates the mechanism of vessel aging caused by UV exposure and the anti-aging effects of royal jelly through the involvement of microRNA.

Keywords: Endothelial cells, microRNA, photoaging, royal jelly, skin aging

1. Introduction

Skin aging is known to be enhanced by ultraviolet (UV) rays, smoking, stress, and eating habits. These factors affect skin cells, including keratinocytes and fibroblasts, causing epidermal atrophy and denaturation of the extracellular matrix (ECM), which contains collagen

and elastic fibers. In addition, aging of endothelial cells has been reported to result in the loss of normal capillaries and in irregular dilation of the remaining vessels (1-4). Maintenance of normal vasculature becomes difficult because of these changes, and impaired blood circulation, decreased skin temperature, subcutaneous hematoma (referred to as senile purpura), and delayed wound healing are frequently noticed. The changes in vasculature are thought to play an important role in the problems that occur in aged skin.

Royal jelly is a product synthesized from pollen and is secreted by worker honeybees. It is fed to larvae, and is used in large quantities for the morphological development of queen bees. Although the queen bee and worker bees are genetically identical, the queen's intake of royal jelly prolongs its lifespan by an order-

*Address correspondence to:

Dr. Katsunari Makino, Department of Dermatology and Plastic Surgery, Faculty of Life Sciences, Kumamoto University, 1-1-1 Honjo, Kumamoto 860-8556, Japan.
E-mail: katsuderma@gmail.com

Dr. Masatoshi Jinnin, Department of Dermatology, Wakayama Medical University Graduate School of Medicine, 811-1 Kimiidera, Wakayama, Japan
E-mail: mjjin@wakayama-med.ac.jp

of-magnitude over that of worker bees (5). In humans, the administration of royal jelly affects various cell types, and its efficacy against aging, hypertension (6), and impairment of the motor function (7) have been described. Skin aging is also thought to be prevented by the intake of royal jelly (8), however, the detailed mechanism for it remains to be elucidated.

In the present study, we sought to determine the role of microRNAs in preventing the skin aging. MicroRNAs are ~22-nucleotide long non-coding RNAs. They regulate gene expression by binding to complementary sequences of 3' untranslated region of their target mRNAs, and thereby, inhibit their translation. Around 2,500 microRNAs have been found in the human genome, which control more than 60% of mRNAs, and are involved in regulating the activity or function of various cell types.

The present study aimed at determining the effect of royal jelly on the expression of microRNAs in skin cells. Furthermore, we elucidated the role microRNAs in the pathogenesis of skin aging and its prevention by the administration of royal jelly.

2. Materials and Methods

2.1. Reagents

The royal jelly powder (YDP-M-140830), standardized to contain a minimum of 3.85% (E)-10-hydroxy-2-decenoic acid and 0.67% 10-hydroxydecanoic acid, was obtained from Yamada Bee Co. Inc. (Okayama, Japan). The enzyme-treated royal jelly powder (YRP-M-140906) was standardized to contain a minimum of 3.5% (E)-10-hydroxy-2-decenoic acid and 0.67% 10-hydroxydecanoic acid. The powder was dissolved in distilled water, and used at a dose of 10 µg/mL.

2.2. Patient samples

Skin samples were obtained from routinely discarded facial skin of three elderly (aged 80-100 years) and three young (aged 0-15 years) individuals undergoing skin grafting. In the elderly individuals, the collected skin showed manifestations of photoaging, including wrinkles and sagging. Immediately after the removal, the skin samples were fixed in formalin and were embedded in paraffin. The study was approved by the institutional review board, and written informed consent was obtained from the patients in accordance with the Declaration of Helsinki.

2.3. Cell culture

Human dermal microvascular endothelial cells (HDMEC) were purchased from Takara (Shiga, Japan), and were cultured in a growth medium (EGM-2MV, Lonza, Walkersville, MD). Normal human epidermal

keratinocytes (NHEK) were obtained from Lonza, and were cultured in KGM-Gold (Lonza). Normal human dermal fibroblasts (NHDF) (ATCC, Manassas, VA) were cultured in Minimum Essential Medium (Sigma, St. Louis, MO).

2.4. PCR array analysis and real-time PCR of microRNAs

MicroRNAs were extracted from formalin-fixed, paraffin-embedded tissue sections with RNeasy FFPE Kit (QIAGEN, Valencia, CA). Total RNA from cultured cells was extracted using ISOGEN (Nippon Gene, Tokyo, Japan), and microRNAs were separated from total RNA using RT² qPCR-Grade miRNA Isolation Kit (SABiosciences, Frederick, MD). For the RT² Profiler PCR Array (QIAGEN), RNAs were reverse-transcribed into first-strand cDNAs using the RT² miRNA First Strand Kit (QIAGEN). The cDNAs were mixed with RT² SYBR Green/ROX qPCR Master Mix, and the mixture was added to the human cell differentiation and development-focused miScript[®] miRNA PCR Array (96-well format, QIAGEN), which includes primer pairs for 84 human microRNAs. PCR was performed on Takara Thermal Cycler Dice (TP800) (Takara Bio Inc., Shiga, Japan) in accordance with the manufacturer's protocol. The threshold cycle (Ct) for each microRNA was determined using the Thermal Cycler Dice Real Time System Ver.2.10B. The raw Ct values were normalized using the mean of Ct values for small RNA housekeeping genes. The primer sets for U6 (5'-cgettcacgaatttgctg tcat-3'), miR-129-5p (5'-cttttgcggctctggcctgc-3'), let-7i-5p (5'-tgaggtagtagtttgctgtt-3'), miR-124-3p (5'-taaggcagcgggtaatgcc-3'), miR-127-5p (5'-ctgaagctcagaggctctgat-3'), and miR-302a-3p (5'-taagtctccatggtttgtga-3') were used in this study.

For quantitative real-time PCR, the primers for miR-129-5p or U6 (QIAGEN) and the templates were mixed with SYBR Premix Ex TaqII (Takara Bio Inc.) (9). DNA was amplified for 60 cycles employing a denaturation step of 5 s at 95°C and an annealing step of 20 s at 60°C. The transcript levels of miR-129-5p were normalized to those of U6.

2.5. Transient transfection

The mimics and inhibitors of miR-129-5p were obtained from QIAGEN, and Lipofectamine RNAiMAX (Invitrogen) was used as the transfection reagent (10). The control mimic and inhibitor were also obtained from QIAGEN. For reverse transfection, microRNA mimics and inhibitors were mixed with the transfection reagent, and then added to the cells at the time of plating.

2.6. Cell counting

The cells were detached from the wells by trypsin

Table 1. Expression profiles of microRNAs in cultured cells treated with royal jelly, as measured by PCR array

Items	Endothelial cells			Keratinocytes		Fibroblasts	
	Control	RJ +	RJ -	control	RJ +	control	RJ +
let-7i-5p	1	0.37 ± 0.22*	0.43 ± 0.27*	1	1.84	1	2.89
miR-129-5p	1	0.18 ± 0.18*	0.17 ± 0.18*	1	1.77	1	2.64
miR-302a-3p	1	0.21 ± 0.21*	1.24 ± 1.12	1	93.70	0	0.0039
miR-124-3p	1	60.20 ± 54.95*	24.45 ± 18.79	1	2.14	0	2.87
miR-127-5p	1	0.13 ± 0.10*	1.96 ± 1.62	1	0.37	1	0.58

MicroRNAs were obtained from human dermal microvascular endothelial cells ($n = 3$), keratinocytes ($n = 1$), and fibroblasts ($n = 1$) cultured in the presence or absence of royal jelly (enzymatically treated [RJ+] or untreated [RJ-]) for 24 h. The microRNA expression profile for each cell was determined using the PCR array. The raw threshold cycle (Ct) was normalized using the Ct values for small RNA housekeeping genes. The fold-change was calculated as $1/2^{(\text{raw Ct of each microRNA} - \text{mean Ct of small RNA housekeeping genes})}$. The mean value obtained for the untreated control cells was set as '1'. For endothelial cells, the mean fold-change and standard deviation of each microRNA is shown. * p values < 0.05 compared with the values in control cells.

treatment, and counted using Coulter® Particle Counter (Beckman Coulter, Fullerton, CA), as described previously (11).

2.7. Statistical analysis

Mann-Whitney test was used for comparison of the median values. The values of means ± SD from three separate experiments are shown in each bar graph. A p value less than 0.05 was considered to be significant.

3. Results

3.1. Identification of microRNAs regulated by royal jelly in skin cells

To identify the microRNAs whose expression is regulated by royal jelly, HDMEC (at passages 7, 8, and 9) were cultured in the presence of enzyme-treated (RJ+) or untreated (RJ-) royal jelly for 24 h. For reference, we also added keratinocytes ($n = 1$) and fibroblasts ($n = 1$), exposed to enzyme-treated royal jelly, in this array. The expression profiles of 84 microRNAs involved in the differentiation and development of human cells were evaluated in the presence of royal jelly using the PCR array.

The expression levels of five microRNAs were significantly altered (as assessed by Mann-Whitney test) by more than 2-fold in the presence of enzyme-treated royal jelly (Table 1). The expression levels of let-7i-5p and miR-129-5p were significantly reduced by royal jelly that was not treated enzymatically (by 0.43- and 0.17-fold, respectively) as well as by enzyme-treated royal jelly (by 0.37- and 0.18-fold, respectively). Upon enzyme treatment, the proteins present in royal jelly are digested into small peptides, resulting in their better absorption. Given that enzyme-treated and untreated royal jelly suppress the expression of miR-129-5p to the same extent, the down-regulation of miR-129-5p seems to be the main effect of royal jelly. On the other hand, the expression of miR-302a-3p and miR-127-5p was significantly downregulated (by

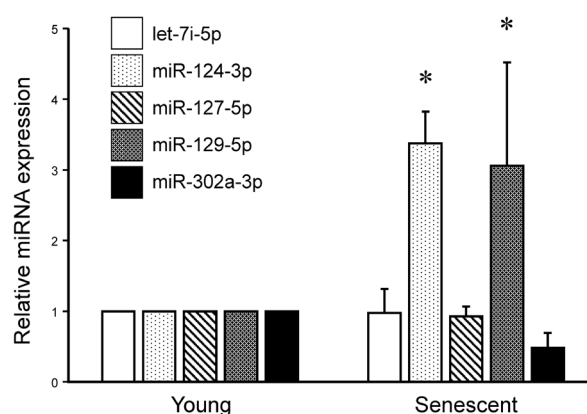


Figure 1. Total microRNA was extracted from skin samples of young ($n = 3$) and senescent ($n = 3$) facial skin. The relative expression levels of the five indicated microRNAs (normalized to the expression level of U6) were determined by using quantitative real-time PCR. The values for young skin were set as '1'. Bars indicate the mean values. $p < 0.05$, as assessed by Mann-Whitney test.

0.21- and 0.13-fold, respectively) only by the enzyme-treated royal jelly, but not by enzyme-untreated royal jelly (by 1.24- and 1.96-fold, respectively). In addition, the expression of miR-124-3p was only upregulated (by 60.2-fold) by enzyme-treated royal jelly.

3.2. Expression of miR-129-5p in senescent skin

The levels of the abovementioned five microRNAs were compared between the facial skin of three young individuals (0-15 years old) and three aging individuals (80-100 years old) (Figure 1). The expression levels of miR-124-3p and miR-129-5p were significantly enhanced ($p < 0.05$) in senescent facial skin. We focused on miR-129-5p because it was the only microRNA whose level was increased in senescent skin by both enzyme-treated and untreated royal jelly. Interestingly, the miR-129-5p levels were not altered by enzyme-treated royal jelly in cultured epidermal keratinocytes or in dermal fibroblasts, as assessed using the array (Table 1). This suggests that miR-129-5p is downregulated by royal jelly specifically in the

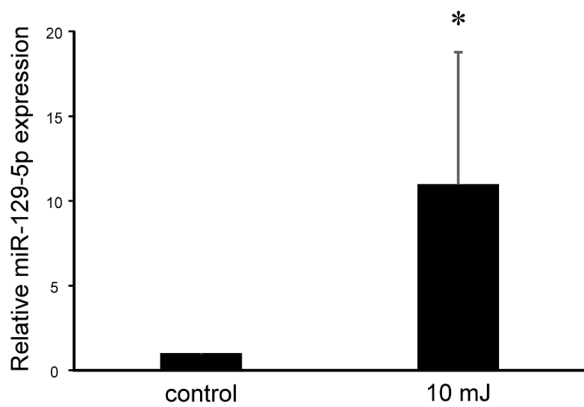


Figure 2. Human dermal microvascular endothelial cells (HDMEC) were exposed to UVB radiation at a dose of 10 mJ/cm²/day for three days. After 24 h, total microRNA was extracted, and the relative level of miR-129-5p (normalized to the expression level of U6) was determined by quantitative real-time PCR ($n = 3$). Bars show the mean values. * $p < 0.05$ compared to the values obtained for the untreated cells (1.0).

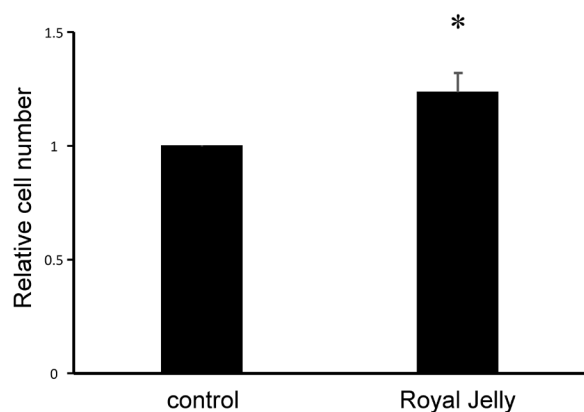


Figure 3. Human dermal microvascular endothelial cells (HDMEC; 1.5×10^5 cells/well) were incubated in 6-well culture plates in the presence or absence of enzyme-treated royal jelly (10 μ g/mL) for 48 h. The number of cells was counted as described in Materials and Methods section. The value for the untreated cells was set as '1'. * $p < 0.05$ ($n = 3$).

endothelial cells. Furthermore, miR-129-5p expression was significantly induced by UV irradiation in HDMEC (Figure 2), indicating that it is the microRNA that is related to photoaging. These findings led us to examine the mechanism through which miR-129-5p affects the function of HDMEC.

3.3. Significance of reduction in miR-129-5p levels in endothelial cells upon royal jelly treatment

Next, we determined the function of miR-129-5p in skin aging. Treatment with enzyme-treated royal jelly significantly increased the number of HDMEC ($p < 0.05$, Figure 3). Royal jelly did not affect the cell viability at 10 μ g/mL concentration. On the other hand, the transfection of microRNA mimic specific to

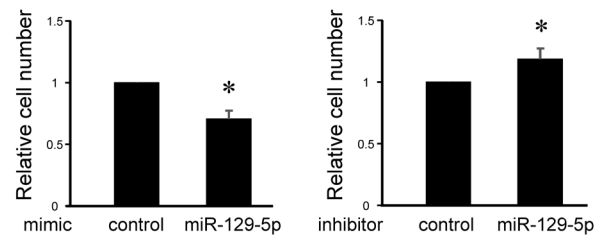


Figure 4. (Left) Human dermal microvascular endothelial cells (HDMEC), at a density of 1.5×10^5 cells/well, were transfected in 6-well culture plates with control or miR-129-5p mimic. (Right) HDMEC at a density of 1.5×10^5 cells/well were transfected in 6-well culture plates with control or miR-129-5p inhibitor. After 48 h, the number of cells was counted, as described in Materials and Methods section. The values for the cells transfected with the controls were set as '1'. * $p < 0.05$ compared to the value for the control cells ($n = 3$).

miR-129-5p significantly decreased the cell number compared to that in the case of control transfection, whereas treatment with the specific miR-129-5p inhibitor increased the cell number (Figure 4).

Based on these results, royal jelly may be thought to induce the cell number of HDMEC through the suppression of miR-129-5p, which is one of the microRNAs related to photoaging.

4. Discussion

Propolis has previously been shown to play a protective role against the arteriosclerosis of vessels by inducing the expression of miR-181a, miR-20b, and miR-106a (12). However, to the best of our knowledge, no association has been established between royal jelly and microRNAs, as of date. The present study, which was conducted to test our hypothesis that royal jelly controls skin aging through the regulation of microRNAs, provides three novel insights, as discussed below.

First, as for propolis, herein, we tried to identify microRNAs that are up- or downregulated in human skin cells (endothelial cells, keratinocytes, and fibroblasts), especially in endothelial cells, upon treatment with royal jelly. We performed PCR array of microRNAs involved in the differentiation and development of cells, and identified five microRNAs (let-7i-5p, miR-129-5p, miR-302a-3p, miR-124-3p, and miR-127-5p) that were regulated by royal jelly.

Next, when the expression of five microRNAs was compared between young facial skin and senescent skin, miR-124-3p and miR-129-5p were found to be significantly upregulated in the latter. Consistently, the expression of miR-129-5p in vascular endothelial cells was significantly increased upon exposure to UVB radiation. UVB is one of the main exogenous factors that mediate skin aging. The association between UVB and several microRNAs, such as miR-23a and -23b, was previously reported for other cell types (13,14), and our results show, for the first time, that miR-129-5p is also a photoaging-related microRNA in endothelial cells.

Lastly, we evaluated the possibility that royal jelly prevents skin aging through the suppression of miR-129-5p. The number of HDMEC was increased upon addition of royal jelly. Furthermore, the forced overexpression of miR-129-5p resulted in a significant suppression in the number of HDMEC, and forced downregulation of miR-129-5p induced it. It is reported that miR-129-5p negatively controls the proliferation of cells by regulating the cell cycle (15). Taken together, our results indicate that miR-129-5p is induced in damaged endothelial cells by UV radiation, which decreases the cell number. Furthermore, the administration of royal jelly downregulated the expression of miR-129-5p in endothelial cells, and may prevent skin aging by maintaining the number of cells. As described in the Introduction section, the number and density of vessels was reported to decrease in aged skin (1-4). Herein, we elucidated the mechanism of vessel aging by UV exposure and the anti-aging effects of the royal jelly through the involvement of microRNAs. Also, we previously reported that the expression of miR-124-3p is downregulated in squamous cell carcinoma (SCC), which is one of the most common skin cancers induced by chronic and cumulative UV irradiation (16). Because royal jelly enhanced the expression of miR-124-3p in keratinocytes in the present study, it may have preventive effects against SCC.

Further *in vivo* experiments would be required to prove that royal jelly can reduce the expression of miR-129-5p and can prevent photoaging of skin. Furthermore, miR-129-5p might not only be involved in increasing the number of cells, but might also prevent skin aging through the regulation of its target genes. However, further work would be needed to explore these molecular mechanisms. Many genes are predicted as putative targets of miR-129-5p using Targetscan (<http://www.targetscan.org>). These include calcium signaling-related molecules, such as calcium channel, voltage-dependent, γ subunit 2 (CACNG), calcium/calmodulin-dependent protein kinase II inhibitor 1 (CAMK2N1), FK506 binding protein 2, 13 kDa (FKBP2), and calmodulin 1 (phosphorylase kinase, delta) (CALM1). Considering the reported association between skin aging and calcium signaling (17), miR-129-5p could be one of the important microRNAs involved in skin aging. In addition, the regulation of calcium signaling by miR-129-5p may cause several changes, such as calcification or arteriosclerosis, in aged vessels.

Acknowledgements

We acknowledge Benjamin Phillis, Clinical Study Support Center, Wakayama Medical University, Japan for proofreading the manuscript. This study was supported in part by the Yamada Research Grant.

Conflict of Interest

Royal Jelly, both enzymatically treated and untreated, was provided in powdered form by Yamada Bee Company Inc., Okayama, Japan. The company had no role in the study design, data collection and analysis, decision to publish, or in the preparation of the manuscript. There are no other conflicts of interests to declare.

References

1. Kelly RI, Pearse R, Bull RH, Leveque JL, de Rigo J, Mortimer PS. The effects of aging on the cutaneous microvasculature. *J Am Acad Dermatol.* 1995; 33:749-756.
2. Kligman AM. Perspectives and problems in cutaneous gerontology. *J Invest Dermatol.* 1979; 73:39-46.
3. Gilchrist BA, Stoff JS, Soter NA. Chronologic aging alters the response to ultraviolet-induced inflammation in human skin. *J Invest Dermatol.* 1982; 79:11-15.
4. Chung JH, Eun HC. Angiogenesis in skin aging and photoaging. *J Dermatol.* 2007; 34:593-600.
5. Haddad LS, Delbert L, Hubert AJ. Extended longevity of queen honey bees compared to workers is associated with peroxidation-resistant membranes. *Exp Gerontol.* 2007; 42:601-609.
6. Niu K, Guo H, Guo Y, Ebihara S, Asada M, Ohru T, Furukawa K, Ichinose M, Yanai K, Kudo Y, Arai H, Okazaki T, Nagatomi R. Royal jelly prevents the progression of sarcopenia in aged mice *in vivo* and *in vitro*. *J Gerontol A Biol Sci Med Sci.* 2013; 68:1482-1492.
7. Okumura N, Toda T, Ozawa Y, Watanabe K, Ikuta T, Tatefuji T, Hashimoto K, Shimizu T. Royal jelly delays motor functional impairment during aging in genetically heterogeneous male mice. *Nutrients.* 2018; 10:1191.
8. Park HM, Hwang E, Lee KG, Han SM, Cho Y, Kim SY. Royal jelly protects against ultraviolet B-induced photoaging in human skin fibroblasts *via* enhancing collagen production. *J Med Food.* 2011; 14:899-906.
9. Makino K, Jinnin M, Aoi J, Hirano A, Kajihara I, Makino T, Sakai K, Fukushima S, Inoue Y, Ihn H. Discoidin domain receptor 2-microRNA 196a-mediated negative feedback against excess type I collagen expression is impaired in scleroderma dermal fibroblasts. *J Invest Dermatol.* 2013; 133:110-119.
10. Makino K, Jinnin M, Hirano A, Yamane K, Eto M, Kusano T, Honda N, Kajihara I, Makino T, Sakai K, Masuguchi S, Fukushima S, Ihn H. The downregulation of microRNA let-7a contributes to the excessive expression of type I collagen in systemic and localized scleroderma. *J Immunol.* 2013; 190:3905-3915.
11. Jinnin M, Ihn H, Mimura Y, Asano Y, Yamane K, Tamaki K. Regulation of fibrogenic/fibrolytic genes by platelet-derived growth factor C, a novel growth factor, in human dermal fibroblasts. *J Cell Physiol.* 2005; 202:510-517.
12. Cuevas A, Saavedra N, Cavalcante MF, Salazar LA, Abdalla DS. Identification of microRNAs involved in the modulation of pro-angiogenic factors in atherosclerosis by a polyphenol-rich extract from propolis. *Arch Biochem Biophys.* 2014; 557:28-35.

13. Zhang JA, Zhou BR, Xu Y, Chen X, Liu J, Gozali M, Wu D, Yin ZQ, Luo D. MiR-23a-depressed autophagy is a participant in PUVA- and UVB-induced premature senescence. *Oncotarget*. 2016; 7:37420-37435.
14. Kraemer A, Chen IP, Henning S, Faust A, Volkmer B, Atkinson MJ, Moertl S, Greinert R. UVA and UVB irradiation differentially regulate microRNA expression in human primary keratinocytes. *PLoS One*. 2013; 8:e83392.
15. Gu X, Gong H, Shen L, Gu Q. MicroRNA-129-5p inhibits human glioma cell proliferation and induces cell cycle arrest by directly targeting DNMT3A. *Am J Transl Res*. 2018; 10:2834-2847.
16. Harada M, Jinnin M, Wang Z, Hirano A, Tomizawa Y, Kira T, Igata T, Masuguchi S, Fukushima S, Ihn H. The expression of miR-124 increases in aged skin to cause cell senescence and it decreases in squamous cell carcinoma. *Biosci Trends*. 2017; 10:454-459.
17. Rinnerthaler M, Streubel MK, Bischof J, Richter K. Skin aging, gene expression and calcium. *Exp Gerontol*. 2015; 68:59-65.

(Received September 4, 2019; Revised October 27, 2019; Accepted October 28, 2019)

Profile and predictors of hepatitis and HIV infection in patients on hemodialysis of Quetta, Pakistan

Ammara Lodhi¹, Ashif Sajjad^{1,*}, Khalid Mehmood¹, Ayesha Lodhi², Sabeena Rizwan³, Ayesha Ubaid³, Kulsoom Baloch¹, Sheikh Ahmed¹, Mohkam ud din⁴, Zahid Mehmood¹

¹Institute of Biochemistry, University of Balochistan, Sariab Road, Quetta, Pakistan;

²Chengde Medical University, Chengde, Hebei, China;

³Department of Chemistry, Sardar Bahadur Khan, Women's University, Quetta, Pakistan;

⁴Balochistan Institute of Nephrology and Urology, Quetta, Pakistan.

Summary

Hemodialysis (HD) is the most commonly used treatment in patients with end-stage renal failure or disease (ESRD) worldwide. Blood-borne viral diseases are the major causes of mortality and morbidity in patients on HD. This study aims to analyze the prevalence and to concentrate on the key risk factors that are responsible for hepatitis B virus (HBV), hepatitis C virus (HCV), and human immunodeficiency virus (HIV) infection in patients on HD visiting two dialysis centers in the city of Quetta in southwestern Pakistan. The overall incidence of HBV was found to be 16.1%, the overall incidence of HCV was found to be 43.2%, and two patients (1.6%) were found to be positive for both HBV and HCV. HIV was not found among patients seen at both hospitals during the study period. The main risk factors for development of a viral infection were the length of time on HD ($p = 0.007$), number of sessions ($p = 0.001$), and level of education ($p = 0.092$). Biochemical and hematological parameters including urea, creatinine, uric acid, and calcium levels, red blood cell count, white blood cell count, hemoglobin levels, and platelet count were also studied in patients on HD. HD is becoming one of the major factors causing a viral infection because a patient can possibly become infected during an HD session via a blood transfusion, dialysis machines, instruments and/or other contaminated equipment. In order to control the spread of viral infections, increased public awareness, vaccinations, and health education programs for both health care providers and patients are needed, and proper screening programs should be instituted before dialysis is performed.

Keywords: Hemodialysis, hepatitis B, hepatitis C, HIV infection

1. Introduction

Hepatitis B virus (HBV), hepatitis C virus (HCV), and human immunodeficiency virus (HIV) infections are becoming major public health problems. Patients with chronic kidney failure or end-stage renal disease usually undergo hemodialysis (HD) (1) and are at increased risk of developing a viral infection. The major reason for the high prevalence of HBV and HCV in patients on HD is related to vascular access. Patients on HD are at

high risk of possible exposure to infected individuals due to the lack of standard preventive methods, effective vaccination, and contaminated and/or cross-contaminated dialysis machines (2).

HBV and HCV cause acute and chronic liver inflammation and damage, ranging from a minor liver disorder like cirrhosis to hepatocellular carcinoma, which is the main reason for the high mortality and morbidity rate in patients on HD (3). Measures to detect the incidence of HBV and HCV infections in HD units/centers and to address the risk factors for their spread help health care planners in a country to work more efficiently. The aim of the current study was to analyze the prevalence and to concentrate on the key risk factors causing HBV, HCV, and HIV viral infections

*Address correspondence to:

Dr. Ashif Sajjad, Institute of Biochemistry, University of Balochistan, Sariab Road, Quetta, Pakistan 87300.

Email: ashif.sajjad@um.uob.edu.pk

in patients on HD in the Quetta District of Pakistan. The obtained information would be useful for health education programs, for patients on HD, and for health care personnel to control the further spread of viral infections in dialysis units.

2. Materials and Methods

2.1. Study design

A cross-sectional time-bounded study was conducted from June to September 2018 at two tertiary care public hospitals, Balochistan Institute of Nephrology and Urology, Quetta (BINUQ) and Sandeman Provincial Hospital (SPH), located in the Quetta District of Balochistan Province, Pakistan. BINUQ is a dedicated hospital for kidney diseases, and SPH is a general hospital. Both hospitals have two separate sections for HBV and HCV sero-positive and negative patients.

2.2. Study sampling tools and procedures

Subjects were a total of 118 patients who were diagnosed with either HBV or HCV. Written consent was obtained from each patient. Data were collected using a pre-tested structured questionnaire asking about socio-demographic data (age, gender, locality, marital status, level of education, occupation, and income), patient-related factors (cause of renal failure, co-morbidity, total years since the 1st session, and the length of time on HD), and clinical factors (family history of receiving dialysis, current status of HBV, HCV, and HIV, timing of initial onset, and laboratory results). Patient files were used to supplement information and clinical data. A blood sample of 5 mL was collected in an EDTA tube from each patient using the standard procedures for peripheral venipuncture before commencement of the HD session. The collected blood samples were stored at 4°C for analysis.

2.3. Serological testing

The collected blood samples were tested for HBV, HCV, and HIV with an immunochromatographic test (ICT) and/or chemiluminescence immunoassay (CLIA). Kits were used per the manufacturer's instructions to detect the presence of hepatitis B surface antigen (HBsAg) (HEXAGON HBsAg Immunochromatographic 1-Step test), anti-HCV antibodies (Onsite HCV Ab Plus Rapid Test), and anti-HIV antibodies (OneSite human immunodeficiency virus (HIV)-1/2 Ab Plus Combo Rapid Test). Non-reactive samples were considered to be negative and were not tested further. In the event of a positive or reactive result, the sample was tested again with an alternative testing method such as a CLIA per the manufacturer's instructions before a final diagnosis was made.

The collected blood samples were further tested for creatinine, urea, calcium, and uric acid levels. Commercial kits were used per the manufacturer's instructions. A complete blood count (CBC) was performed on a Medonic hematology analyzer (Stockholm, Sweden). The following parameters were included in the CBC: hemoglobin (HB) level, red blood cell (RBC) count, white blood cell (WBC) count, and platelet (PLTS) count. Controls were provided by the manufacturer and external controls were used.

2.4. Statistical analysis

Data were analyzed using SPSS v 22. Demographic characteristics were analyzed using a basic statistical tool (percentage and frequency for categorical variables and mean standard deviation SD for continuous variables). The presence of an infection was predicted with an inferential statistic using the chi-square test to determine the association between demographic characteristics and the presence of an infection.

3. Results

In the current study, 118 patients received HD at two government-run dialysis centers in the Quetta District. Of the patients studied, 93 were received dialysis at the BINUQ dialysis center and 25 received dialysis at the Civil Hospital in the Quetta District. All of the patients were on HD for more than one month, and a blood sample was collected during the first dialysis session. Of the 118 patients tested, 71 were male and 47 were female; 18 (15.3%) were positive for HBV, 52 (44.1%) were positive for HCV, 2 (1.69%) were positive for an HBV/HCV co-infection, and none were positive for HIV (Table 1). Patients ranged in age from 33-42 years. The mean age of HBV-positive patients on HD was 42.56 ± 16.80 years while the mean age of HBV-negative patients on HD was 43.36 ± 14.56 years. The incidence of HBV among the patients studied was found to be 16.1%. Positivity for HBV was higher among males than females ($p = 0.929$) (Table 2). An analysis of the obtained data revealed no significant association between HBV infection and patient age ($p = 0.663$). HBV infection was not significantly related to biochemical and/or hematological parameters such as

Table 1. Frequency distribution and percentage of several variables in patients on hemodialysis

Variable	Description	Frequency	%
Gender	Males	71	60.1
	Females	47	39.8
Viral Infection	HBV	18	15.3
	HCV	52	44.1
	HBV/HCV (co-infection)	02	1.69
	HIV	–	–

Table 2. Comparison between HBV, HCV, and HIV infection with risk factors in patients on hemodialysis

Variable	HBV Positive	HBV Negative	P value	HCV-positive	HCV-negative	P value
Age (Mean Age)	42.56 ± 16.80	43.36 ± 14.56	0.663	43.02 ± 13.69	43.41 ± 15.84	0.993
Gender						
Male	11 (61.1%)	60 (60.0%)	0.929	30 (57.7%)	41 (62.1%)	0.626
Female	7 (38.9%)	40 (40.0%)		22 (42.3%)	25 (37.9%)	
Marital Status						
Married	15 (83.3%)	87 (87.0%)	0.676	47 (90.4%)	55 (83.3%)	0.267
Single	3 (16.7%)	13 (13.0%)		5 (9.6%)	11 (16.7%)	
Locality						
Rural	5 (27.8%)	34 (34.0%)	0.605	17 (32.7%)	22 (33.3%)	0.941
Urban	13 (72.2%)	66 (66.0%)		35 (67.3%)	44 (66.7%)	
Education						
Illiterate	10 (55.6%)	35 (35.0%)	0.431	25 (48.1%)	20 (30.3%)	0.092
Religious	0 (0.0%)	7 (7.0%)		4 (7.7%)	3 (4.5%)	
Primary school	1 (5.6%)	9 (9.0%)		5 (9.6%)	5 (7.6%)	
Middle school	2 (11.1%)	8 (8.0%)		4 (7.7%)	6 (9.1%)	
Matriculated	4 (22.2%)	18 (18.0%)		6 (11.5%)	16 (24.2%)	
Intermediate	0 (0.0%)	8 (8.0%)		5 (9.6%)	3 (4.5%)	
Graduate	1 (5.6%)	15 (15.0%)		3 (5.8%)	13 (19.7%)	
Occupation						
Unemployed	6 (33.3%)	18 (18.0%)	0.520	9 (17.3%)	15 (22.7%)	0.702
Working part-time while studying	1 (5.6%)	11 (11.0%)		4 (7.7%)	8 (12.1%)	
Employee of private firm	2 (11.1%)	5 (5.0%)		2 (3.8%)	5 (7.6%)	
Government employee	3 (16.7%)	15 (15.0%)		8 (15.4%)	10 (15.2%)	
Self-employed	1 (5.6%)	20 (20.0%)		11 (21.2%)	10 (15.2%)	
Housewife	5 (27.8%)	30 (30.0%)		17 (32.7%)	18 (27.3%)	
Retired	0 (0.0%)	1 (1.0%)		1 (1.9%)	0 (0.0%)	
Income per month in USD						
Less than 50 USD	4 (22.2%)	21 (21.0%)	0.427	11 (21.2%)	14 (21.2%)	0.211
From 50-100	5 (27.8%)	17 (17.0%)		13 (25.0%)	9 (13.6%)	
More than 100	7 (38.9%)	34 (34.0%)		19 (36.5%)	22 (33.3%)	
No income	2 (11.1%)	28 (28.0%)		9 (17.3%)	21 (31.8%)	
Length of Time on Hemodialysis						
Less than 3 Months	0 (0.0%)	5 (5.0%)	0.007	2 (3.8%)	3 (4.5%)	0.409
3-6 months	5 (27.8%)	8 (8.0%)		4 (7.7%)	9 (13.6%)	
7-12 months	3 (16.7%)	15 (15.0%)		7 (13.5%)	11 (16.7%)	
1-3 years	3 (16.7%)	55 (55.0%)		29 (55.8%)	29 (43.9%)	
4-6 years	7 (38.9%)	15 (15.0%)		8 (15.4%)	14 (21.2%)	
7-9 years	0 (0.0%)	2 (2.0%)		2 (3.8%)	0 (0.0%)	
Frequency of Hemodialysis Sessions						
Twice weekly	18 (100.0%)	75 (75.0%)	0.017	51 (98.1%)	42 (63.6%)	0.001
Thrice weekly	0 (0.0%)	25 (25.0%)		1 (1.9%)	24 (36.4%)	

urea, creatinine, uric acid, and calcium levels, the RBC count, WBC count, HB level, and platelet count. HBV-positive patients had a mean blood urea level of 145.60 ± 48.45 mg/dL while HBV-negative patients had a mean blood urea level of 144.98 ± 56.60 mg/dL ($p = 0.818$). HBV-positive patients had a mean creatinine level of 7.46 ± 2.33 mg/dL while HBV-negative patients had a mean creatinine level of 7.50 ± 1.74 mg/dL ($p = 0.817$). HBV-positive patients had a mean uric acid level of 7.26 ± 2.21 mg/dL while HBV-negative patients had a mean uric acid level of 6.97 ± 1.74 mg/dL ($p = 0.99$). HBV-positive patients had a mean calcium level of 8.12 ± 0.26 mg/dL while HBV-negative patients had a mean calcium level of 7.36 ± 1.90 mg/dL ($p = 0.446$). HBV-positive patients had a mean RBC count of 3.11 ± 0.32 million cells/mcL while HBV-negative patients had a mean RBC count of 13.51 ± 20.41 million cells/mcL ($p = 0.218$). HBV-positive patients had a mean WBC count of 7.45 ± 4.12 thousand cells/mcL while HBV-

negative patients had a mean WBC count of 11.30 ± 15.63 thousand cells/mcL ($p = 0.767$). HBV-positive patients had a mean HB level of 8.60 ± 1.49 gm/dL while HBV-negative patients had a mean HB level of 13.51 ± 20.41 gm/dL ($p = 0.530$). HBV-positive patients had a mean platelet count of 179.80 ± 65.15 platelets/mcL while HBV-negative patients had a mean platelet count of 208.55 ± 87.89 platelets/mcL ($p = 0.408$) (Table 3). HBV infection was significantly related to the length of time on HD ($p = 0.007$) and the frequency of HD sessions ($p = 0.017$) (Table 2).

The overall prevalence of HCV was 43.2% among patients on HD the two dialysis centers in the Quetta District. HBV infection was not significantly related to patient age ($p = 0.993$). The mean age of HCV-positive patients on HD was 43.02 ± 13.69 years while the mean age of HCV-negative patients on HD was 43.41 ± 15.84 years (Table 2). Positivity for HCV was higher among males than females ($p = 0.626$) (Table 2). HCV

Table 3. Comparison between HBV and HCV infection and biochemical and hematological parameters in patients on hemodialysis.

Variable (mean values)	HBV Positive	HBV Negative	P value	HCV-positive	HCV-negative	P value
Urea (mg/dL)	145.60 ± 48.45	144.98 ± 56.60	0.818	144.98 ± 56.60	145.60 ± 48.45	0.916
Creatinine (mg/dL)	7.46 ± 2.33	7.50 ± 1.74	0.817	7.50 ± 1.74	7.40 ± 2.33	0.88
Uric Acid (mg/dL)	7.26 ± 2.21	6.97 ± 1.74	0.99	6.97 ± 1.64	7.26 ± 2.21	0.99
Calcium (mg/dL)	8.12 ± 0.26	7.36 ± 1.90	0.446	7.36 ± 1.90	8.12 ± 0.26	0.446
WBC (thousand cells/mcL)	7.45 ± 4.12	11.30 ± 15.63	0.767	11.30 ± 15.63	7.45 ± 4.12	0.766
RBC (million cells/mcL)	3.11 ± 0.32	13.51 ± 20.41	0.218	3.60 ± 0.69	3.11 ± 0.32	0.218
HB (g/dL)	8.60 ± 1.49	13.51 ± 20.41	0.530	13.51 ± 20.41	8.60 ± 1.49	0.530
Platelets (platelets/mcL)	179.80 ± 65.15	208.55 ± 87.89	0.408	208.55 ± 87.89	178.80 ± 65.15	0.408

positivity was not significantly related to patient gender ($p = 0.626$) (Table 2). The incidence of HCV infection and level of education were significantly related ($p = 0.092$). Most of the patients with an HCV infection were illiterate (48.1%) or had matriculated (11.5%). Additional risk factors for HCV positivity included the frequency of HD sessions ($p = 0.001$) (Table 2). HCV was not significantly related to serum levels of urea, creatinine, uric acid, calcium, or HB or to RBC, WBC, or platelet counts. HCV-positive patients had a mean urea level of 144.98 ± 56.60 mg/dL while HCV-negative patients had a mean urea level of 145.60 ± 48.45 mg/dL ($p = 0.916$). HCV-positive patients had a mean creatinine level of 7.50 ± 1.74 mg/dL while HCV-negative patients had a mean creatinine level of 7.40 ± 2.33 mg/dL ($p = 0.88$). HCV-positive patients had a mean uric acid level of 6.97 ± 1.64 of mg/dL while HCV-negative patients had a mean uric acid level of 7.26 ± 2.21 mg/dL ($p = 0.99$). HCV-positive patients had a mean calcium level of 7.36 ± 1.90 mg/dL while HCV-negative patients had a mean calcium level of 8.12 ± 0.26 mg/dL ($p = 0.44$). HCV-positive patients had a mean RBC count of 3.60 ± 0.69 million cells/mcL while HCV-negative patients had a mean RBC count of 3.11 ± 0.32 million cells/mcL ($p = 0.218$). HCV-positive patients had a mean WBC count of 11.30 ± 15.63 thousand cells/mcL while HCV-negative patients had a mean WBC count of 7.45 ± 4.12 thousand cells/mcL ($p = 0.766$). Patients positive for HCV had a mean HB level of 13.51 ± 20.41 g/dL while patients negative for HCV had a mean HB level of 8.60 ± 1.49 g/dL ($p = 0.53$). HCV-positive patients had a mean platelet count of 208.55 ± 87.89 platelets/mcL, while HCV-negative patients had a mean platelet count of 178.80 ± 65.15 platelets/mcL ($p = 0.408$) (Table 3). The obtained values were compared with normal reference ranges, but a direct relationship between the studied parameters and both HBV and HCV infection was not noted.

4. Discussion

An HBV, HCV, or HIV viral infection is considered to be a major health hazard for patients on HD and the medical staff of dialysis units/centers (4). Among the patients studied, the prevalence of HBV was 16.1%.

The observed prevalence is quite high compared to that in other studies conducted in different countries and regions like Jordan (5.9%), Gaza (8.1%), Saudi Arabia (10%), and Bahrain (11.8%) (5). This observed difference in prevalence of infection might remain because of the variation in the extent of the implementation of universal safety measures in order to prevent the nosocomial spread of viral diseases. In the current study, there was a significant association between HBV and the frequency of HD sessions and the years on HD, and this finding agrees with the results of a study conducted in Jordan (6). In general, most of the patients with a chronic kidney disease in the Quetta District and those who need major surgery are treated in different hospitals in different cities in Pakistan. Some of the patients had undergone HD during treatment in another city. A previous study in India reported that traveling to other cities is also associated with an increased risk of becoming infected with the hepatitis virus and/or HIV, and this risk would presumably increase when traveling to distant areas (4). As mentioned above, the observed difference between the incidence of HBV and the length of time on HD and the frequency of HD sessions might be due to variation in the type of surgical procedure, the medical facility, and associated factors in countries where surgery is performed. An HBV infection was not significantly related to patient age or income. Patients younger than 42 years of age had a greater risk of infection with HBV than older patients. Among the patients undergoing HD in the Quetta District in the current study, those 33 to 42 years of age had the highest incidence of HBV infection. Males had a higher risk of HBV infection than females. This might be related to the fact that males are more socially active and exposed to risk factors for development of an HBV infection (*e.g.* hair dressing, contaminated razors for shaving, blood donation, unsterilized instruments, and needles used in different types of surgery) than females. These findings are in accordance with the results of a previous study of the general population in the Karachi District of Pakistan (7). The reported incidence of HCV among patients on HD in Karachi was 43.2%, indicating that the observed prevalence of HCV in the current study was higher than that in Tunisia (19.1%),

Lebanon (27%), and Jordan (34.6%) and lower than that in Syria (75%) (8,9). The prevalence of HCV differed among HD units/centers; as stated earlier, the difference in prevalence of infection was due to different types of universal safety measures that are implemented in different units. Similar results were reported in previous studies conducted in Jordan and Lebanon (8,10). The current study noted no relationship between the incidence of HCV and patient gender, age, or income. This finding agrees with the results of a previous study (11), but HCV was significantly related to the frequency of HD sessions and conditions for HD, indicating that the risk factors for development of an HCV in patients on HD increased with a longer time on HD. Previous studies in different regions around the world have reported similar results (12,13). In the current study, most of the HCV-positive patients were illiterate or had matriculated (10 years of schooling). This finding agrees with the results of a previous large-scale study reporting that less educated people had a higher prevalence of HCV infection than educated people (14). Two patients in the current study (1.6%) were positive for both HBV and HCV, which is quite low when compared to the results of a study conducted in Moldavia that reported co-infection at a rate of 17% (6). Laboratory results were not significantly related to HBV, HCV, or HIV. In Pakistan, the prevalence of HBV and HCV is quite high, and nationwide efforts are required to identify people who are infected. In the current study, none of the patients studied were infected with HIV. This finding is similar to the results of a previous study conducted in Baghdad, Iraq (15). The prevalence of HIV among patients on HD was 0% in the Jenin District of Palestine, 6% in Nigeria, and 7% in the US; these rates are much lower than 33% in Kosovo, 39% in Morocco, 50% in France, and 51% in Spain (16).

5. Conclusion

To the extent known, the prevalence of HBV, HCV, and HIV among patients on HD has never been examined in the Quetta District of Balochistan. This study of viral infections among patients on HD was conducted to obtain baseline information for medical personnel. In the current study, HBV and HCV infections were prevalent among patients on HD in the Quetta District. None of the patients studied had HIV, which could be due to socio-cultural beliefs and practices. HD is becoming one of the major factors causing viral infections like HBV, HCV, or HIV because a patient on HD can contract an infection *via* blood transfusion, dialysis machines, instruments or other contaminated equipment. In order to control the spread of viral infections, increased public awareness, vaccinations, and health education programs for both health care providers and patients are needed, and

proper screening programs should be instituted before dialysis is performed.

Acknowledgments

The authors wish to thank all of the patients who provided blood samples for this study. The authors also wish to thank the Chief Executive Officer of the Balochistan Institute of Nephrology and Urology, Quetta (BINUQ) and the Medical Superintendent of Sandeman Provincial Hospital (SPH), Quetta, for their cooperation.

References

1. Go AS, Chertow GM, Fan D, McCulloch CE, Hsu CY. Chronic kidney disease and the risks of death, cardiovascular events, and hospitalization. *N Engl J Med.* 2004; 351:1296-305.
2. Fabrizi F, De Vecchi AF, Como G, Lunghi G, Martin P. De novo HCV infection among dialysis patients: A prospective study by HCV core antigen ELISA assay. *Aliment Pharmacol Ther.* 2005; 21:861-9.
3. Idrees MK, Batool S, Ahmed E. Hepatitis B virus among maintenance haemodialysis patients: A report from Karachi, Pakistan. *J Pak Med Assoc.* 2011; 34:12-68.
4. Jauréguiberry S, Grandière-Pérez L, Ansart S, Laklache H, Métivier S, Caumes E. Acute hepatitis C virus infection after a travel in India. *J Travel Med.* 2005; 12:55-56.
5. Al Hijazat M, Ajlouni YM. Hepatitis B infection among patients receiving chronic hemodialysis at the Royal Medical Services in Jordan. *Saudi J Kidney Dis Transpl.* 2008; 19:260.
6. Covic A, Iancu L, Apetrei C, Scripcaru D, Volovat C, Mititiuc I, Covic M. Hepatitis virus infection in haemodialysis patients from Moldavia. *Nephrol Dial Transplant.* 1999; 14:40-45.
7. Akhtar S, Younus M, Adil S, Hassan F, Jafri SH. Epidemiologic study of chronic hepatitis B virus infection in male volunteer blood donors in Karachi, Pakistan. *BMC Gastroenterol.* 2005; 5:26.
8. Ayed K, Gorgi Y, Ben TA, Aouadi H, Jendoubi-Ayed S, Sfar I, Makni H. Hepatitis C virus infection in hemodialysis patients from Tunisia: National survey by serologic and molecular methods. *Transplant Proc.* 2003; 35:2573-2575.
9. Bdoor S. Hepatitis C virus infection in Jordanian haemodialysis units: Serological diagnosis and genotyping. *J Med Microbiol.* 2002; 51:700-704.
10. Naman RE, Mansour I, Klayme S, Khalil G. Hepatitis C virus in hemodialysis patients and blood donors in Lebanon. *J Med Liban.* 1996; 44:4-9.
11. Lopes EP, Gouveia EC, Albuquerque AC, Sette LH, Mello LA, Moreira RC, Coelho MR. Determination of the cut-off value of serum alanine aminotransferase in patients undergoing hemodialysis, to identify biochemical activity in patients with hepatitis C viremia. *J Clin Virol.* 2006; 35:298-302.
12. Mohtasham AZ, Jaefari SA, Toorchi RM. Seroprevalence of hepatitis C and risk factors in hemodialysis patients in Guilan province, Iran. *PAYESH.* 2003; 2:291-295.
13. Zahedi MJ, Moghaddam SD, Alavian SM, Dalili M.

- Seroprevalence of hepatitis viruses B, C, D and HIV infection among hemodialysis patients in Kerman Province, South-East Iran. *Hepat Mon.* 2012; 12:339-343.
14. El-Sadawy M, Ragab H, El-Toukhy H, el-Mor AL, Mangoud AM, Eissa MH, Afefy AF, El-Shorbagy E, Ibrahim IA, Mahrous S, Abdel-Monem A. Hepatitis C virus infection at Sharkia Governorate, Egypt: Seroprevalence and associated risk factors. *J Egypt Soc Parasitol.* 2004; 3:67-84.
 15. Kamal IM, Mahdi BM. Seroprevalence occurrence of viral hepatitis and HIV among hemodialysis patients. *Ann Med Surg.* 2018; 29:1-4.
 16. Abumwais JQ, Idris OF. Prevalence of hepatitis C, hepatitis B, and HIV infection among hemodialysis patients in Jenin District (Palestine). *Iran J Virol.* 2010; 4:38-44.

(Received June 16, 2019; Revised August 27, 2019; Re-revised October 21, 2019; Accepted October 23, 2019)

Catheter tips are a possible resource for biological study on catheter failure

Toshiaki Takahashi¹, Takeo Minematsu^{2,3}, Ryoko Murayama^{3,4}, Gojiro Nakagami^{3,5}, Taketoshi Mori^{1,3}, Hiromi Sanada^{3,5,*}

¹ Department of Life Support Technology (Molten), Graduate School of Medicine, The University of Tokyo, Tokyo, Japan;

² Department of Skincare Science, Graduate School of Medicine, The University of Tokyo, Tokyo, Japan;

³ Division of Care Innovation, Global Nursing Research Center, Graduate School of Medicine, The University of Tokyo, Tokyo, Japan;

⁴ Department of Advanced Nursing Technology, Graduate School of Medicine, The University of Tokyo, Tokyo, Japan;

⁵ Department of Gerontological Nursing/Wound Care Management, Graduate School of Medicine, The University of Tokyo, Tokyo, Japan.

Summary

Few studies have investigated the molecular mechanisms of catheter failure (CF). Herein, we performed histological and molecular biological analyses of the catheter tip to demonstrate its potential as a resource for biological investigation. Additionally, we searched for risk factors for the development of inflammation and coagulation, which are pathological conditions clarified by biological analysis. The CF group included 30 failed catheters involving thrombus and subcutaneous edema identified by ultrasonography. The No-CF group included 26 catheters with no complications. The removed catheter tips were fixed for hematoxylin-eosin (HE) staining with the application of a real-time reverse transcriptase polymerase chain reaction for eukaryotic 18S ribosomal RNA (rRNA), interleukin 1 β , tumor necrosis factor α , tissue plasminogen activator, and plasminogen activator inhibitor 1 (*SERPINE1*). HE staining identified attached nuclear cells on the inner surfaces of both CF and No-CF catheters. The 18S rRNA was amplified in all samples. The expression level of *SERPINE1* was significantly higher in the CF group than in the No-CF group ($p = 0.01$), whereas the expression levels of other genes did not differ between the groups. Symptoms of CF associated with the expression of *SERPINE1* were analyzed. The catheter being in contact with blood vessels during placement was a suggested factor related to the high expression of *SERPINE1* ($p = 0.04$). Catheter tips are a potential resource for biological investigation, and expression analysis of the attached cells can reflect the pathological condition of the catheterized tissue. Further studies using catheter tips are required to elucidate the molecular mechanisms of CF.

Keywords: Catheter failure, catheter tips, histological analysis, thrombus

1. Introduction

Peripheral catheters are commonly used for the administration of fluids and medications. A recent study reported that more than 70% of all patients in

acute care hospitals use peripheral intravenous catheters (PIVCs) (1,2). In addition, more than 30% of PIVCs are reportedly removed for unplanned reasons rather than replaced when clinically indicated, which is termed catheter failure (CF) (3,4). Peripheral intravenous CF is a generic term used to refer to local complications associated with PIVCs, such as phlebitis and infiltration (5-7). CF is associated with clinical signs and symptoms, such as erythema, swelling, induration, bleeding and pain, and an insufficient infusion rate. CF negatively affects the patient's comfort and continuous fluid therapy. Catheter replacement, which

*Address correspondence to:

Dr. Hiromi Sanada, Department of Gerontological Nursing/Wound Care Management, Graduate School of Medicine, University of Tokyo, Faculty of Medicine Bldg. No. 5-306, 7-3-1 Hongo, Bunkyo-ku, Tokyo 113-0033, Japan.
E-mail: hsanada-ky@umin.ac.jp

is unavoidable in CF, increases patient discomfort (8,9), labor costs, and the cost of medical resources (3,10-14). For these reasons, it is important to prevent CF in PIVCs and to pay special attention to signs, symptoms, and changes in the infusion rate.

The lack of effective preventive methods for CF may be due to insufficient investigation into the etiology of CF. Intravascular thrombus, subcutaneous edema, and catheter dislodgment have been previously discussed as possible etiologies of peripheral intravenous CF. Our previous study investigated the relationship between the etiology of CF confirmed by ultrasonography and the occurrence of peripheral intravenous CF (15). Notably, no catheter dislodgment was found among the cases of peripheral intravenous CF. On the other hand, thrombus with subcutaneous edema was found to be significantly related to the occurrence of peripheral intravenous CF.

In our previous study, we identified etiologies (dislodgment, thrombosis, and subcutaneous edema) by ultrasonography. Ultrasonography is useful to identify the structural changes at tissue or organ levels. However, it is very labor-intensive to perform an ultrasound examination just before removing a catheter at the bedside, especially difficult when doing at night or in situations where catheter removal is urgent. Here, instead, we wanted to focus on the removed catheter itself and to examine whether it is possible to clarify the condition of the blood vessels and surrounding tissue at the time of removal.

Therefore, we thought that we could explain the phenomenon of CF by the biological analysis of the removed catheter. With this new evaluation method, it would become possible to evaluate changes that are difficult to detect on the skin, and it may be possible to elucidate the causes of CF in detail and to evaluate the differences between varying devices and placement depths. Many studies have evaluated the status of catheter infection (16-19). For example, reports on the estimation of the infection route have been made by analyzing bacterial flora using next generation sequencing for the collected catheter (16). However, few studies have focused on the tissues and cells in the vicinity where the catheter is inserted.

Investigation at the cellular and molecular levels is essential for the development of an effective method to prevent CF. Here, we hypothesized that the cells, including erythrocytes, lymphocytes, vascular endothelial cells, and fibroblasts, attach to the inner and outer surfaces of the catheter, and they are a possible resource for molecular biological investigation.

The purpose of this preliminary study was to show the possibility of cytological and molecular biological investigation of the catheter tip by microscopic observation of the adhered host cells on the surface of the removed catheter tips and real-time reverse transcriptase polymerase chain reactions of housekeeping genes and genes related to inflammation

and thrombosis. In this study, we searched for risk factors for the development of inflammation and coagulation, which are pathological conditions that can be clarified by biological analysis.

2. Materials and Methods

2.1. Study setting and participants

We recruited participants who had been admitted to a medical ward of a university hospital located in a metropolitan city in Japan who required PIVC for fluid therapy between January and June 2014. Any patients who received chemotherapy, were under 20 years of age, had a low cognitive level, or had an unstable physical condition were excluded. We repeatedly observed the patients who received PIVCs multiple times in order to include all PIVCs in this analysis. In this prospective observational study, we observed all PIVCs just before catheter removal. We defined PIVC with thrombus and subcutaneous edema detected on ultrasound and related to CF as "CF". We defined PIVC with no complications detected on ultrasound and no CF as "No-CF".

2.2. Data collection procedure

The patients' characteristics were collected either from medical records or from observations of the indwelling site before infusion therapy started. We asked the nurses to call us just before catheter removal. We then observed the signs and symptoms from macroscopic observation and observed the vessel lumen and surrounding tissues by ultrasound.

2.3. Investigation items

The researchers confirmed with the nurses the reasons for catheter removal. Accidental catheter removal was defined as CF. In this study, the ultrasound scanning technique was based on our previous study (20,21). The motion images were recorded on a hard disk attached to the ultrasound equipment (Noblus[®]; Hitachi Aloka Medical, Ltd., Tokyo, Japan), which included a linear-array (5.0-18.0 MHz) transducer. The identifications of thrombus, subcutaneous edema, and catheter tip position on ultrasound images were performed by a certified sonographer with over 10 years of experience. The sonographer was blinded to the condition of the PIVC.

The definitions of thrombus and subcutaneous edema were based on those of our previous study (15,22). Intravenous thrombus was defined as a marked echogenic mass with an uneven surface. Final judgments were made using both transverse and longitudinal ultrasound images. Subcutaneous edema was defined by a homogeneous cobblestone appearance

in the subcutaneous fat layer.

2.4. PIVC collection

PIVCs removed by the medical staff were collected. All catheters used in the target ward were Sure Shield Surflew II® (Terumo Corp., Tokyo, Japan). The catheter material was Teflon®, and the length was 19-25 mm. PIVC tips removed by a nurse (or researcher) were cut off at the base of the catheter with scissors, immersed in 1 ml RNAlater® (Sigma-Aldrich Corp., MO, USA), and subsequently stored at -20°C.

2.5. HE Staining

The catheter tips were removed from the RNAlater and cut into two pieces longitudinally through the center of the tips. Both pieces of the catheter tip were placed in hematoxylin (Muto Pure Chemicals, Tokyo, Japan) for 2 minutes. Next, the pieces of the catheter were transferred to tap water and washed 5 times. Following incubation in hot water (55°C) for 10 minutes, the catheter pieces were transferred to eosin (Muto Pure Chemicals Corp. Tokyo, Japan) for 10 seconds. Finally, the catheter pieces were dehydrated with a series of ethanol washes (90%, 100%, 100%, and 100%), and stored in 100% ethanol. The pieces of the catheter tips were placed in a droplet of glycerin and observed with an optical microscope.

2.6. Real time reverse transcription polymerase chain reaction (real-time RT-PCR)

Total RNA was extracted using a RNeasy Plus Mini Kit (QIAGEN, Venlo, Netherlands). The pieces of the catheter tips were immersed in a lysis buffer and flushed repeatedly with a 25 G needle. Next, RNA was extracted according to the manufacturer's instructions. Reverse transcription was carried out by the TM100™ Thermal Cycler (Bio-Rad, Hercules, CA) and the High Capacity cDNA Reverse Transcription Kit (Thermo Fisher Scientific, Waltham, MA). Real-time RT-PCR was performed with a real-time PCR system (Agilent, Santa Clara, CA) and TaqMan Gene Expression assays (Thermo Fisher Scientific) for tumor necrosis factor α (*TNF*), interleukin-1 β (*IL1B*), serpin family E member 1 (*SERPINE1*) plasminogen activator inhibitor 1), and tissue plasminogen activator (*PLAT*). *IL1B* and *TNF* were biomarkers for inflammation, and *PLAT* and *SERPINE1* were biomarkers for thrombosis. As an internal standard, 18S ribosomal RNA (rRNA) was simultaneously amplified. Each reaction was performed in triplicate.

At first, the amplifications were qualitatively evaluated. Samples showed typical amplification curves, and any cycle threshold (Ct) values were considered as "detected". Samples with Ct values of 35 or lower were

evaluated as "quantified". Subsequently, qualitative analysis was conducted only in the quantified samples. Relative expression levels of target genes (*TNF*, *IL1B*, *SERPINE1*, and *PLAT*) were calculated by the comparative Ct method with the following formulas and the $\Delta\Delta Ct$ values were used for the statistical analysis.

$$\begin{aligned}\Delta Ct &= (Ct \text{ target gene} - Ct 18S \text{ rRNA}) \\ \Delta\Delta Ct &= \Delta Ct - \text{Average of } \Delta Ct \text{ CF negative} \\ \text{Relative expression level} &= 2^{-\Delta\Delta Ct}\end{aligned}$$

2.7. Statistical analyses

Results are presented as mean \pm standard deviation. Statistical differences between the CF and No-CF groups were determined using Student's *t*-test or the rank sum test. For risk factor analysis, we compared CF with high gene expression ($\Delta\Delta Ct > 1$) of biomarkers and No-CF with low gene expression ($\Delta\Delta Ct < 1$) of biomarkers. A *p* value of < 0.05 was considered statistically significant. All statistical analyses were performed using STATA/SE 15.0 software (StataCorp LP, College Station, TX, USA).

2.8. Ethical considerations

The study protocol was approved by the Research Ethics Committee of The University of Tokyo (#10348). Written informed consent was obtained from all patients or their proxies prior to participation in the study.

3. Results

3.1. Participants and PIVC characteristics

In this study, the researchers investigated 186 catheters using an ultrasonography device just before catheter removal. The study included 26 CF patients whose PIVC had thrombus with subcutaneous edema-related CF and 30 No-CF patients whose PIVC had no complications. Thirty of the 56 participants were men. The patients' mean age (SD) was 69.1 (± 12.8) years, and the mean body mass index was 22.4 (± 3.5) kg/m² (Table 1).

3.2. Presence of adhered cells

HE staining showed the presence of adhered cells on the surface of the catheter tips. Erythrocytes, which have no nucleus, were stained only with eosin, and a double positive for hematoxylin and eosin revealed the presence of nucleated cells, such as white blood cells, endothelial cells, and fibroblasts. In all samples, a large number of erythrocytes and nucleated cells were observed only on the inner surface of the catheter tips. The morphology of the nucleated cells was round

in shape, suggesting that they were white blood cells (Figure 1).

3.3. Expression analysis

Expression of *18S rRNA*, an internal standard, was examined by real-time RT-PCR. All samples showed the specific amplification curves and their Ct values less than 35. The median (interquartile) Ct value of *18S rRNA* were 22.4 (19.7-24.5) and 24.5 (20.6-27.9) in CF and NO-CF groups, respectively ($p = 0.06$).

The expression of target genes was qualitatively evaluated (Figure 2). The proportion of the detected samples for *TNF*, *IL1B*, *SERPINE1*, and *PLAT* was

75% (42/56), 94.6% (53/56), 98.2% (55/56), and 19.6% (11/56), respectively. The proportion of the quantified samples for *TNF*, *IL1B*, *SERPINE1*, and *PLAT* was 64.3% (36/56), 60.7% (34/56), 71.4% (40/56), and 7.1% (4/56), respectively.

3.4. Effects of the number of adhered cells on expression analysis

In order to confirm the effect of the number of adhered cells on the quantification of target gene expression, the number of adhered cells and the expression level of *18S rRNA* were compared between quantified and not quantified samples for *TNF*. The median (interquartile) numbers of adhered cells were 21.3 (19.7-23.2) and 27.4 (25.3-29.0) in the quantified and the not quantified groups, respectively ($p = 0.01$).

3.5. Comparison between the CF and No-CF groups

Tables 2 and 3 show the proportion of detected and quantified samples for the target genes, respectively. There was no significant difference in the proportion of detected samples for all genes between groups. The frequency of quantified samples was significantly high in *IL1B* and *SERPINE1* and tended to be high in *TNF* in the CF group compared with those in the No-CF group. In other words, it suggests that whether a sample is quantified or not depends on the number of cells that can be collected.

The expression levels of target genes only in the quantified samples were compared between the CF and

Table 1. Participants and PIVC characteristics

Items	No-CF	<i>n</i> = 30	CF	<i>n</i> = 26
Age; years*	69.8	(12.0)	68.3	(12.0)
Sex	17	(56.7)	13	(50.0)
BMI*	22.6	(3.2)	22.3	(3.7)
History of present illness				
Neoplasms	18	(60.0)	14	(53.8)
Digestive system	25	(83.3)	20	(76.9)
Certain infectious	4	(13.3)	1	(3.8)
Diabetes	9	(30.0)	7	(26.9)
Anticoagulant drug use	4	(13.3)	1	(3.8)
Catheter size				
22G	22	(73.3)	22	(84.6)
24G	8	(26.7)	4	(15.4)
Catheter anatomical site (forearm)	28	(93.3)	25	(96.2)
Catheter dwell time*	65.0	(32.0)	53.6	(27.4)

N (%), * mean (SD). BMI: body mass index; CF: catheter failure; PIVC: peripheral intravenous catheters.

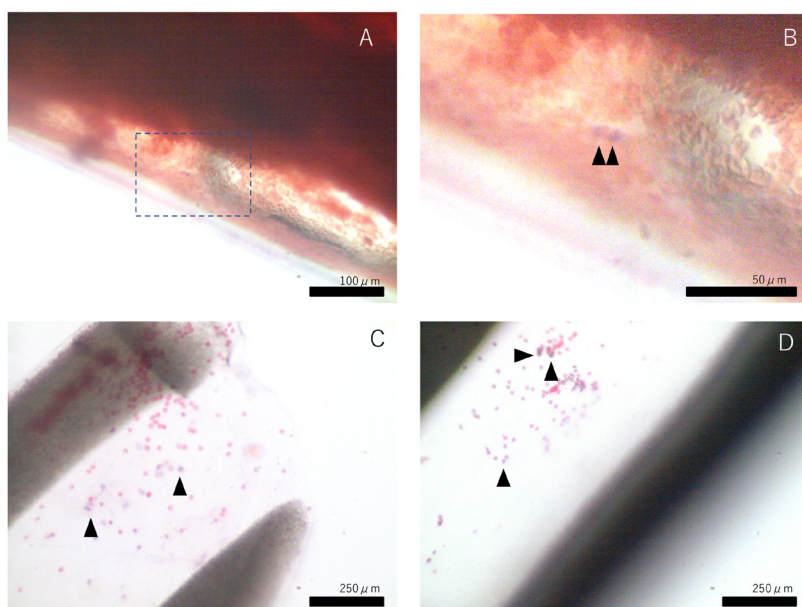


Figure 1. Hematoxylin-eosin staining of catheter tips. A few, round, nucleated cells (arrowheads) were observed among many enucleated cells. Two catheters are represented: A and B are images of one catheter, and C and D are images of another catheter. In A and B, many red blood cell aggregates and some cells with nuclei are present; B is an enlarged image of the broken line portion of A. Panels C and D show some cells adhering to the lumen of the catheter.

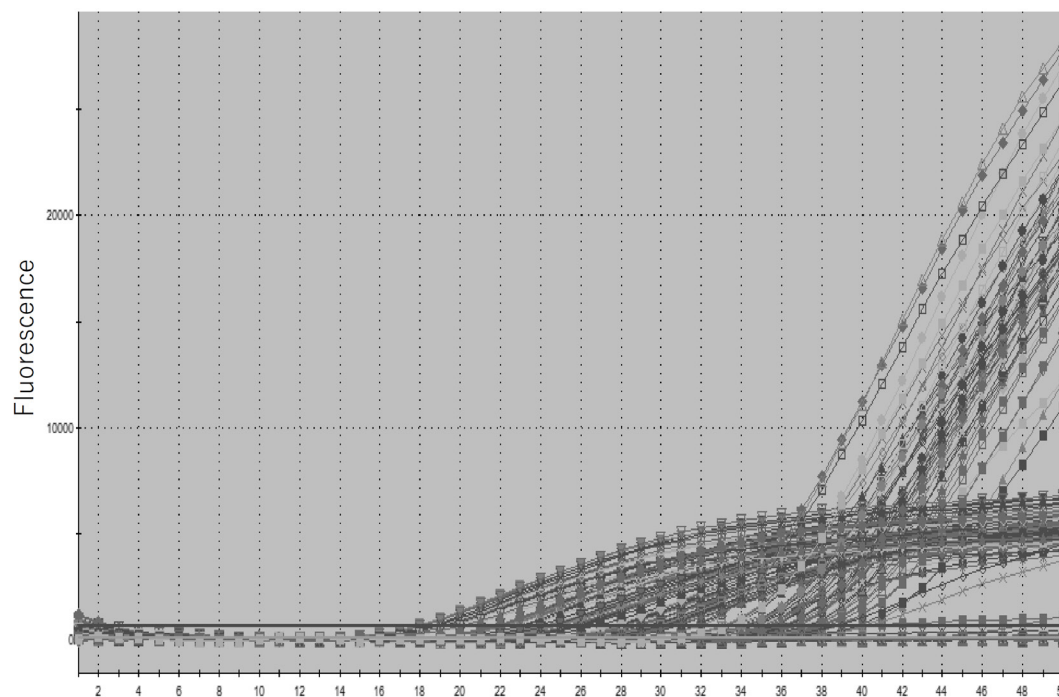


Figure 2. Amplification curve.

Table 2. The proportion of the detected samples for target genes

Detected	No-CF 30 N (%)	CF 26 N (%)	<i>p</i> value
<i>TNF</i>	20 (66.7)	22 (84.6)	0.112
<i>IL1B</i>	27 (90.0)	26 (100.0)	0.097
<i>SERPINE1</i>	29 (96.7)	26 (100.0)	0.348
<i>PLAT</i>	5 (16.7)	6 (23.1)	0.547

χ^2 test

CF: Catheter failure; TNF: tumor necrosis factor; IL1B: interleukin-1 β ; SERPINE1: serpin family E member 1; PLAT: plasminogen activator, tissue type.

Table 3. The proportion of the quantified samples for target genes

Quantified	No-CF 30 N (%)	CF 26 N (%)	<i>p</i> value
<i>TNF</i>	16 (53.3)	20 (76.9)	0.066
<i>IL1B</i>	14 (46.7)	20 (76.9)	0.021
<i>SERPINE1</i>	18 (60.0)	22 (84.6)	0.042
<i>PLAT</i>	2 (06.7)	2 (07.7)	0.882

χ^2 test

CF: Catheter failure; TNF: tumor necrosis factor; IL1B: interleukin-1 β ; SERPINE1: serpin family E member 1; PLAT: plasminogen activator, tissue type.

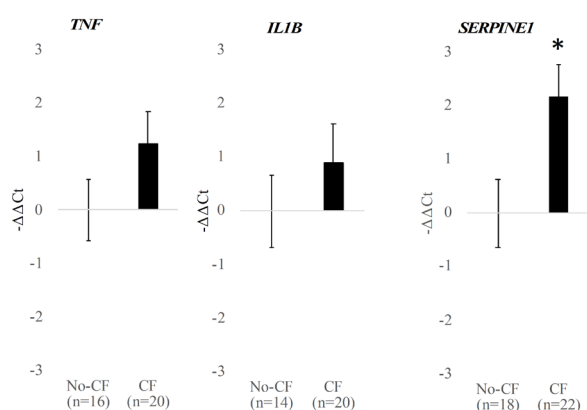


Figure 3. Comparison of expression levels of target genes between the catheter failure (CF) and No-CF groups. Data are presented as means \pm Standard Division of $-\Delta\Delta C_t$. **p* < 0.05.

No-CF groups (Figure 3). The $-\Delta\Delta C_t$ values of *TNF* expression were 1.24 ± 0.60 in the CF group and $0.0 \pm$

0.57 in the No-CF group (*p* = 0.15). The $-\Delta\Delta C_t$ values of *IL1B* expression were 0.90 ± 0.73 in the CF group and 0.0 ± 0.68 in the No-CF group (*p* = 0.39). The $-\Delta\Delta C_t$ values of *SERPINE1* expression were 2.18 ± 0.60 in the CF group and 0.0 ± 0.63 in the No-CF group (*p* < 0.01). The $-\Delta\Delta C_t$ values of *PLAT* expression were -8.15 ± 6.04 in the CF group and 0.0 ± 0.66 in the No-CF group. Statistical analysis was not performed because only two samples were confirmed the expression of *PLAT*.

The risk factors for CF that have been identified in previous studies were compared between *SERPINE1* expression groups (Table 4). As a result, the catheter coming into contact with blood vessels during placement was suggested as a factor related to the high expression of *SERPINE1* (*p* = 0.04) rather than any other patient characteristics.

4. Discussion

To the best of our knowledge, this is the first study to

Table 4. The proportion of the quantified samples for target genes

Items	No-CF with <i>SERPINE1</i> < 1 mean/n	n = 12 (SD)/(%)	CF with <i>SERPINE1</i> > 1 mean/n	n = 14 (SD)/(%)	p
Age (y)	63.5	(12.8)	65.6	(15.3)	0.71
Sex (male)	8	(66.7)	9	(64.3)	0.90
BMI	21.6	(3.1)	21.8	(3.1)	0.89
Disease (digestive system disease)	11	(91.7)	12	(85.7)	0.89
Disease (neoplastic)	9	(75.0)	8	(57.1)	0.91
Oral administration of anticoagulant	3	(25.0)	1	(7.1)	0.21
Part (forearm)	12	(100.0)	13	(92.9)	0.89
Gauge (22G)	9	(75.0)	13	(92.9)	0.21
Heparin lock time more than 12 hours	9	(75.0)	12	(85.7)	0.24
Irritant drug	1	(8.3)	3	(21.4)	0.36
Antibacterial drug	5	(41.7)	9	(64.3)	0.25
Total dose of drug solution (mL)	2,165.0	(2,179.8)	2,464.9	(3,121.6)	0.78
Heparin lock total time (h)	36.5	(26.0)	20.8	(17.7)	0.09
Contact with the blood vessels by catheter	0	(0.0)	4	(28.6)	0.04*
Blood vessel diameter	2.45	(1.0)	2.55	(0.8)	0.79

CF: catheter failure; *SERPINE1*: serpin family E member 1; BMI: body mass index.

biologically analyze the extracted PIVC. Our results suggest that catheter tips are a potential resource for biological investigation, and expression analysis of the attached cells can reflect the pathological condition of the catheterized tissue. Further studies using catheter tips are required to elucidate the molecular mechanisms of CF. Furthermore, we performed an analysis of *SERPINE1*, which was related to CF. These results suggested that in cases with high expression of *SERPINE1*, the catheter may stimulate the blood vessel wall by coming in contact with it. Keeping this in mind could be useful when considering future CF precautions.

There were three main findings from this study. The first finding was the presence of the attached human-derived cells on the inside surface of the removed catheter tips. Prior research has reported that blood in the lumen of the catheter is coagulated at the catheter tip if there is no infusion (23). In particular, it has been shown that backflow of blood occurs owing to the locking procedure performed when the catheter use is interrupted (24-26). In the wards covered in this study, a needleless connector was used to connect the infusion tube, and a positive pressure heparin flush was performed at least once every 24 hours. Nevertheless, HE staining and the amplification of *18S rRNA* indicated the adherence of abundant enucleated erythrocytes and nucleated cells on the inner surface of tips even in the No-CF catheters.

Secondly, analysis of the cells attached to the removed catheter showed that *SERPINE1* mRNA, which is an inhibitor of thrombus removal, was highly expressed in the CF group as compared to the No-CF group. Although this mRNA may be derived from vascular endothelial cells, we believe that the most likely candidate may be derived from monocytes (27). *SERPINE1* is expressed by various kinds of cells, including endothelial cells, monocytes, hepatocytes, granulosa cells, and vascular smooth muscle cells, and

inhibits the activities of urinary-type and tissue-type plasminogen activators (28). Performing catheterization is foreign to the human body, and the coagulation reaction is caused by disturbance of all three factors of Virchow's triad (29). Especially in the distal end of the catheter, a fibrin sheath is formed. Erythrocytes and monocytes are entangled by the fibrin sheath, and thrombus is formed. In this study, the monocytes may express *SERPINE1* and may inhibit thrombus removal and promote thrombus formation. A significant difference was not detected between *IL1B* and *TNF*, as hypothesized by the present study. This may be owing to the fact that vascular endothelial cells and surrounding tissues could not be collected. Vascular endothelial cells and surrounding tissues should have been in contact with the catheter, but it is thought that these were scraped off in the catheter removal process. *PALT* is a marker closely related to *SERPINE1* (30,31), but its expression was not observed in most samples in this study. This may be owing to *PALT* being tissue derived rather than monocyte derived. In the future, it may be better to verify the chemotactic factors of MF and monocytes as inflammation markers.

Finally, CF associated with the expression of *SERPINE1* was analyzed. The catheter being in contact with blood vessels during placement was suggested to be a factor related to high expression of *SERPINE1* ($p = 0.04$). Mechanical stimulation of the blood vessel wall by a catheter is a risk factor for CF that has been pointed out in our previous studies (32). It is suggested that inflammation by simulation occurs when the tip of the catheter contacts the vascular endothelial cells (33). This study suggested that neutrophils were more aggregated in the fibrin sheath, causing coagulation to progress further.

Some studies have been conducted in the past to detect infection using removed catheters. We believed that our method by real time RT-PCR would contribute to the detection of coagulation. As mentioned in the

background section, we performed ultrasonography just before catheter removal to detect the etiology of catheter failure. This allowed real-time assessment and direct observation of the blood vessel; however, it may be difficult to conduct ultrasonography at night or in situations where removal is urgent. In such situations, conventional analysis is useful to detect the etiology of CF. Our suggested technique might be useful to evaluate new vascular access devices, fixation devices, or other medical devices.

This study showed that it is possible to elucidate a biological cause of CF. Furthermore, real-time RT-PCR, using cells extracted from catheters after removal, may be a useful new method to evaluate peripheral venous catheters. Our findings suggest that catheter contact is related not only to inflammation but also to coagulation. This result will be useful for devising and evaluating future measures to prevent CF in clinical nursing. The prevention of mechanical stimuli for the prevention of CF has been advocated in recent years (32-34). Since this study suggested that the catheter tip has an effect on the blood vessel wall and coagulation, it may be advisable that clinical nurses need to pay attention to the fixation of the catheter for confirmation. Confirmation of catheter position by ultrasonography is likely to be effective for the prevention of CF, and future clinical application is expected.

There were limitations to the variations of clinical samples dealt with in this study, and only one type of catheter was used. In order to extrapolate these results, it is necessary to consider the type and coating of the catheter. Furthermore, peripheral intravenous catheter infections have been reported (35) and may have been associated with CF. However, we did not include cases in which the target catheter was diagnosed as an infection source. Factor analysis of *SERPINE1* expression in this study could not be performed using multivariate analysis owing to the small sample size. However, a relationship between *SERPINE1* and vessel wall contact can be suggested because this was not related to patient factors such as oral anticoagulant administration or age.

Our findings suggest that catheter tips are a potential resource for biological investigation, and expression analysis of the attached cells can reflect the pathological condition of the catheterized tissue. This result implicates the involvement of *SERPINE1* in drip failure and pain as a new pathological condition. In addition, the etiology of *SERPINE1* expression was suggested to be mechanical stimulation by the catheter coming into contact with the vessel wall. Further studies using catheter tips are required to elucidate the molecular mechanisms of CF.

Acknowledgements

This work was conducted as a part of a project funded

by the JSPS KAKENHI Grant Number 26670915 and 18074373.

References

- Zingg W, Pittet D. Peripheral venous catheters: an under-evaluated problem. *Int J Antimicrob Agents*. 2009; 34 (Suppl 4):S38-42.
- Waitt C, Waitt P, Pirmohamed M. Intravenous therapy. *Postgrad Med J*. 2003; 80:1-6.
- Rickard CM, Webster J, Wallis MC, Marsh N, McGrail MR, French V, Foster L, Gallagher P, Gowardman JR, Zhang L, McClymont A, Whitby M. Routine versus clinically indicated replacement of peripheral intravenous catheters: a randomised controlled equivalence trial. *Lancet*. 2012; 380:1066-1074.
- Murayama R, Uchida M, Oe M, Takahashi T, Oya M, Komiyama C, Sanada H. Patient risk factors for developing sign- and symptom-related peripheral intravenous catheter failure: A retrospective study. *J Jpn WOCM*. 2015; 19:13594-13402.
- Gorski LA. Infusion nursing standards of practice. *J Infus Nurs*. 2007; 30:20-21.
- Pujol M, Hornero A, Saballs M, Argerich MJ, Verdaguier R, Ciscal M, Pena C, Ariza J, Gudiol F. Clinical epidemiology and outcomes of peripheral venous catheter-related bloodstream infections at a university-affiliated hospital. *J Hosp Infect*. 2007; 67:22-29.
- Dougherty L. IV therapy: recognizing the differences between infiltration and extravasation. *Br J Nurs*. 2008; 17:896-891.
- Bregenzer T, Conen D, Sakmann P, Widmer AF. Is routine replacement of peripheral intravenous catheters necessary? *Arch Intern Med*. 1998; 158:151-156.
- Xu L, Hu Y, Huang X, Fu J, Zhang J. Clinically indicated replacement versus routine replacement of peripheral venous catheters in adults: A nonblinded, cluster-randomized trial in China. *Int J Nurs Pract*. 2017; 23(6). doi: 10.1111/ijn.12595.
- Ansel B, Boyce M, Embree JL. Extending short peripheral catheter dwell time: A best practice discussion. *J Infus Nurs*. 2017; 40:143-146.
- Rickard CM, Marsh NM, Webster J, et al. Intravascular device administration sets: replacement after standard versus prolonged use in hospitalised patients-a study protocol for a randomised controlled trial (The RSVP Trial). *BMJ Open*. 2015; 5:e007257.
- Rickard CM, McCann D, Munnings J, McGrail MR. Routine resite of peripheral intravenous devices every 3 days did not reduce complications compared with clinically indicated resite: a randomised controlled trial. *BMC Med*. 2010; 8:53.
- Webster J, Osborne S, Rickard CM, New K. Clinically-indicated replacement versus routine replacement of peripheral venous catheters. *Cochrane Database Syst Rev*. 2013; 1:CD007798.
- Tuffaha HW, Rickard CM, Webster J, Marsh N, Gordon L, Wallis M, Scuffham PA. Cost-effectiveness analysis of clinically indicated versus routine replacement of peripheral intravenous catheters. *Appl Health Econ Health Policy*. 2014; 12:51-58.
- Takahashi T, Murayama R, Oe M, Nakagami G, Tanabe H, Yabunaka K, Arai R, Komiyama C, Uchida M, Sanada H. Is thrombus with subcutaneous edema detected by

- ultrasonography related to short peripheral catheter failure? A prospective observational study. *J Infus Nurs.* 2017; 40:313-322.
16. Choudhury MA, Marsh N, Banu S, Paterson DL, Rickard CM, McMillan DJ. Molecular comparison of bacterial communities on peripheral intravenous catheters and matched skin swabs. *PLoS One.* 2016; 11:e0146354.
 17. Choudhury MA, Sidjabat HE, Rathnayake IU, Gavin N, Chan RJ, Marsh N, Banu S, Huygens F, Paterson DL, Rickard CM, McMillan DJ. Culture-independent detection of chlorhexidine resistance genes *qacA/B* and *smr* in bacterial DNA recovered from body sites treated with chlorhexidine-containing dressings. *J Med Microbiol.* 2017; 66:447-453.
 18. Cicolini G, Manzoli L, Simonetti V, Flacco ME, Comparcini D, Capasso L, Di Baldassarre A, Eltaji Elfarouki G. Phlebitis risk varies by peripheral venous catheter site and increases after 96 hours: a large multi-centre prospective study. *J Adv Nurs.* 2014; 70:2539-2549.
 19. Cinel I, Dellinger RP. Guidelines for severe infections: are they useful? *Curr Opin Crit Care.* 2006; 12:483-488.
 20. Tanabe H, Murayama R, Yabunaka K, Oe M, Takahashi T, Komiyama C, Sanada H. Low-angled peripheral intravenous catheter tip placement decreases phlebitis. *J Vasc Access.* 2016; 17:542-547.
 21. Tanabe H, Takahashi T, Murayama R, Yabunaka K, Oe M, Matsui Y, Arai R, Uchida M, Komiyama C, Sanada H. Using Ultrasonography for vessel diameter assessment to prevent infiltration. *J Infus Nurs.* 2016; 39:105-111.
 22. Yabunaka K, Takahashi T, Tanabe H, Kawamoto A, Oe M, Arai R, Sanada H. Ultrasonographic appearance of infusion *via* the peripheral intravenous catheters. *J Nurs Sci Eng.* 2015; 2:40-46.
 23. Baekgaard N, Broholm R, Just S, Jorgensen M, Jensen LP. Long-term results using catheter-directed thrombolysis in 103 lower limbs with acute iliofemoral venous thrombosis. *Eur J Vasc Endovasc Surg.* 2010; 39:112-117.
 24. Keogh S, Flynn J, Marsh N, Mihala G, Davies K, Rickard C. Varied flushing frequency and volume to prevent peripheral intravenous catheter failure: a pilot, factorial randomised controlled trial in adult medical-surgical hospital patients. *Trials.* 2016; 17:348.
 25. Hamze B, Vaillancourt R, Sharp D, Villarreal G. A comparison of taste and odor perception in pediatric patients receiving a 0.9% sodium chloride flush from 2 different brands of prefilled 0.9% sodium chloride syringes. *J Infus Nurs.* 2016; 39:18-24.
 26. Upadhyay A, Verma KK, Lal P, Chawla D, Sreenivas V. Heparin for prolonging peripheral intravenous catheter use in neonates: a randomized controlled trial. *J Perinatol.* 2015; 35:274-277.
 27. Hamilton JA, Whitty GA, Wojta J, Gallichio M, McGrath K, Ianches G. Regulation of plasminogen activator inhibitor-1 levels in human monocytes. *Cell Immunol.* 1993; 152:7-17.
 28. Sprengers ED, Kluft C. Plasminogen activator inhibitors. *Blood.* 1987; 69:381-387.
 29. Kyrle PA, Eichinger S. Is Virchow's triad complete? *Blood.* 2009; 114:1138-1139.
 30. Cao C, Lawrence DA, Li Y, Von Arnim CA, Herz J, Su EJ, Makarova A, Hyman BT, Strickland DK, Zhang L. Endocytic receptor LRP together with tPA and PAI-1 coordinates Mac-1-dependent macrophage migration. *EMBO J.* 2006; 25:1860-1870.
 31. Nassar T, Akkawi S, Shina A, Haj-Yehia A, Bdeir K, Tarshis M, Heyman SN, Higazi AA. *In vitro* and *in vivo* effects of tPA and PAI-1 on blood vessel tone. *Blood.* 2004; 103:897-902.
 32. Murayama R, Takahashi T, Tanabe H, Yabunaka K, Oe M, Oya M, Uchida M, Komiyama C, Sanada H. The relationship between the tip position of an indwelling venous catheter and the subcutaneous edema. *Biosci Trends.* 2015; 9:414-419.
 33. Piper R, Carr PJ, Kelsey LJ, Bulmer AC, Keogh S, Doyle BJ. The mechanistic causes of peripheral intravenous catheter failure based on a parametric computational study. *Sci Rep.* 2018; 8:3441.
 34. Rickard CM, Marsh N, Webster J, *et al.* Dressings and securements for the prevention of peripheral intravenous catheter failure in adults (SAVE): A pragmatic, randomised controlled, superiority trial. *Lancet.* 2018; 392:419-430.
 35. Ray-Barruel G. Infection prevention: Peripheral intravenous catheter assessment and care. *Aust Nurs Midwifery J.* 2017; 24:34.

(Received September 30, 2019; Revised October 24, 2019; Accepted October 26, 2019)

Characteristics of subcutaneous tissues at the site of insertion of peripheral infusion in patients undergoing paclitaxel and carboplatin chemotherapy

Ryoko Murayama^{1,2,*}, Maiko Oya³, Mari Abe-Doi¹, Makoto Oe², Chieko Komiyama⁴, Hiromi Sanada^{2,3}

¹ Department of Advanced Nursing Technology, Graduate School of Medicine, The University of Tokyo, Tokyo, Japan;

² Global Nursing Research Center, Graduate School of Medicine, The University of Tokyo, Tokyo, Japan;

³ Department of Gerontological Nursing/Wound Care Management, Graduate School of Medicine, The University of Tokyo, Tokyo, Japan;

⁴ The University of Tokyo Hospital, Tokyo, Japan.

Summary

Paclitaxel, a taxane, is frequently administered intravenously as an anticancer agent. When a peripheral intravenous catheter is used for paclitaxel infusion, clinical nurses often observe signs such as slight swelling at the catheter placement site, lack of blood return, and difficulty in continuing the infusion. However, the cause(s) of such phenomena at the puncture site has not yet been elucidated. The aim of this study was to obtain ultrasonography images of subcutaneous tissues and veins of patients undergoing paclitaxel and carboplatin chemotherapy and compare ultrasonography images taken immediately before catheter removal with those of patients receiving other types of taxanes. We studied 24 patients receiving chemotherapy, including seven receiving paclitaxel and carboplatin chemotherapy, through a peripheral intravenous catheter in a chemotherapy unit for outpatients of a university hospital in Japan. Ultrasonography images of venipuncture sites were obtained before catheter insertion and immediately before catheter removal. We observed subcutaneous edema in the absence of visible manifestations at the puncture sites of all patients undergoing paclitaxel and carboplatin chemotherapy, but not in any patients receiving other types of taxanes. When vesicant agents and vehicles have caused subclinical subcutaneous edema, clinical nurses may detect early slight extravasation by using ultrasonography.

Keywords: Chemotherapy, peripheral intravenous catheter, subcutaneous edema, ultrasonography

1. Introduction

Paclitaxel, a taxane, is frequently administered intravenously as an anticancer agent because there is published evidence that weekly administration of paclitaxel after a standard adjuvant chemotherapy regimen improves disease-free and overall survival in women with breast cancer (1). Needless to say, clinical nurses must take precise care to avoid extravasation during administration of vesicant drugs, including

paclitaxel.

Extravasation is the process by which any liquid accidentally leaks out of a blood vessel into the surrounding tissue. Specifically, in the context of cancer therapy, extravasation refers to the inadvertent infiltration of chemotherapy agents into the subcutaneous or subdermal tissues surrounding an intravenous or intra-arterial administration site (2). Such inadvertent infiltration of vesicant anticancer agents (e.g., taxanes) can cause adverse events such as tissue necrosis or induration in the region of catheter placement (3-5). The reported incidence of extravasation varies greatly because there is no shared register of chemotherapy extravasation events; however, several studies have been published, most of which have reported that the incidence of extravasation is greater with paclitaxel than

*Address correspondence to:

Dr. Ryoko Murayama, Department of Advanced Nursing Technology, Graduate School of Medicine, The University of Tokyo, 7-3-1 Hongo, Bunkyo-ku, Tokyo 113-8655, Japan.
E-mail: rymurayama-tyk@umin.ac.jp

with other taxanes (6,7).

Therefore, maximal detection and assessment of abnormalities suggestive of extravasation is required to better manage administration of taxanes, especially paclitaxel. When a peripheral intravenous catheter is used for paclitaxel infusion, clinical nurses often observe phenomena such as slight swelling, lack of blood return and resistance to infusion at the catheter placement site. The causes of such phenomena at the puncture site have not yet been clearly elucidated except for identification of extravasation and flare reactions; whereas systemic adverse effects of taxane chemotherapy such as arthralgia and myalgia have been better documented (8-11). There remains a lack of data concerning subcutaneous tissue or vessel damage in patients undergoing taxane infusion at the catheter placement site because these adverse effects cannot be directly observed. We may know the cause of phenomena such as lack of blood return or resistance to infusion, if we can observe directly the subcutaneous tissue, blood vessel and placed catheter.

We therefore implemented ultrasonography, which has the advantages of being non-invasive, providing real-time information, and being easy to use in the clinic, to enable visualization of subcutaneous tissues and veins (12,13). We visualized the puncture sites for infusion therapy with ultrasonography and examined the tissues surrounding the catheterized veins (14,15), to determine whether ultrasonography would enable early detection of subcutaneous abnormalities, even in patients who had completed treatment and had no symptoms or visible evidence of such abnormalities.

It has recently been shown in Japan that conventional-TC (paclitaxel with carboplatin every 3 weeks) and dose dense TC (dose-dense paclitaxel once a week in combination with carboplatin every 3 weeks) are effective regimens for paclitaxel administration (16). The target hospital also adopted these regimens. Therefore, we obtained typical ultrasonography images of subcutaneous tissues and veins of patients undergoing paclitaxel and carboplatin chemotherapy and compared images obtained immediately before catheter removal with those of patients receiving other types of taxane-based chemotherapy.

2. Materials and Methods

2.1. Study design and setting

We did cross sectional observational study of patients (over 20 years old) undergoing taxane-based chemotherapy through a peripheral intravenous catheter in a chemotherapy unit for outpatients in a university hospital in Japan, from February to October 2015.

2.2. Ultrasound scanning technique

We visualized venipuncture sites by ultrasonography

before catheter insertion and immediately before catheter removal. We evaluated the subcutaneous tissues around the relevant vein using portable ultrasonography equipment (Noblus; Hitachi, Tokyo, Japan) with a linear-array transducer (5-18.0 MHz) under the following conditions: echo gain, 25 dB; dynamic range, 65 dB; and focus range and image depth, 1.5-2.5 cm to show the catheterized vein clearly. In this study, one well-trained researcher performed all ultrasonographic examinations and identified all visible subcutaneous-edema related manifestations and another ultrasonographer with more than 20 years of experience evaluated the ultrasonography images. We defined subcutaneous edema as a cobblestone-like pattern in the subcutaneous fat layer on ultrasound images (14,15).

2.3. Study procedure

Characteristics of participants (age, sex, body mass index, and site of cancer) were collected from medical records. In macroscopic observation, a clinical nurse and researcher made the judgment of signs (swelling and redness). The information was classified into three types of taxane-based chemotherapy (paclitaxel and carboplatin, docetaxel, and nab-paclitaxel chemotherapy) and showed. Also, we described one conventional-TC case as representative case.

2.4. Ethical considerations

This study was approved by the Research Ethics Committee of the Graduate School of Medicine, The University of Tokyo (No. 10712). All participants were informed about the purpose of the research and methods of this study and advised that they were free to withdraw their consent at any time. The researchers obtained written consent from all participants before enrollment in the study.

3. Results and Discussion

3.1. Characteristics of participants

Table 1 shows the characteristics of the patients undergoing chemotherapy. The study cohort comprised 24 patients, including seven patients undergoing paclitaxel and carboplatin chemotherapy, eight undergoing docetaxel chemotherapy, and nine undergoing nab-paclitaxel chemotherapy. Patients undergoing paclitaxel and carboplatin chemotherapy received more doses of taxanes over a longer infusion time (average dose of taxanes 206.4 ± 79.4 mg and duration 2.5 hours or 1.0 hour) than those receiving the other two types of taxane-based chemotherapy (105.5 ± 18.5 mg, 1.0 hour, and 185.6 ± 67.2 mg, 0.5 hour, respectively) (Table 1). One patient (paclitaxel and carboplatin chemotherapy group) was needed catheter

placement again, because extravasation occurred due to pulling out catheter accidentally with moving to the toilet. All other patients were able to complete administration of anticancer agents.

Figure 1 shows typical transverse ultrasound images of puncture sites. We observed severe subcutaneous edema after administration of paclitaxel and carboplatin (A2) in patients who had no detectable edema before the infusion (A1). The catheter tip was characteristically visible but the vein not clearly identifiable because of compression by the edema and the absence of an intraluminal anechoic area around the catheter (A2).

In comparison, we observed no such changes in the subcutaneous tissues in patients receiving the other two types of chemotherapy (B1, B2, C1, C2). The vessel lumens were clearly visible (anechoic area) in images obtained both before and after administration of docetaxel or nab-paclitaxel (B2, C2).

Table 2 shows our findings concerning subcutaneous edema and related visible manifestations. We observed neither subcutaneous edema nor related visible manifestations around the puncture sites of patients receiving docetaxel or nab-paclitaxel, whereas all patients receiving paclitaxel and carboplatin showed

Table 1. Demographic characteristics and anticancer agents

Items	Paclitaxel and Carboplatin (n = 7)	Docetaxel (n = 8)	Nab-paclitaxel (n = 9)
Age (years)	59.3 ± 12.4	60.9 ± 12.7	62.1 ± 8.6
Sex / female	7 (100.0)	5 (62.5)	5 (55.6)
Body mass index (kg/m ²)	19.2 ± 3.3	22.3 ± 2.6	21.9 ± 2.9
Cancer	Ovary, 4 (57.1) Uterine, 3 (42.9)	Breast, 5 (62.5) Prostate, 3 (37.5)	Pancreas, 7 (77.8) Breast, 2 (22.2)
Anticancer agents	PTX + CBDCA, 6 (85.7) PTX + CBDCA + BEV, 1 (14.3)	DOC, 5 (62.5) DOC + CPA, 2 (25.0) DOC + PER + TRA, 1 (12.5)	Nab-PTX + GEM, 7 (77.8) Nab-PTX, 2 (22.2)
Dose of taxanes (mg)	206.4 ± 79.4	105.5 ± 18.5	185.6 ± 67.2
Drip rate of taxens (mL/h)	225.7 ± 44.3	280.0 ± 0.0	75.6 ± 26.1
Drip time of taxens	2.5 hours, 5 (71.4) 1.0 hour, 2 (28.6)	1.0 hour, 8 (100.0)	0.5 hour, 9 (100.0)

Mean ± SD or n (%). PTX; paclitaxel, CBDCA; carboplatin, BEV; Bevacizumab, DOC; docetaxel, CPA; cyclophosphamide, PER; pertuzumab, TRA; Trastuzumab, Nab-PTX; nab-paclitaxel, GEM; gemcitabine.

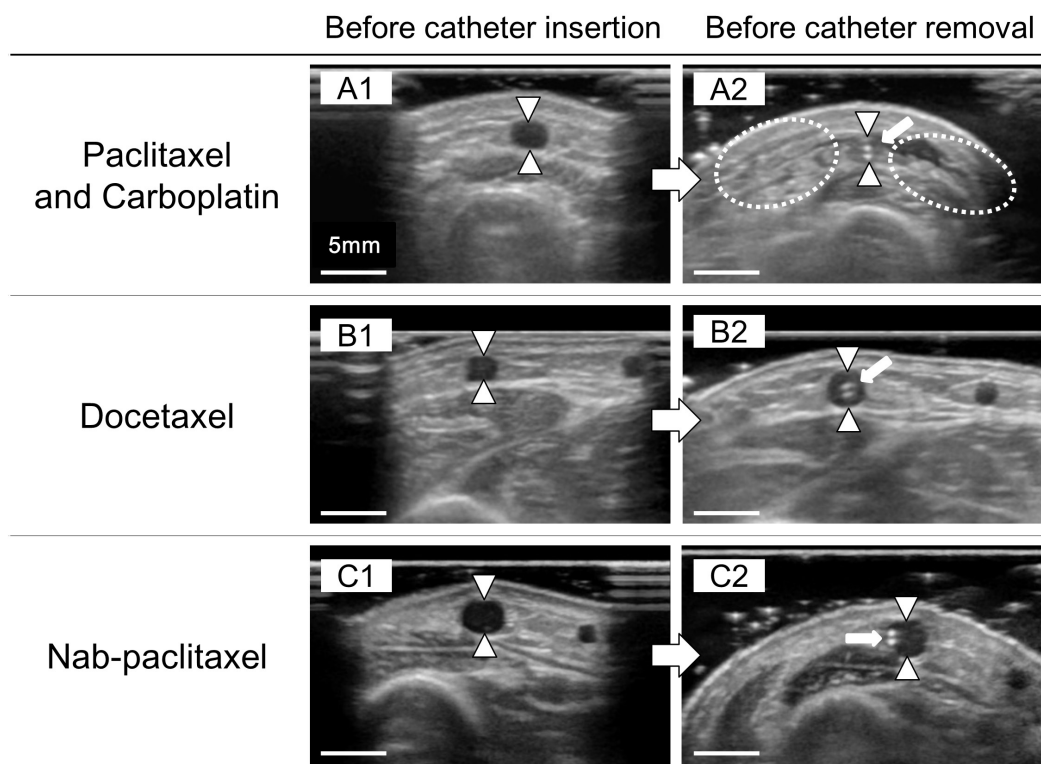


Figure 1. Ultrasound images of veins and subcutaneous tissues at puncture sites of patients undergoing three types of taxane-based chemotherapy. Transverse ultrasound images of puncture sites obtained before catheter insertion (A1, B1, C1) and after administration (before catheter removal: A2, B2, C2). Arrowheads indicate the catheterized vein and allow indicate the catheter tip; the catheter tip can be seen as two bright points in the vein. Subcutaneous edema is visible around the catheterized vein in the area circled by a dotted line in a patient undergoing paclitaxel and carboplatin administration (A2).

ultrasonographic evidence of subcutaneous edema at their puncture sites after administration of these chemotherapy agents. Furthermore, we encountered clinical problems such as lack of blood return, difficulty in continuing the infusions, and swelling during administration of paclitaxel and carboplatin. Only one patient who received this regimen did not show macroscopic symptoms. Extravasation occurred in one patient, necessitating reinsertion of the catheter to complete the chemotherapy.

3.2. Representative case: conventional-TC (paclitaxel with carboplatin every 3 weeks)

A 79-year-old woman with ovary cancer developed severe subcutaneous edema around her puncture site after paclitaxel and carboplatin administration (Figure 2). The nurse had inserted a 24G peripheral intravenous catheter into a forearm vein. There were no visible abnormalities at the puncture site during pre-medication and paclitaxel infusion (paclitaxel 80 mg + natural saline 250 mL, 280 mL/h for one hour). However, no

return of blood occurred when a nurse tried to exchange the infusion bags from paclitaxel to carboplatin. The nurse determined that the catheter appeared to be correctly positioned in the vein; however, the catheter tip may have been touching the vein wall. The nurse shifted the catheter tip a little after peeling off the dressing. After adjustment, return of blood was achieved, enabling complete administration of the carboplatin infusion without reinsertion. An ultrasound image after administration showed severe subcutaneous edema (D1, D2), compressing the catheterized vein and thus likely causing a lack of blood return in the absence of any visible manifestations or pain (D3). Ultrasonography confirmed that the tip of the catheter had not dislodged from the vein.

These findings indicate that ultrasonography can identify subcutaneous edema after administration of taxane in patients without visible manifestations or symptoms other than a lack of blood return. Also, paclitaxel may cause subcutaneous edema at the infusion site. Such

Table 2. The subcutaneous edema observed by ultrasonography and macroscopic symptoms

Items	Paclitaxel and Carboplatin (n = 7)	Docetaxel (n = 8)	Nab-paclitaxel (n = 9)
Subcutaneous edema (ultrasonographic observation)	7 (100.0%)	0 (0.0%)	0 (0.0%)
Macroscopic symptoms	Lack of blood return + difficulty of drip + swelling, 2 (28.6%) Lack of blood return + difficulty of drip, 1 (14.3%) Slight swelling, 3 (42.9%) No symptoms, 1 (14.3%)	No symptoms, 8 (100.0%)	No symptoms, 9 (100.0%)

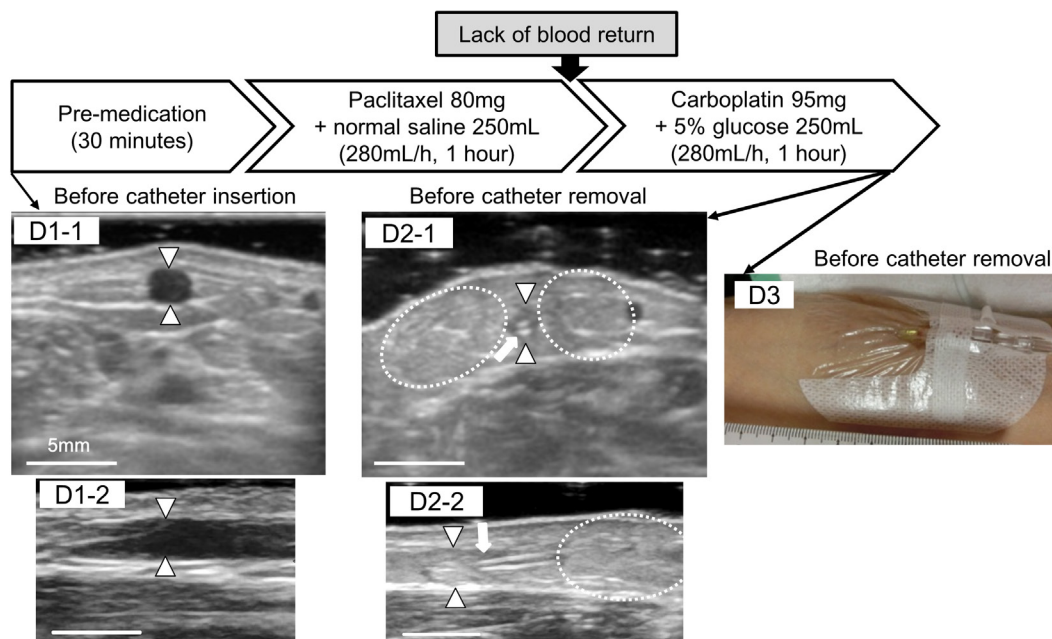


Figure 2. Ultrasound images and a photograph of the puncture site of a 79-year-old female patient. Transverse images (D1-1, D2-1) and longitudinal images (D1-2, D2-2) at puncture sites obtained before catheter insertion and after administration (before catheter removal). Arrowheads indicate the catheterized vein and allow indicate the catheter tip; the catheter tip can be seen as two bright points and lines in the vein. Subcutaneous edema is visible around the catheterized vein in the areas circled by dotted lines (D2-1, D2-2). Clinical image of the insertion site taken with a digital camera (D3).

edema may compress the vein, leading to a lack of blood return and difficulty in continuing the infusion.

All seven study patients who underwent paclitaxel and carboplatin chemotherapy showed subcutaneous edema after their infusions, whereas we identified no such changes in the ultrasound images of patients receiving docetaxel or nab-paclitaxel chemotherapy. Paclitaxel, docetaxel and nab-paclitaxel are classified as the same taxane; however, the preparations incorporate different vehicles. The vehicle comprises polyethoxylated castor oil and anhydrous ethanol in paclitaxel infusions (10). This vehicle reportedly often causes hypersensitivity and vascular irritability (17,18). In comparison, polyethoxylated castor oil is not the vehicle for docetaxel and nab-paclitaxel. Some studies have reported that classifying taxanes (including paclitaxel) as vesicants is debatable and that there is insufficient evidence to formally classify antineoplastic agents according to their vesicant properties (6). In the current study, patients receiving paclitaxel and carboplatin received more doses of taxanes over a longer infusion time than did patients receiving docetaxel or nab-paclitaxel. The subcutaneous edema may have developed because of stimulation of the vessel wall by antineoplastic agents and/or their vehicle (polyethoxylated castor oil) during lengthy infusions; however, it is unclear whether the subcutaneous edema was attributable to the amount of taxanes or total administration time. Furthermore, it is noteworthy the vein may be compressed by subcutaneous edema when the nurses cannot achieve blood return.

Also, there is a published report of a patient who presented with severe and progressive pain at the infusion site on day 11 after paclitaxel administration, despite having had no evidence of complications during the infusion (19). We, therefore, speculated that some changes can occur in the subcutaneous tissue and vein even when there are not significant visible abnormalities or symptoms by the end of chemotherapy. It is possible that ultrasound would provide more detailed information than the infiltration scale (15), including enabling detection of early slight extravasation.

Our findings indicate that stimulation by vesicant agents such as paclitaxel may cause subcutaneous edema at the infusion site. Such edema may compress the vein, leading to a lack of blood return and difficulty in continuing the infusion. Prevention of subcutaneous edema stimulated by vesicant agents and their vehicles may require consideration of varying the mode of venipuncture, for example, by choosing a larger vein and selecting a different catheter gauge. Furthermore, both the nurse and patient should be alert to the possibility of subcutaneous edema and inspect the infusion site repeatedly, since such edema may be present by the completion of infusion in the absence of visible manifestations or symptoms.

Because this study was observational study and the number of subjects was small, we could not investigate

the cause of the subcutaneous edema. However, the ultrasound findings reported here may be a key to further exploring the adverse events of paclitaxel.

In conclusion, we have here presented typical ultrasound images of the subcutaneous tissues around the catheterized vein after taxane administration and documented ultrasound evidence of severe subcutaneous edema immediately before catheter removal in the absence of significant visible manifestations or symptoms in patients undergoing paclitaxel and carboplatin chemotherapy but not in those receiving other taxane-based chemotherapy regimens.

Both subcutaneous edema stimulated by vesicant agents and their vehicles and early slight extravasation may be identified by clinical nurses by using ultrasonography.

Acknowledgements

This study was supported by a grant from the Japanese Society of Wound, Ostomy and Continence Management. We would like to acknowledge Dr. Koichi Yabunaka, who assisted to evaluate ultrasonographic images. We thank all participants and the healthcare professionals of the chemotherapy unit in The University of Tokyo Hospital.

Conflicts of interest

This study was a joint research program with Terumo Corporation and was conducted under the sponsorship of Terumo Corporation. Ryoko Murayama and Mari Abe-Doi are belonging to the laboratory supported by Terumo Co. Makoto Oe, Chieko Komiyama and Hiromi Sanada have no conflicts of interest.

References

1. Sparano JA, Wang M, Martino S, Jones V, Perez EA, Saphner T, Wolff AC, Sledge GW Jr., Wood WC, Davidson NE. Weekly paclitaxel in the adjuvant treatment of breast cancer. *N Engl J Med*. 2008; 358:1663-1671.
2. Pérez Fidalgo JA, García Fabregat L, Cervantes A, Margulies A, Vidall C, Roila F; ESMO Guidelines Working Group. Management of chemotherapy extravasation: ESMO-EONS Clinical Practice Guidelines. *Ann Oncol*. 2012; 23 (Suppl 7):vii167-173.
3. Hahn JC, Shafritz AB. Chemotherapy extravasation injuries. *J Hand Surg Am*. 2012; 37:360-362.
4. Schulmeister L. Extravasation management: clinical update. *Semin Oncol Nurs*. 2011; 27:82-90.
5. Raley J, Geisler JP, Buekers TE, Sorosky JI. Docetaxel extravasation causing significant delayed tissue injury. *Gynecol Oncol*. 2000; 78:259-260.
6. Barbee MS, Owonikoko TK, Harvey RD. Taxanes: vesicants, irritants, or just irritating? *Ther Adv Med Oncol*. 2014; 6:16-20.
7. Pérez Fidalgo JA, García Fabregat L, Cervantes A, Margulies A, Vidall C, Roila F. ESMO Guidelines

- Working Group. Management of chemotherapy extravasation: ESMO-EONS Clinical Practice Guidelines. *Ann Oncol*. 2012; 23 (Suppl 7):vii167-173.
8. Chiu N, Chiu L, Chow R, Lam H, Verma S, Pasetka M, Chow E, DeAngelis C. Taxane-induced arthralgia and myalgia: A literature review. *J Oncol Pharm Pract*. 2017; 23:56-67.
 9. Stanford BL, Hardwicke F. A review of clinical experience with paclitaxel extravasations. *Support Care Cancer*. 2003; 11:270-277.
 10. Bicher A, Levenback C, Burke TW, Morris M, Warner D, DeJesus Y, Gershenson DM. Infusion site soft-tissue injury after paclitaxel administration. *Cancer*. 1995; 76:116-120.
 11. Boyle DM, Engelking C. Vesicant extravasation: Myth and realities. *Oncol Nurs Forum*. 1995; 22:57-67.
 12. Yabunaka K, Iizaka S, Nakagami G, Aoi N, Kadono T, Koyanagi H, Uno M, Ohue M, Sanada S, Sanada H. Can ultrasonographic evaluation of subcutaneous fat predict pressure ulceration? *J Wound Care*. 2009; 18:192-196.
 13. Yabunaka K, Konishi H, Nakagami G, Sanada H, Iizaka S, Sanada S, Ohue M. Ultrasonographic evaluation of geniohyoid muscle movement during swallowing: a study on healthy adults of various ages. *Radiol Phys Technol*. 2012; 5:34-39.
 14. Yabunaka K, Murayama R, Takahashi T, Tanabe H, Kawamoto A, Oe M, Arai R, Sanada H. Ultrasonographic appearance of infusion via the peripheral intravenous catheters. *J Nurs Sci Eng*. 2015; 2:40-46.
 15. Yabunaka K, Murayama TR, Tanabe H, Takahashi T, Oe M, Oya M, Fujioka M, Sanada H. Ultrasonographic classification of subcutaneous edema caused by infusion via peripheral intravenous catheters. *J Med Ultrasound*. 2016; 24:60-65.
 16. Katsumata N, Yasuda M, Takahashi F, Isonishi S, Jobo T, Aoki D, Tsuda H, Sugiyama T, Kodama S, Kimura E, Ochiai K, Noda K; Japanese Gynecologic Oncology Group. Dose-dense paclitaxel once a week in combination with carboplatin every 3 weeks for advanced ovarian cancer: A phase 3 open-label, randomized trial. *Lancet*. 2009; 374:1331-1338.
 17. Kawano S, Kondoh H, Ishikawa K, Koizumi S, Kadota T, Takahashi N. Irritability study of paclitaxel in rabbit ear vein. *J Toxicol Sci*. 1994; 19:123-130.
 18. Singla AK, Garg A, Aggarwal D. Paclitaxel and its formulations. *Int J Pharm*. 2002; 235:179-192.
 19. Herrington JD, Figueroa JA. Severe necrosis due to paclitaxel extravasation. *Pharmacotherapy*. 1997; 17:163-165.

(Received September 9, 2019; Revised October 18, 2019; Accepted October 23, 2019)

Pediatric case of Graham Little Piccardi Lassueur syndrome – A rare entity

Ayan Basu^{1,*}, Dyuti Basu², Arpita Chattopadhyay³, Rhik Sanyal⁴, Mehebubar Rahman⁴, Rama Prosad Goswami⁴

¹DM Infectious Diseases, All India Institute of Medical Sciences, New Delhi, India;

²Department of Obstetrics and Gynaecology, Calcutta Medical College, Kolkata, West Bengal, India;

³All India Institute of Medical Sciences, New Delhi, India;

⁴Department of Tropical Medicine, School of Tropical Medicine, Kolkata, West Bengal, India.

Summary Graham Little Piccardi Lassueur syndrome (GLPLS) is a rare dermatosis characterized by patchy cicatricial alopecia of scalp, rapidly developing keratosis pilaris like follicular papules over trunk and extremities, and noncicatricial loss of axillary and pubic hair. This syndrome which is mostly seen in middle aged post-menopausal females (between ages 30-70) has rarely ever been described in the pediatric age group. We report a case of a 15 year old girl presenting to us with this rare syndrome.

Keywords: Graham Little Piccardi Lassueur syndrome, alopecia, lichen planopilaris, pediatric

1. Introduction

Graham Little Piccardi Lassueur syndrome (GLPLS) was first described by Piccardi (1914) who reported a case with progressive cicatricial scalp alopecia associated with non-cicatricial alopecia of axillary and pubic areas and a follicular lichenoid eruption on the trunk and extremities. In 1915, Ernst Graham-Little also published a similar case observed by Lassueur, which he called 'folliculitis decalvans et atrophicans' (1). GLPLS is a rare variant of lichen planopilaris usually occurring in middle-aged Caucasian women (2-6). No pediatric case has been reported till date. Herein, we present a case of E/beta thalassemia with GLPLS and its classical triad of clinical features.

2. Case Report

A 15 year old girl presented with intermittent episodes of mild yellowish discolouration of eyes since 5 years of age, each episode lasting 7-10 days which

spontaneously disappeared without any medications only to recur 2 months later. These episodes happened several times, each of similar duration and symptom free intervals. Her mother noticed poor growth during this period compared to her siblings. Six months before presentation, she noticed multiple discrete small spiky black spots over the skin of epigastric region. The lesions gradually increased over the whole anterior abdominal wall within 2-3 months (Figure 1). There was associated scalp hair loss over the past 6 months with 2 small areas of baldness with distinct margin over left parietal region (Figure 2) and left posterior auricular region. A patchy lesion over medial aspect of right leg with distinct margin had also appeared progressively increasing in size over last 2-3 months. Antenatal and birth history were uneventful. She was developmentally appropriate and had good scholastic performance. She had not attained menarche and there was no development of her secondary sexual characters. She never required any hospitalization or any blood transfusions during this period. Topical steroid ointments were prescribed in the past but did not relieve her symptoms. On general survey, there was mild pallor and icterus. She was stunted and had no hair over the both axilla (Figure 3) and pubic region with no breast development. There were plenty of discrete black spiky elevated spots dispersed over whole anterior abdomen. There was 2 areas of alopecia areata over scalp and a 3 cm by 4 cm patchy lesion with distinct

Released online in J-STAGE as advance publication October 27, 2019.

*Address correspondence to:

Dr. Ayan Basu, DM Infectious Diseases, Department of Internal Medicine, All India Institute of Medical Sciences, New Delhi-110029, India.

E-mail: ayanbasustm@gmail.com



Figure 1. Multiple discrete black spiky elevated lesions over skin of abdomen.



Figure 2. Cicatricial scalp alopecia over left parietal region.

margin over the medial aspect of right leg. On systemic examination there was hepatosplenomegaly, both being 2 cm from costal margin, firm in consistency and nontender. Her laboratory reports showed a microcytic hypochromic anemia with haemoglobin 8 g/dL, MCV-62 fl, MCH-18.4 pg, MCHC-24.7 g/dL, red cell distribution width-23.1%. Liver function tests showed total bilirubin was 2.32 mg/dL and conjugated fraction was 1.58 mg/dL with normal transaminases. Thyroid stimulating hormone level was 2.62 μ IU/mL. Haemoglobin electrophoresis was done in two occasions and showed haemoglobin F was 23-27.3%, haemoglobin A was 6.2-9.9%, haemoglobin A2+E was 49.8-54.8%. Haemoglobin electrophoresis of her mother showed haemoglobin E carrier and father showed beta thalassemia carrier. Our dermatology department diagnosed skin lesions over abdomen as Lichen planopilaris and leg lesions as lichen planus.



Figure 3. Bilateral loss of axillary hair.

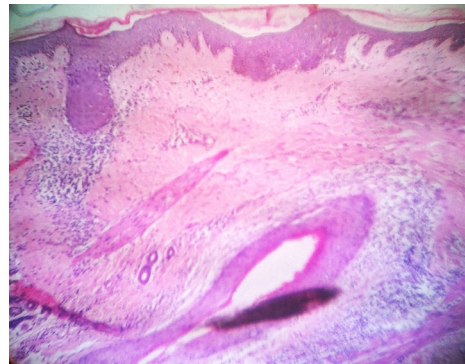


Figure 4. Microscopic findings. Skin biopsy showed perfollicular lymphocytic infiltrate with damage to follicular basal cells which is suggestive of lichen planopilaris.

Skin biopsy was taken from abdominal lesion showed perfollicular lymphocytic infiltrate with damage to follicular basal cells which is suggestive of lichen planopilaris (Figure 4).

3. Discussion

We report a pediatric case of E/beta thalassemia with GLPLS which has never been described before. This dermatosis which is a variant of lichen planus may have a human leukocyte antigen (HLA) induced T cell response behind its clinical expression (7). Rodríguez Bayona *et al.* reported autoantibodies against Inner Centromere Protein INCENP, a protein responsible for chromosomal segregation and mitosis regulation, in one patient with GLPLS (8).

Though typically sporadic and nonfamilial, one case of familial pattern has been described (7), an association with hepatitis B vaccination (9) and a phenotypically female (genetically XY) patient with androgen insensitivity syndrome (testicular feminization) have also been reported (10). Our patient, however, did not receive any hepatitis B vaccination in the past. We performed abdominal ultrasound to confirm the female phenotype but karyotyping was not done as we lost the

patient to follow up.

In early lesions of lichen planopilaris there is perifollicular lymphocytic infiltrate at the level of isthmus and infundibulum, along with vacuolar changes of the outer root sheath. Progression of disease shows perifollicular fibrosis and epithelial atrophy at the level of isthmus and infundibulum which gives rise to a characteristic hourglass configuration. In advanced cases there is alopecia with vertically oriented elastic fibers that replace the destroyed hair follicles. Similar findings were seen in our case. End stage scarring alopecia without any visible hair follicle is called pseudopelade of Brocq (11).

Topical and systemic glucocorticoids, retinoids, and PUVA (psoralen and ultraviolet A) photochemotherapy have not shown to halt progression of the disease. Treatment with cyclosporine (4 mg/kg/day) has shown improvement in erythema, hyperkeratotic papules, and induction of partial hair growth in previous reports (12,13). In some cases improvement with thalidomide have also been described (14,15).

4. Conclusion

The main aim of reporting this rare case is to make the clinicians aware of the occurrence of this rare syndrome in pediatric age group. If a patient presented with progressive cicatricial scalp alopecia associated with non-cicatricial alopecia of axillary and pubic areas and a follicular lichenoid eruption on the trunk and extremities then clinician should suspect GLPLS.

References

- Graham Little EG. Folliculitis decalvans et atrophicans. *Br J Dermatol.* 1915; 27:1835.
- Varadraj V Pai, Naveen N Kikkeri, Tukaram Sori, US Dinesh. Graham little piccardi lassueur syndrome: an unusual variant of follicular lichen planus. *Int J Trichology.* 2011; 3:28-30.
- Vashi N, Newlove T, Chu J, Patel R, Stein J. Graham Little Piccardi Lassueur syndrome. *Dermatol Online J.* 2011; 17:30.
- Zegarska B, Kallas D, Schwartz RA, Czajkowski R, Uchanska G, Placek W. Graham Little syndrome. *Acta Dermatovenerol Alp Panonica Adriat.* 2010; 19:39-42.
- László FG. Graham Little Piccardi Lassueur syndrome: case report and review of the syndrome in men. *Int J Dermatol.* 2014; 53:1019-1022.
- Somani N, Bergfeld WF. Cicatricial alopecia: classification and histopathology. *Dermatol Ther.* 2008; 21:221-237.
- Viglizzo G, Verrini A, Rongioletti F. Familial Lassueur Graham Little Piccardi syndrome. *Dermatology.* 2004; 208:142-144.
- Rodríguez-Bayona B, Ruchaud S, Rodríguez C, Linares M, Astola A, Ortiz M, Earnshaw WC, Valdivia MM. Autoantibodies against the chromosomal passenger protein INCENP found in a patient with Graham Little Piccardi Lassueur syndrome. *J Autoimmune Dis.* 2007; 4:1.
- Rebora A, Rongioletti F, Drago F, Parodi. Lichen planus as a side effect of HBV vaccination. *Dermatology.* 1999; 198:1-2.
- Vega Gutiérrez J, Miranda-Romero A, Pérez Milán F, Martínez García G. Graham Little Piccardi Lassueur syndrome associated with androgen insensitivity syndrome (testicular feminization). *J Eur Acad Dermatol Venereol.* 2004; 18:463-466.
- Mobini N, Loussaint S, Kamino H. Non-infectious erythematous papular and squamous disease. In: *Lever's Histopathology of skin.* (Elder DE, Elenitsas R, Johnson BL, Murthy GF, editors). 9th ed., Philadelphia: Lippincott William Wilkins, 2005; pp. 179-214.
- Bottoni U, Innocenzi D, Carlesimo M. Treatment of Piccardi Lassueur Graham Little syndrome with cyclosporin A. *Eur J Dermatol.* 1995; 5:216-219.
- Mirmirani P, Willey A, Price VH. Short course of oral cyclosporine in lichen planopilaris. *J Am Acad Dermatol.* 2003; 49:667-671.
- George SJ, Hsu S. Lichen planopilaris treated with thalidomide. *J Am Acad Dermatol.* 2001; 45:965.
- Boyd AS, King LE Jr. Thalidomide induced remission of lichen planopilaris. *J Am Acad Dermatol.* 2002; 47:967-968.

(Received September 29, 2018; Revised July 10, 2019; Re-revised September 2, 2019; Accepted October 19, 2019)

A case of overlap syndrome (scleroderma and polymyositis) associated with the development of sudden chest pain due to myocardial damage

Akira Kaneko, Ikko Kajihara*, Azusa Miyashita, Hironobu Ihn

Department of Dermatology and Plastic Surgery, Faculty of Life Sciences, Kumamoto University, Kumamoto, Japan.

Summary Myocardial injury with systemic sclerosis (SSc) causes pericarditis and arrhythmia, and polymyositis-induced muscle inflammation causes myocarditis. We report a rare case of overlap syndrome (SSc and polymyositis) who presented with sudden chest pain secondary to myocardial fibrosis. Although the etiology of chest symptoms in collagen disease was difficult to identify, cardiac magnetic resonance imaging (MRI) revealed not myocarditis but myocardial fibrosis in our case. Synthetic judgement of serum brain natriuretic peptide/troponin T levels and cardiac MRI is useful in the search for the cause of chest symptoms even in patients with collagen diseases.

Keywords: Scleroderma, polymyositis, myocardial fibrosis, myocarditis

1. Introduction

Cardiac involvement is rare in patients with collagen diseases; however, this is a serious condition when it does occur. Myocardial injury with systemic sclerosis (SSc) causes pericarditis and arrhythmia, and polymyositis-induced muscle inflammation causes myocarditis (1,2). We report a rare case of overlap syndrome (SSc and polymyositis) who presented with sudden chest pain secondary to myocardial fibrosis.

2. Case Report

A 20-year-old man presented with a 3-year history of Raynaud's phenomenon and fingertip ulceration in winter. He noticed muscle weakness 3 months prior to presentation to our hospital. Physical examination revealed pitting scars and skin sclerosis (modified Rodnan's total skin thickness score, 16). Manual muscle testing revealed normal results; however, we observed decreased grip strength (10 kg [right], 8 kg [left]) and myalgia in both thighs. Laboratory investigations revealed the following results: white blood cell count

5,200 cells/mm³, serum creatine kinase 763 IU/L (59-248 IU/L), aldolase 15.3 IU/L (2.7-7.5 IU/L), anti-Smith antibody 3.6 IU/mL (< 10 U/mL), anti-U1 ribonucleoprotein antibody > 550 IU/mL (< 10 U/mL). Biopsy of the skin of the forearm showed edematous and increased collagen fibers in the dermis, and these findings were compatible with SSc (Figure 1A). Muscle biopsy of the biceps brachii revealed dense and diffuse perivascular lymphocytic infiltration (Figure 1B). Chest computed tomography (CT) revealed mild interstitial pneumonia in the basal segments of the lungs. We diagnosed him with overlap syndrome (diffuse cutaneous SSc and polymyositis) and treated with oral prednisolone (0.5 mg/kg/day, 35 mg/day). On the first day of oral steroid therapy, he developed sudden chest pain and dyspnea. Electrocardiography (ECG), echocardiography (UCG), and coronary CT revealed no abnormalities. However, the serum troponin T level was 0.0427 ng/mL (< 0.014 ng/mL), and serum brain natriuretic peptide (BNP) was 55.9 pg/mL (< 18.4 ng/mL). Cardiac magnetic resonance imaging (MRI) revealed that the extracellular volume fraction (ECV) was 35% (normal range 20-30%), and the value of native T1 mapping at the left ventricular wall was 1,320 ms (normal range approximately 950 ms). These findings indicated significant myocardial fibrosis (not myocarditis). Based on the aforementioned findings, we concluded that his chest symptoms were secondary to myocardial fibrosis caused by SSc. This symptom

*Address correspondence to:

Dr. Ikko Kajihara, Department of Dermatology and Plastic Surgery, Faculty of Life Sciences, Kumamoto University, 1-1-1 Honjo, Chuo-ku, Kumamoto City, Kumamoto, 860-8556, Japan.

E-mail: kajiderma@gmail.com

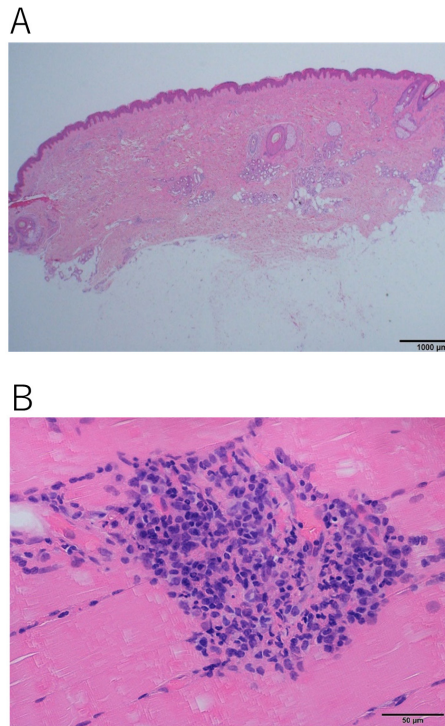


Figure 1. (A) Swollen and increased collagen fibers in the dermis. (B) Dense and diffuse infiltration of lymphocytes around vascular wall in the muscle.

disappeared spontaneously within 4 hours. Follow-up cardiac MRI performed 9 months later showed improved ECV and native T1 values.

3. Discussion

Serum BNP and troponin T levels are useful predictors

of myocardial injury in patients with SSc (3,4). Our patient showed the elevation of both serum BNP and troponin T levels. To our knowledge, this is a rare case report that describes overlap syndrome (SSc and polymyositis) with sudden onset of chest pain secondary to myocardial fibrosis. The exact etiology of chest symptoms (SSc and/or polymyositis) was difficult to identify because ECG and UCG may not accurately identify abnormalities in conditions that may be clinically indistinguishable, as was observed in our patient. We dermatologists must recognize that synthetic judgement of serum BNP/troponin T levels and cardiac MRI is useful in the search for the cause of chest symptoms even in patients with collagen diseases.

References

1. Gabrielli A, Avvedimento EV, Krieg T. Scleroderma. *N Engl J Med.* 2009; 360:1989-2003.
2. Zhang L, Wang GC, Ma L, Zu N. Cardiac involvement in adult polymyositis or dermatomyositis: a systematic review. *Clin Cardiol.* 2012; 35:686-691.
3. Ivanovic BA, Tadic MV, Zlatanovic MM, Damjanov NN, Ostojić PM, Bonaci-Nikolic BN. Which factors impact myocardial function in systemic sclerosis? *Echocardiography.* 2012; 29:307-317.
4. Bosello S, De Luca G, Berardi G, Canestrari G, de Waure C, Gabrielli FA, Di Mario C, Forni F, Gremese E, Ferraccioli G. Cardiac troponin T and NT-proBNP as diagnostic and prognostic biomarkers of primary cardiac involvement and disease severity in systemic sclerosis: A prospective study. *Eur J Intern Med.* 2019; 60:46-53.

(Received September 23, 2019; Revised October 16, 2019; Accepted October 26, 2019)

Guide for Authors

1. Scope of Articles

Drug Discoveries & Therapeutics welcomes contributions in all fields of pharmaceutical and therapeutic research such as medicinal chemistry, pharmacology, pharmaceutical analysis, pharmaceuticals, pharmaceutical administration, and experimental and clinical studies of effects, mechanisms, or uses of various treatments. Studies in drug-related fields such as biology, biochemistry, physiology, microbiology, and immunology are also within the scope of this journal.

2. Submission Types

Original Articles should be well-documented, novel, and significant to the field as a whole. An Original Article should be arranged into the following sections: Title page, Abstract, Introduction, Materials and Methods, Results, Discussion, Acknowledgments, and References. Original articles should not exceed 5,000 words in length (excluding references) and should be limited to a maximum of 50 references. Articles may contain a maximum of 10 figures and/or tables.

Brief Reports definitively documenting either experimental results or informative clinical observations will be considered for publication in this category. Brief Reports are not intended for publication of incomplete or preliminary findings. Brief Reports should not exceed 3,000 words in length (excluding references) and should be limited to a maximum of 4 figures and/or tables and 30 references. A Brief Report contains the same sections as an Original Article, but the Results and Discussion sections should be combined.

Reviews should present a full and up-to-date account of recent developments within an area of research. Normally, reviews should not exceed 8,000 words in length (excluding references) and should be limited to a maximum of 100 references. Mini reviews are also accepted.

Policy Forum articles discuss research and policy issues in areas related to life science such as public health, the medical care system, and social science and may address governmental issues at district, national, and international levels of discourse. Policy Forum articles should not exceed 2,000 words in length (excluding references).

Case Reports should be detailed reports of the symptoms, signs, diagnosis, treatment, and follow-up of an individual patient. Case reports may contain a demographic profile of the patient but usually describe an unusual or novel occurrence. Unreported or unusual side effects or adverse interactions involving medications will also be considered. Case

Reports should not exceed 3,000 words in length (excluding references).

News articles should report the latest events in health sciences and medical research from around the world. News should not exceed 500 words in length.

Letters should present considered opinions in response to articles published in Drug Discoveries & Therapeutics in the last 6 months or issues of general interest. Letters should not exceed 800 words in length and may contain a maximum of 10 references.

3. Editorial Policies

Ethics: Drug Discoveries & Therapeutics requires that authors of reports of investigations in humans or animals indicate that those studies were formally approved by a relevant ethics committee or review board.

Conflict of Interest: All authors are required to disclose any actual or potential conflict of interest including financial interests or relationships with other people or organizations that might raise questions of bias in the work reported. If no conflict of interest exists for each author, please state "There is no conflict of interest to disclose".

Submission Declaration: When a manuscript is considered for submission to Drug Discoveries & Therapeutics, the authors should confirm that 1) no part of this manuscript is currently under consideration for publication elsewhere; 2) this manuscript does not contain the same information in whole or in part as manuscripts that have been published, accepted, or are under review elsewhere, except in the form of an abstract, a letter to the editor, or part of a published lecture or academic thesis; 3) authorization for publication has been obtained from the authors' employer or institution; and 4) all contributing authors have agreed to submit this manuscript.

Cover Letter: The manuscript must be accompanied by a cover letter signed by the corresponding author on behalf of all authors. The letter should indicate the basic findings of the work and their significance. The letter should also include a statement affirming that all authors concur with the submission and that the material submitted for publication has not been published previously or is not under consideration for publication elsewhere. The cover letter should be submitted in PDF format. For example of Cover Letter, please visit <http://www.ddtjournal.com/downloadcentre.php> (Download Centre).

Copyright: A signed JOURNAL PUBLISHING AGREEMENT (JPA) must be provided by post, fax, or as a scanned file before acceptance of the article. Only forms with a hand-written signature are accepted. This copyright will ensure the widest possible dissemination of information. A form facilitating transfer of copyright can be downloaded by clicking the appropriate link and can be returned to the e-mail address or fax number noted on the form (Please visit

Download Centre). Please note that your manuscript will not proceed to the next step in publication until the JPA form is received. In addition, if excerpts from other copyrighted works are included, the author(s) must obtain written permission from the copyright owners and credit the source(s) in the article.

Suggested Reviewers: A list of up to 3 reviewers who are qualified to assess the scientific merit of the study is welcomed. Reviewer information including names, affiliations, addresses, and e-mail should be provided at the same time the manuscript is submitted online. Please do not suggest reviewers with known conflicts of interest, including participants or anyone with a stake in the proposed research; anyone from the same institution; former students, advisors, or research collaborators (within the last three years); or close personal contacts. Please note that the Editor-in-Chief may accept one or more of the proposed reviewers or may request a review by other qualified persons.

Language Editing: Manuscripts prepared by authors whose native language is not English should have their work proofread by a native English speaker before submission. If not, this might delay the publication of your manuscript in Drug Discoveries & Therapeutics.

The Editing Support Organization can provide English proofreading, Japanese-English translation, and Chinese-English translation services to authors who want to publish in Drug Discoveries & Therapeutics and need assistance before submitting a manuscript. Authors can visit this organization directly at <http://www.iacmhr.com/iac-eso/support.php?lang=en>. IAC-ESO was established to facilitate manuscript preparation by researchers whose native language is not English and to help edit works intended for international academic journals.

4. Manuscript Preparation

Manuscripts should be written in clear, grammatically correct English and submitted as a Microsoft Word file in a single-column format. Manuscripts must be paginated and typed in 12-point Times New Roman font with 24-point line spacing. Please do not embed figures in the text. Abbreviations should be used as little as possible and should be explained at first mention unless the term is a well-known abbreviation (e.g. DNA). Single words should not be abbreviated.

Title page: The title page must include 1) the title of the paper (Please note the title should be short, informative, and contain the major key words); 2) full name(s) and affiliation(s) of the author(s); 3) abbreviated names of the author(s); 4) full name, mailing address, telephone/fax numbers, and e-mail address of the corresponding author; and 5) conflicts of interest (if you have an actual or potential conflict of interest to disclose, it must be included as a footnote on the title page of the manuscript; if no conflict of interest exists for each author, please state "There is no conflict of interest to disclose"). Please visit [Download Centre](#) and refer to the title page of the manuscript sample.

Abstract: The abstract should briefly state the purpose of the study, methods, main findings, and conclusions. For article types including Original Article, Brief Report, Review, Policy Forum, and Case Report, a one-paragraph abstract consisting of no more than 250 words must be included in the manuscript. For News and Letters, a brief summary of main content in 150 words or fewer should be included in the manuscript. Abbreviations must be kept to a minimum and non-standard abbreviations explained in brackets at first mention. References should be avoided in the abstract. Key words or phrases that do not occur in the title should be included in the Abstract page.

Introduction: The introduction should be a concise statement of the basis for the study and its scientific context.

Materials and Methods: The description should be brief but with sufficient detail to enable others to reproduce the experiments. Procedures that have been published previously should not be described in detail but appropriate references should simply be cited. Only new and significant modifications of previously published procedures require complete description. Names of products and manufacturers with their locations (city and state/country) should be given and sources of animals and cell lines should always be indicated. All clinical investigations must have been conducted in accordance with Declaration of Helsinki principles. All human and animal studies must have been approved by the appropriate institutional review board(s) and a specific declaration of approval must be made within this section.

Results: The description of the experimental results should be succinct but in sufficient detail to allow the experiments to be analyzed and interpreted by an independent reader. If necessary, subheadings may be used for an orderly presentation. All figures and tables must be referred to in the text.

Discussion: The data should be interpreted concisely without repeating material already presented in the Results section. Speculation is permissible, but it must be well-founded, and discussion of the wider implications of the findings is encouraged. Conclusions derived from the study should be included in this section.

Acknowledgments: All funding sources should be credited in the Acknowledgments section. In addition, people who contributed to the work but who do not meet the criteria for authors should be listed along with their contributions.

References: References should be numbered in the order in which they appear in the text. Citing of unpublished results, personal communications, conference abstracts, and theses in the reference list is not recommended but these sources may be mentioned in the text. In the reference list, cite the names of all authors when there are fifteen or fewer authors; if there are sixteen or more authors, list the first three followed by *et al.* Names of journals should

be abbreviated in the style used in PubMed. Authors are responsible for the accuracy of the references. Examples are given below:

Example 1 (Sample journal reference):
Nakata M, Tang W. Japan-China Joint Medical Workshop on Drug Discoveries and Therapeutics 2008: The need of Asian pharmaceutical researchers' cooperation. *Drug Discov Ther.* 2008; 2:262-263.

Example 2 (Sample journal reference with more than 15 authors):
Darby S, Hill D, Auvinen A, *et al.* Radon in homes and risk of lung cancer: Collaborative analysis of individual data from 13 European case-control studies. *BMJ.* 2005; 330:223.

Example 3 (Sample book reference):
Shalev AY. Post-traumatic stress disorder: Diagnosis, history and life course. In: *Post-traumatic Stress Disorder, Diagnosis, Management and Treatment* (Nutt DJ, Davidson JR, Zohar J, eds.). Martin Dunitz, London, UK, 2000; pp. 1-15.

Example 4 (Sample web page reference):
World Health Organization. The World Health Report 2008 – primary health care: Now more than ever. http://www.who.int/whr/2008/whr08_en.pdf (accessed September 23, 2010).

Tables: All tables should be prepared in Microsoft Word or Excel and should be arranged at the end of the manuscript after the References section. Please note that tables should not in image format. All tables should have a concise title and should be numbered consecutively with Arabic numerals. If necessary, additional information should be given below the table.

Figure Legend: The figure legend should be typed on a separate page of the main manuscript and should include a short title and explanation. The legend should be concise but comprehensive and should be understood without referring to the text. Symbols used in figures must be explained.

Figure Preparation: All figures should be clear and cited in numerical order in the text. Figures must fit a one- or two-column format on the journal page: 8.3 cm (3.3 in.) wide for a single column, 17.3 cm (6.8 in.) wide for a double column; maximum height: 24.0 cm (9.5 in.). Please make sure that artwork files are in an acceptable format (TIFF or JPEG) at minimum resolution (600 dpi for illustrations, graphs, and annotated artwork, and 300 dpi for micrographs and photographs). Please provide all figures as separate files. Please note that low-resolution images are one of the leading causes of article resubmission and schedule delays. All color figures will be reproduced in full color in the online edition of the journal at no cost to authors.

Units and Symbols: Units and symbols conforming to the International System of Units (SI) should be used for physicochemical quantities. Solidus notation (*e.g.* mg/kg, mg/mL, mol/mm²/min) should be used. Please refer to the SI Guide www.bipm.org/en/si/ for standard units.

Supplemental data: Supplemental data might be useful for supporting and enhancing your scientific research and Drug Discoveries & Therapeutics accepts the submission of these materials which will be only published online alongside the electronic version of your article. Supplemental files (figures, tables, and other text materials) should be prepared according to the above guidelines, numbered in Arabic numerals (*e.g.*, Figure S1, Figure S2, and Table S1, Table S2) and referred to in the text. All figures and tables should have titles and legends. All figure legends, tables and supplemental text materials should be placed at the end of the paper. Please note all of these supplemental data should be provided at the time of initial submission and note that the editors reserve the right to limit the size and length of Supplemental Data.

5. Submission Checklist

The Submission Checklist will be useful during the final checking of a manuscript prior to sending it to Drug Discoveries & Therapeutics for review. Please visit [Download Centre](#) and download the Submission Checklist file.

6. Online submission

Manuscripts should be submitted to Drug Discoveries & Therapeutics online at <http://www.ddtjournal.com>. The manuscript file should be smaller than 5 MB in size. If for any reason you are unable to submit a file online, please contact the Editorial Office by e-mail at office@ddtjournal.com

7. Accepted manuscripts

Proofs: Galley proofs in PDF format will be sent to the corresponding author *via* e-mail. Corrections must be returned to the editor (proof-editing@ddtjournal.com) within 3 working days.

Offprints: Authors will be provided with electronic offprints of their article. Paper offprints can be ordered at prices quoted on the order form that accompanies the proofs.

Page Charge: A page charge of \$140 will be assessed for each printed page of an accepted manuscript. The charge for printing color figures is \$340 for each page. Under exceptional circumstances, the author(s) may apply to the editorial office for a waiver of the publication charges at the time of submission.

(Revised February 2013)

Editorial and Head Office:

Pearl City Koishikawa 603
2-4-5 Kasuga, Bunkyo-ku
Tokyo 112-0003
Japan
Tel: +81-3-5840-9697
Fax: +81-3-5840-9698
E-mail: office@ddtjournal.com

JOURNAL PUBLISHING AGREEMENT (JPA)

Manuscript No.:

Title:

Corresponding author:

The International Advancement Center for Medicine & Health Research Co., Ltd. (IACMHR Co., Ltd.) is pleased to accept the above article for publication in Drug Discoveries & Therapeutics. The International Research and Cooperation Association for Bio & Socio-Sciences Advancement (IRCA-BSSA) reserves all rights to the published article. Your written acceptance of this JOURNAL PUBLISHING AGREEMENT is required before the article can be published. Please read this form carefully and sign it if you agree to its terms. The signed JOURNAL PUBLISHING AGREEMENT should be sent to the Drug Discoveries & Therapeutics office (Pearl City Koishikawa 603, 2-4-5 Kasuga, Bunkyo-ku, Tokyo 112-0003, Japan; E-mail: office@ddtjournal.com; Tel: +81-3-5840-9697; Fax: +81-3-5840-9698).

1. Authorship Criteria

As the corresponding author, I certify on behalf of all of the authors that:

- 1) The article is an original work and does not involve fraud, fabrication, or plagiarism.
- 2) The article has not been published previously and is not currently under consideration for publication elsewhere. If accepted by Drug Discoveries & Therapeutics, the article will not be submitted for publication to any other journal.
- 3) The article contains no libelous or other unlawful statements and does not contain any materials that infringes upon individual privacy or proprietary rights or any statutory copyright.
- 4) I have obtained written permission from copyright owners for any excerpts from copyrighted works that are included and have credited the sources in my article.
- 5) All authors have made significant contributions to the study including the conception and design of this work, the analysis of the data, and the writing of the manuscript.
- 6) All authors have reviewed this manuscript and take responsibility for its content and approve its publication.
- 7) I have informed all of the authors of the terms of this publishing agreement and I am signing on their behalf as their agent.

2. Copyright Transfer Agreement

I hereby assign and transfer to IACMHR Co., Ltd. all exclusive rights of copyright ownership to the above work in the journal Drug Discoveries & Therapeutics, including but not limited to the right 1) to publish, republish, derivate, distribute, transmit, sell, and otherwise use the work and other related material worldwide, in whole or in part, in all languages, in electronic, printed, or any other forms of media now known or hereafter developed and the right 2) to authorize or license third parties to do any of the above.

I understand that these exclusive rights will become the property of IACMHR Co., Ltd., from the date the article is accepted for publication in the journal Drug Discoveries & Therapeutics. I also understand that IACMHR Co., Ltd. as a copyright owner has sole authority to license and permit reproductions of the article.

I understand that except for copyright, other proprietary rights related to the Work (e.g. patent or other rights to any process or procedure) shall be retained by the authors. To reproduce any text, figures, tables, or illustrations from this Work in future works of their own, the authors must obtain written permission from IACMHR Co., Ltd.; such permission cannot be unreasonably withheld by IACMHR Co., Ltd.

3. Conflict of Interest Disclosure

I confirm that all funding sources supporting the work and all institutions or people who contributed to the work but who do not meet the criteria for authors are acknowledged. I also confirm that all commercial affiliations, stock ownership, equity interests, or patent-licensing arrangements that could be considered to pose a financial conflict of interest in connection with the article have been disclosed.

Corresponding Author's Name (Signature):

Date:

